Doctoral dissertation: Molecularly imprinted polymer based sensors for bio-sensing applications.

PhD Candidate:	Evelien Kellens
Promotor:	Prof. Dr. A. Ethirajan
Copromotors:	Prof. Dr. R. Thoelen
	Prof. Dr. T. Junkers
Research group:	Nanobiophysics and soft matter interfaces (NSI)
Faculty/School:	Institute for Material Research (IMO), Hasselt University

Promotor:	Prof. Dr. Anitha Ethirajan
Copromotors:	Prof. Dr. Tanja Junkers
	Prof. Dr. Ronald Thoelen
Members of the jury:	Prof. Dr. Dirk Vanderzande
	Prof. Dr. Anna Musyanovych
	Prof. Dr. Sarah De Saeger

Table of Contents

Acknowledgements

I wish to express my sincere appreciation to those who have contributed to this thesis and supported me in one way or the other during this journey. First of all, I am grateful to my promotor, Anitha, for giving me the chance to work on this topic, her guidance and all the useful discussions and brainstorming sessions. Your insights helped me at various stages of my research.
My sincere gratitude is also reserved for my co-promotors Tanja and Ronald for their invaluable insights and suggestions on several aspects during my PhD.

I want to thank Dirk Vanderzande, Anna Musyanovych and Sarah De Saeger for being part of my PhD jury.

Many thanks to Hannelore, Jolien, Marten, Sorel, Jeroen, Matthias, Jeroen S. and Thijs. Without these people, my thesis would not be what it is now!

Very special thanks to Hasselt University – Institute for material research and Instituut voor Innovatie door Wetenschap en Technologie in Vlaanderen (IWT) for giving me the opportunity to carry out my doctoral research and for their financial support. It would have been impossible for me to even start my study had they not given me the facilities and scholarship.

A big thank you goes to Christel, Hilde, Johnny, Jan, Lieven, Erik, Relinde, Ellen and Marina for always being ready to help!

Special mention goes to my IMO-besties Lien and Inge for going far beyond the call of duty ;). I also want to thank 'the office' : Thijs, Andreas, Christopher, Yasin, Srujan, Senne, Martijn, Sumit, Mehran and Gideon and the lunch/fitlink/coffee squads: Ronald, Steven, Bert, Tanya, Jorne, Gilles, Seppe, Jeroen S., Frederik, Glen, Philippe, Tim V., Marijn, Sien, Rozita, Patricia (especially for the biscotti), Jeroen D., Wieland, Aslihan, Shova, Ilaria, Michael, Dieter and for all the support and laughs.

The BDE group: Flushed away, but the IMPRINT is permanent!

Then there are the girls who also deserve a special place in this section: Svennie, Esther and Vio. I don't even dare to mention our squad name in this thesis ;). I

also want to thank Lys, An, Maarten, Martine, Karen, Wim, Kris and Gaëlle for the support and the laughs.

Words cannot express the love I have for my parents, my brother and his girlfriend and my in-laws for their constant unconditional support - both emotionally, financially and gastronomically ;). I would not be here if it was not for you all. This also holds for the two gangsters of the Daal: Binkie and Cadee 'Kat met de grote K'. <3

Finally, I would like to acknowledge the most important person in my life, Lars. He has been a constant source of strength and inspiration. I can honestly say that it was his determination and constant encouragement (and sometimes an "Evelien, stel u niet aan jong" when I needed one) that ultimately made it possible for me to see this project through to the end.

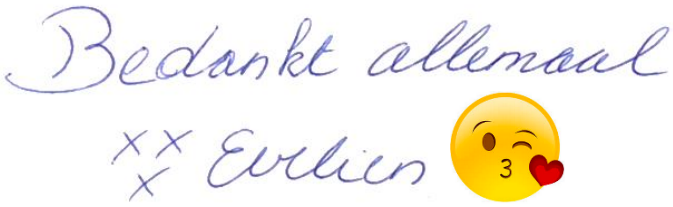

Nederlandse samenvatting

Gebruiksvriendelijke en goedkope sensoren die een biologisch relevant doelmolecule in zijn fysiologische concentraties kunnen detecteren en kwantificeren op een consistente en accurate manier, zijn zeer interessant voor toepassingen in de medische diagnostiek en voedsel- en omgevingsveiligheid. Vandaag de dag wordt de concentratie van een doelmolecule in een staal doorgaans bepaald in gespecialiseerde laboratoria door gespecialiseerd personeel dat gebruik maakt van dure en tijd consumerende detectietechnieken zoals immunoassays, vloeistof- en gaschromatografie. Bijgevolg, richten vele onderzoekers zich op de ontwikkeling van een gebruiksvriendelijke, goedkope en betrouwbare diagnostische sensor die buiten het laboratorium kan gebruikt worden als alternatief. Biosensoren gebruiken biologische receptoren als detectie element omdat deze zeer specifiek en selectief zijn tijdens het binden van het doelmolecule. Biologische receptoren hebben echter ook grote nadelen betreffende de kostprijs en de stabiliteit. Daarnaast zijn er veel doelmoleculen waarvoor er geen stabiele biologische receptoren bestaan. In dit opzicht zouden synthetische moleculair geïmprinte polymeren (MIPs) een interessant alternatief zijn aangezien ze voordelen bieden op gebied van stabiliteit en kostprijs terwijl ze toch nog voldoende affiniteit en selectiviteit voor het doelmolecule tonen. MIPs worden gemaakt door het polymeriseren van functionele en crosslinkende monomeren in de aanwezigheid van het sjabloon doelmolecule. Na het polymeriseren en het verwijderen van de sjabloon doelmoleculen, blijft er een afdruk in het polymeer over dat complementair is aan het doelmolecule betreffende de grootte, de vorm en de functionele groepen. Bij gevolg kunnen deze afdrukken, ook wel imprints genoemd, het doelmolecule met een hoge affiniteit en specificiteit binden. Niet geïmprinte polymeren (NIPs) worden als negatieve controle gebruikt. MIP gebaseerde sensoren werden eerder al ontwikkeld in het Instituut voor Materiaalonderzoek voor de detectie van verschillende doelmoleculen en werden vervolgens continu geoptimaliseerd om hun prestatie, betrouwbaarheid en herbruikbaarheid te verbeteren.

Aan het begin van mijn doctoraat, waren bulk MIP gebaseerde sensoren voor de detectie van nicotine, histamine, cafeïne en serotonine reeds ontwikkeld. Hierbij

werd er gebruik gemaakt van stempelen en een polymeer lijm als afzet en immobilisatie techniek, respectievelijk. Impedantie spectroscopie, de heat-transfer methode (HTM) en de kwarts kristal microbalans werden hierbij gebruikt als uitleestechnieken. Echter, wanneer bulk polymerisatie gebruikt wordt als synthese techniek om MIPs te maken, verkrijgt men partikels met een onregelmatige vorm, een brede grootte verdeling (0.1 – 50 µm) en een relatief klein detectieoppervlak. Omwille van deze redenen zijn de toepassingsmogelijkheden van bulk MIPs voor commercieel verkrijgbare diagnostische sensoren eerder gelimiteerd. De stempel techniek werd gebruikt om de MIP partikels op het sensor substraat af te zetten. Deze techniek is tijd consumerend en zeer afhankelijk van de kunde van de operator wat leidt tot grote variaties in en tussen verschillende sensor substraten betreffende de hoeveelheid en de verdeling van de MIP partikels. Bijkomend is het mogelijk dat de polymere lijmlaag die gebruikt werd om de MIP partikels te immobiliseren, verschillende imprints fysiek zal blokkeren en los kan komen tijdens de sensor meting. Dit kan leiden tot een verlaagde sensor gevoeligheid en onvoorziene foutieve detectie van het doelmolecule en limiteert de mogelijkheden voor herbruikbare sensoren. In deze thesis, focust elk hoofdstuk zich op verschillende efficiënte en eenvoudige strategieën om de voorgenoemde problemen te omzeilen. Aangezien het zeer interessant is om een goedkope, hoog performante, reproduceerbare en herbruikbare sensor te ontwikkelen voor de detectie van (bio-) moleculen in biologische stalen in fysiologische concentraties, werd elk hoofdstuk in deze thesis gewijd aan het realiseren van één of meerdere van deze eigenschappen.

De belangrijkste resultaten en toekomst perspectieven in dit werk werden hieronder volgens hoofdstuk samengevat.

Tijdens het eerste deel van mijn doctoraat (hoofdstuk 2), werd de focus gelegd op het ontwikkelen van MIP partikels met een verbeterde herkenning van het doelmolecule doordat ze aan de ene kant homogeen waren in grootte, vorm en materiaal verdeling en aan de andere kant een verhoogd detectie oppervlak vertoonden door hun kleine sub-micron diameter. Om dit doel te bereiken, werden er twee strategieën gecombineerd. De eerste strategie was de implementatie van de veelzijdige miniemulsie techniek om colloïde MIP partikels in de vorm van water gebaseerde dispersies te maken. De bekomen colloïde MIP partikels vertoonden een kleinere diameter (± 500 nm), een sferische vorm en een relatief kleine

grootte verdeling. Vervolgens, om nog een stap verder te gaan en ook controle te krijgen over de homogeniteit van de materiaalverdeling binnenin de MIP partikels, werd een tweede strategie gebruikt. Doorgaans worden MIPs verkregen door het combineren van een crosslinkend monomeer (± 80 – 90 %) met een functioneel monomeer (± 10 – 20 %) dat groepen bevat die kunnen interageren met de doelmoleculen. Om een homogene verdeling van het crosslinkend en functioneel monomeer te verzekeren in het polymeer netwerk, moeten deze twee structureel gelijkend zijn. Daarom moet men een geschikt functioneel monomeer kiezen afhankelijk van het doelmolecule en de crosslinker. Daarenboven hangt de kwaliteit van de MIP ook nog eens af van de onderlinge concentratie ratio's van de individuele componenten. Als alternatief, werd er in deze thesis een al eerder ontwikkeld bifunctioneel crosslinked monomeer: N,O-bismethacryloyl ethanolamine (NOBE) gebruikt. Met dit concept werd er een eenvoudigere route ontwikkeld om colloïde MIP partikels te maken waarbij de nood aan bijkomstige functionele monomeren en de optimalisatie van de relatieve ratio's van functionele en crosslinkende monomeren en doelmoleculen omzeild werd.

NOBE bulk en miniemulsie MIPs geïmprint met testosteron werden succesvol gesynthetiseerd. Om te bewijzen dat de colloïde MIPs wel degelijk superieur zijn aan de conventionele bulk MIPs, werd er een vergelijkende studie uitgevoerd. Dit was mogelijk doordat zowel de bulk als de miniemulsie NOBE MIPs met dezelfde relatieve ratio's van doelmolecule, monomeer, initiator en porogeen samengesteld werden. De moleculaire herkenningscapaciteit van de twee verschillende soorten MIPs werd bestudeerd aan de hand van evenwicht bindingsanalyses in een waterige oplossing. Eerst, werden de bindingseigenschappen van de bulk MIP en NIP partikels getest bij verschillende pH waarden. Na het selecteren van de meest optimale pH, werden de evenwicht bindingsanalyse studies ook uitgevoerd met het miniemulsie MIP-NIP duo. Deze experimenten gaven aan dat de colloïde NIPs significant minder aspecifieke binding vertoonden in vergelijking met de bulk NIPs. De colloïde MIPs vertonen significant meer voordelen die ze te danken hadden aan hun kleine omvang, homogeniteit en vergroot oppervlak wat resulteert in toegenomen imprintfactoren (6.8 vs 2.2) en een verbeterde selectiviteit in vergelijking met bulk MIPs. Ten slotte, werden zowel de bulk als de miniemulsie partikels getest op hun selectiviteit met verschillende moleculen die structureel gelijken op het doelmolecule testosteron, namelijk methyl testosteron, β-estradiol

en estriol. Deze experimenten toonden aan dat de herkenning van de structurele analoge moleculen sterk afhankelijk is van de mate waarop ze gelijken op het doelmolecule. In het kort, in dit hoofdstuk werden voor de eerste keer colloïde MIPs, die testosteron en zijn structureel gelijkende moleculen herkennen, ontwikkeld via een vereenvoudigd synthese protocol dat gebaseerd is op een bifunctioneel monomeer in een waterige oplossing. In de toekomst kan het miniemulsie MIP synthese recept afgesteld worden om partikels met een nog lagere polydispersiteit te verkrijgen. Om dit te bereiken kan er een co-stabilisator toegevoegd worden aan het systeem. Er moet echter wel rekening gehouden worden met de mogelijkheid dat deze laatste component de binding tussen het monomeer en het doelmolecule zou kunnen beïnvloeden. 2-methyl-*N*-(3-methyl-2-oxobut-3-enyl)acrylamide (NAG) is een ander bifunctioneel monomeer dat getest zou kunnen worden om nog beter werkende MIPs te verkrijgen. NAG zou de resolutie van de afdruk van het doelmolecule kunnen verbeteren aangezien deze crosslinker korter is in vergelijking met NOBE. Andere monomeren die verschillende functionaliteiten bevatten kunnen gebruikt worden om doelmoleculen met complementaire functionele groepen te imprinten. Wanneer de niet-covalente imprint methode wordt toegepast, kan men niet enkel gebruik maken van waterstofbindingen tussen het functioneel monomeer en het doelmolecule, maar ook van electrostatische, hydrofobe, etc. interacties.

Na het verkrijgen van deze superieure miniemulsie MIPs, ging onze focus naar hun integratie in een sensor toepassing (hoofdstuk 3). Er zijn twee veelgebruikte manieren om MIPs op een sensor substraat te immobiliseren. De eerste manier maakt gebruik van een polymere adhesielaag (zoals een lijm) en de tweede manier is via chemische koppeling. Aangezien een adhesie polymeer een deel van de MIP imprints blokkeert (wat leidt tot een afgenomen sensor sensitiviteit) en zou kunnen los komen tijdens de meting (wat leidt tot een foutieve doelmolecule kwantificatie), ging in dit werk de voorkeur naar een directe chemische koppeling op het sensor oppervlak. Een gedopeerd silicium substraat bedekt met een gedopeerd nanokristallijn diamant laagje werd gefunctionaliseerd met amorfe koolstoflaag via evaporatie. Vervolgens werden de miniemulsie partikels aan de hand van hun vinyl oppervlakte groepen covalent gekoppeld aan de koolsoflaag door middel van UV licht. Door deze directe koppeling worden er geen imprints geblokkeerd en worden de preparatie stappen gereduceerd terwijl er toch nog

steeds een sterke en betrouwbare binding verkregen wordt. In vergelijking met het gebruik van linker moleculen zoals silanen om de MIP partikels te immobiliseren, laat de directe koppeling een veel kortere afstand tussen het substraat en de receptor toe wat cruciaal is voor oppervlakte gevoelige detectietechnieken. Na het verwijderen van de niet gebonden MIP partikels, tonen de rasterelektronenmicroscoop (SEM) afbeeldingen dat de MIP partikels uniform verdeeld zijn over het sensor oppervlak. Om te testen in welke mate de MIP sensor substraten het doelmolecule selectief kunnen detecteren in biologische stalen, werden testosteron en β-estradiol in bepaalde concentraties in zowel buffer als urine stalen opgelost. Elektrochemische impedantie spectroscopie (EIS) werd hier als uitleestechniek gebruikt. Deze sensor metingen toonden aan dat testosteron selectief en in fysiologische nM concentraties gedetecteerd kon worden in zowel buffer als urine stalen. In het kort, de MIP immobilisatie methode die gebruikt werd in dit hoofdstuk is eenvoudig, vereist een minimaal aantal preparatie stappen en omzeilt het gebruik van een polymere adhesielaag. Om het actieve detectie oppervlak van de sensor te vergroten, zullen naar de toekomst toe optimalisaties gedaan worden. Aan de ene kant zullen de MIP partikels kleiner gemaakt worden en aan de andere kant zal de sensor bedekking met MIP deeltjes verbeterd worden. Ook de sensor flow-cell opstelling kan geoptimaliseerd en geminiaturiseerd worden om lagere detectielimieten en snellere responstijden te verkrijgen.

Een andere interessante strategie om een betrouwbare hoog performante sensor te verkrijgen, is de in situ polymerisatie en hechting van gepatroneerde MIP structuren met specifieke geometrieën direct op het sensor substraat via microfluidische systemen (hoofdstuk 4). Een hoofdstructuur die een specifiek patroon bevat om het uiteindelijke detectie oppervlak te maximaliseren, werd gemaakt met behulp van elektronen straal lithografie. Van deze hoofdstructuur werd vervolgens een afdruk, gebaseerd op het elastische polydimethylsiloxaan, gegoten. Deze vorm werd dan geplaatst op een diamant silicium substraat dat gefunctionaliseerd werd met een laagje amorfe koolstof. De structuren werden gevuld met een prepolymerisatie mix bestaande uit testosteron en NOBE (monomeer). Daarna werden de in situ polymerisatie en koppeling aan het substraat gestart door middel van UV-licht. Deze simpele en kosten efficiënte techniek laat aan de ene kant een stevigere immobilisatie en aan de andere kant

een controleerbare, homogene en reproduceerbare receptor materiaal verdeling op de sensor toe. De methode die hier werd gebruikt reduceert het aantal preparatie stappen aangezien verschillende elastische vormen gemaakt kunnen worden van één hoofdstructuur. Dit betekent dat de dure en tijd consumerende elektronen straal lithografie stap maar één keer doorlopen moet worden. Na het verwijderen van de elastische vorm en de sjabloon doelmoleculen, werd de selectieve detectie van de sensor substraten getest in buffer, urine en speeksel waar testosteron, β-estradiol of estriol in opgelost werd. Tijdens deze testen werd EIS als uitleestechniek gebruikt. Er werd een differentiële flow-cell sensor opstelling ontwikkeld waarin zowel de MIP als de NIP substraten tegelijk getest kunnen worden in dezelfde vloeistof omgeving. Met dit concept wordt het effect van de omgevingsfactoren en staal variaties (complexe samenstellingen) op het signaal geëlimineerd. De sensormetingen toonden aan dat de MIP structuren inderdaad testosteron konden binden op een selectieve manier zowel in buffer als in biologische stalen. Zelfs het staal dat de laagste concentratie testosteron bevatte (0.5 nM), zorgde voor een meetbare stijging in het sensor signaal. Hoewel de sensor respons gemeten in de urine stalen vergelijkbaar is met de respons gemeten in buffer stalen, zorgden de speeksel stalen voor een verlaagd, maar toch nog significant signaal. Dit kan te wijten zijn aan het feit dat speeksel veel meer eiwitten en andere moleculen bevat in vergelijking met urine. Deze eiwitten kunnen een aanzienlijke hoeveelheid imprints blokkeren wat resulteert in een afgenomen sensor gevoeligheid. Na de sensor metingen waarin de MIP structuren onderhevig gesteld werden aan een dynamische vloeistof omgeving, werd aan de hand van optische microscopie vastgesteld dat de structuren nog steeds intact waren. Doordat de MIP een groot oppervlak heeft en stevig gebonden is aan het substraat, wordt regeneratie van de sensor mogelijk aan de hand van een aantal wasstappen. Vervolgens werd er een tweede sensormeting uitgevoerd die wederom een concentratie afhankelijke signaal stijging aangaf bij het toevoegen van testosteron. In het kort, een kostenefficiënte en eenvoudige techniek voor het ontwikkelen van gevoelige, hoog performante, reproduceerbare en gestructureerde MIP sensoren voor het elektronisch detecteren van (bio-) moleculen werd in dit werk voorgesteld. Deze techniek biedt genoeg flexibiliteit om de geometrieën van de MIPs aan te passen door het ontwikkelen van een gepaste hoofdstructuur. Als een volgende stap, om nog lagere doelmolecule

concentraties (pM) te kunnen detecteren, kan langs de ene kant de meetopstelling aangepast en geminiaturiseerd worden en langs de andere kant een groter actief detectie oppervlak ontwikkeld worden. Een groter actief detectie oppervlak zal ook kortere sensor regeneratietijden toelaten. Additioneel kunnen MIP structuren die geïmprint zijn met verschillende doelmoleculen langs elkaar op één sensor substraat geïmmobiliseerd worden. Dit concept laat toe om verschillende doelmoleculen in een staal gelijktijdig te detecteren in één sensormeting.

In hoofdstuk 5, werd er een nieuwe MIP afzettechniek in combinatie met een goedkoper MIP immobilisatie adhesie materiaal verkend met het oog op kostenefficiënte en schaalbare sensoren. Bulk MIP partikels (0.1 – 10 µm) die geïmprint zijn met serotonine, werden succesvol getest op hun vermogen om het doelmolecule te binden via evenwicht bindingsanalyses. Vervolgens werden de MIP partikels geïmmobiliseerd op een vlakke aluminium electrode via een adhesielaag. Hiervoor werd het duur geconjugeerd polymeer namelijk poly[2-methoxy-5-(3',7'-dimethoxyoctyloxy)-1,4-phenylenevinylene] (MDMO-PPV) die in de voorgaande sensoren gebruikt werd vervangen door het goedkoper en meer toegankelijk polymeer polyvinylchloride (PVC). Een PVC oplossing werd bovenop het aluminium substraat gespincoat zodat er een laag van 180 nm bekomen werd. Ook de stempel techniek die in de voorgaande sensoren gebruikt werd om de MIP partikels af te zetten, werd vervangen door de spraycoat techniek. Dit werd gedaan omdat het resultaat van het stempelen zeer afhankelijk is van de kunde van de operator terwijl het spraycoaten reproduceerbaar is, geautomatiseerd kan worden en kan gebruikt worden bij sensor fabricatie op grote schaal. Na het afzetten van de MIP en NIP partikels, werden de substraten verwarmd tot net boven de glas transitie temperatuur van PVC. Op deze manier werd de adhesielaag zacht en konden de partikels er deels in zinken waardoor ze vast kwamen te zitten. Om de twee verschillende MIP afzettechnieken te vergelijken op vlak van oppervlakte bedekking, werden zowel de gestempelde als de gespraycoatte sensorsubstraten vergeleken op basis van optische microscopie en rasterelektronenmicroscopie. Met spraycoaten kan men grote hoeveelheden MIP partikels op het substraat afzetten door het aantal spraycoat passages aan te passen. Langs de ene kant bevatten de gespraycoate substraten een hogere hoeveelheid en een homogenere verdeling van het MIP materiaal op het oppervlak

in vergelijking met de gestempelde substraten. Langs de andere kant werden bij het stempelen de polymeer partikels mechanisch op het sensor substraat geduwd waardoor ze dieper in de PVC laag kwamen te zitten. Dit effect werd bevestigd aan de hand van rasterelektronenmicroscoop beelden van de doorsnede van het substraat. Voor de gespraycoate stalen toonden deze beelden echter aan dat de MIP partikels nauwelijks in de PVC laag verzonken waren. Om de sensor perfomantie te testen, werd de kostenefficiënte en eenvoudige heat transfer methode (HTM) gebruikt als uitleestechniek. De HTM omzeilt de nood aan een gesofisticeerde opstelling aangezien het maar twee thermokoppels, een PID (proportioneel, integrerend en differentiërend) regelaar en een aanpasbare warmte bron vereist. Deze experimenten toonden aan dat de sensorrespons voor beide afzettechnieken in dezelfde range lag. Echter, de gestempelde sensor gaf 10 % meer respons en minder saturatie bij een doelmolecule concentratie van 500 nM in vergelijking met de gespraycoate sensor. Dit resultaat bewijst dat de performantie van de sensor meer beïnvloed werd door de manier waarop de MIP partikels ingebed zaten in de adhesielaag en dus ook hoe kort ze tegen het aluminium substraat aan zaten in vergelijking met de hoeveelheid MIP partikels die op het substraat zaten. Hoewel de gespraycoate sensor performantie nog niet optimaal is, heeft deze afzettechniek duidelijke voordelen inzake automatisatie en schaalbaarheid. De combinatie van het goedkope PVC, de schaalbare en reproduceerbare afzettechniek en de miniaturiseerbare uitleesmethode, laat de ontwikkeling van een kosten efficiënte sensor toe om (bio-) moleculen met een laag moleculair gewicht te detecteren. Als een volgende stap, kunnen de spraycoat condities (zoals bijvoorbeeld de hoeveelheid MIP partikels per substraat) en de dikte van de PVC laag geoptimaliseerd worden met het oog op het bekomen van een grotere sensor respons. Om een beter contact te krijgen tussen de gespraycoate MIP partikels en het sensor substraat, kan men bijvoorbeeld de gesprayde partikels nog eens mechanisch in de PVC laag duwen zodat ze dieper komen te zitten. Lagere detectielimieten en snellere responstijden kunnen verkregen worden door optimalisatie en miniaturisatie van de HTM sensor opstelling. Omdat men met spraycoaten ook een hogere resolutie kan bekomen in vergelijking met stempelen, kunnen ook verschillende MIP structuren die elk een ander doelmolecule binden, afgezet worden op hetzelfde substraat. Dit is

vooral interessant voor het detecteren van meerdere doelmoleculen tegelijkertijd in een volledige staalanalyse.
In dit doctoraat lag de focus op het testen van verschillende manieren om hoog performante MIP gebaseerde sensoren te ontwikkelen die betrouwbaar en goedkoop zijn. De resultaten tonen duidelijk aan dat mits een aantal optimalisatie stappen, deze sensoren het potentieel hebben commercieel gebruikt te worden in de nabije toekomst.

List of publications

E. Kellens, H. Bové, M. Conradi, L. D'Olieslaeger, P. Wagner, K. Landfester, T. Junkers and A. Ethirajan. Improved molecular imprinting based on colloidal particles made from miniemulsion: a case study on testosterone and its structural analogues. Macromolecules, **2016**, 49 (7), 2559–2567.

E. Kellens, S. De León, J. Lambrichts, S. Drijkoningen, T. Vandenryt, L. D'Olieslaeger, J. D'Haen, K. Haenen, R. Thoelen, T. Junkers,A. Ethirajan. Molecularly imprinted polymer nanoparticles on a functionalized diamond sensor interface: A simple and robust sensor platform for the electronic detection of testosterone in biological samples. **2017**, manuscript to be submitted.

E. Kellens, H. Bové, T. Vandenryt, J. Dekens, S. Drijkoningen, J. D'Haen, W. De Ceuninck, R. Thoelen, T. Junkers, K. Haenen, A. Ethirajan. A simple and efficient fabrication of reliable and reusable biosensors using patterned molecularly imprinted polymer structures on functionalized diamond substrates for selective detection of target molecules in body fluids. **2017**, manuscript to be submitted.

E. Kellens, M. Achten, T. Vandenryt, J. Stryckers, N. A. Rivas, L. D'Olieslaeger, W. De Ceuninck, F. Renner, T. Junkers, W. Deferme, R. Thoelen, A. Ethirajan. Fabrication of low cost sensors based on molecularly imprinted polymer particles. **2017**, manuscript to be submitted.

P. Cornelis, T. Vandenryt, G. Wackers, E. Kellens, P. Losada-Pérez, R. Thoelen, W. De Ceuninck, K. Eersels, S. Drijkoningen, K. Haenen, M. Peeters, B. van Grinsven. Heat transfer resistance as a tool to quantify hybridization efficiency of DNA on a nanocrystalline diamond surface. Diamond and Related Materials, **2014**, 48, 32-36.

G. Wackers, T. Vandenryt, P. Cornelis, E. Kellens, R. Thoelen, W. De Ceuninck, P. Losada-Pérez, B. van Grinsven, M. Peeters, P. Wagner. Array Formatting of the Heat-Transfer Method (HTM) for the Detection of Small Organic Molecules by Molecularly Imprinted Polymers. **2014**, 14 (6), 11016-11030.

Conference contributions

E. Kellens, P. Wagner and A. Ethirajan. Polymer nanoparticles for molecular recognition in biomedical applications and for studying nanoparticle cell interactions. July **2012**, International Life Siences Master Student Research Conference, Hasselt, Poster presentation and prize.

E. Kellens, H. Bové, M. Conradi, L. D'Olieslaeger, T. Junkers, A. Ethirajan, P. Wagner. Molecularly imprinted nano and micro particles for the detection of testosterone. May **2013**, BPS, Luik, Poster presentation.

E. Kellens, H. Bové, M. Conradi, T. Junkers, P. Wagner, A. Ethirajan. Molecularly imprinted nanoparticles for the detection of hormone disruptors. June **2013**, Biomedica, Aachen, Poster presentation.

E. Kellens, H. Bové, M. Conradi, T. Junkers, P. Wagner, A. Ethirajan. Molecularly imprinted nanoparticles for the detection of hormone disruptors. July **2013**, ENFI, Hasselt, Poster presentation and oral.

E. Kellens, H. Bové, M. Conradi, T. Junkers, P. Wagner, A. Ethirajan. Molecularly imprinted nanoparticles for the detection of hormone disruptors. August **2013**, Graduate student symposium on Molecular imprinting in Belfast, United Kingdom. Poster presentation and poster prize.

E. Kellens, H. Bové, M. Conradi, T. Junkers, P. Wagner, A. Ethirajan. Micro and nano sized molecularly imprinted polymers as a synthetic receptor for the detection of hormone disruptors. July **2014**, ENFI, Julich, Poster presentation and oral.

E. Kellens, H. Bové, M. Conradi, T. Junkers, P. Wagner, A. Ethirajan. Molecularly imprinted nano and micro particles for the detection of testosterone. June **2014**, Biomedica, Maastricht, Poster presentation.

E. Kellens, H. Bové, M. Conradi, L. D'Olieslaeger, P. Wagner, K. Landfester, T. Junkers, A. Ethirajan. Molecularly imprinted polymer particles targeted for testosterone detection: micro Vs. nano. June **2015**, Biomedica, Genk, Poster presentation.

E. Kellens, H. Bové, M. Conradi, L. D'Olieslaeger, P. Wagner, K. Landfester, T. Junkers, A. Ethirajan. Molecularly imprinted polymer particles targeted for testosterone detection: micro Vs. nano. May **2016**, BPG, Hasselt, Poster presentation.

List of abbreviations

hCG	Human Chorionic Gonadotropin
DNA	Deoxyribonucleic Acid
RNA	Ribonucleic Acid
MOF	Metal Organic Framework
HPLC	Liquid and Gas Chromatography
MIP	Molecularly Imprinted Polymer
NIP	Non-Imprinted Polymer
TRP	Traditional Radical Polymerization
RAFT	Reversible Addition–Fragmentation Chain Transfer
ATRP	Atom Transfer Radical Polymerization
MAA	Methacylic Acid
4-VPY	4-Vinylpyridine
AAM	Acrylamide
DVB	Divinylbenzene
TRIM	Trimethylolpropane Trimethacrylate
EGDMA	Ethylene Glycol Dimethacrylate
NOBE	N,O-Bismethacryloyl Ethanolamine
AIBN	N-N'-Bis Isobutyronitrile
T_g	Glass Transition Temperature
QCM	Quartz Crystal Microbalance
SPR	Surface Plasmon Resonance
CVD	Chemical Vapor Deposition
HTM	Heat Transfer Method
R_{th}	Thermal Resistance
ACN	Acetonitrile
OMNiMIPs	One Monomer MIPs
PBS	Phosphate Buffered Saline
TEA	Triethylamine
CTMA	Cetyltrimethylammonium Chloride
TEM	Transmission Electron Microscope
PDI	Polydispersity Index
C_f	Free Target Molecule Concentration
C_b	Bound Target Molecule Concentration
ME	Miniemulsion

H-bonding	Hydrogen Bonding
NCD	Nano-Crystalline Diamond
EIS	Electrochemical Impedance Spectroscopy
DLS	Dynamic Light Scattering
EtOH	Ethanol
UV	Ultraviolet
VIS	Visible
SEM	Scanning Electron Microscopy
PID	Proportional Integral Derivative
PDMS	Polydimethylsiloxane
MDMO-PPV	Poly[2-methoxy-5-(3',7'-dimethoxyoctyloxy) -1,4-phenylenevinylene]
PVC	Polyvinylchloride
THF	Tetrahydrofuran
AM	Acrylamide
DMSO	Dimethylsulfoxide
FIB	Focused Ion Beam
IF	Imprint Factor

1 General introduction

A living organism consists out of billions of cells. In order for the organism to sustain itself, these cells need to respond to external stimuli, regulate numerous cellular processes and communicate with other cells. In order to do this, the cell makes use of natural receptors (such as antibodies, enzymes, DNA, etc.) which are able to bind their target molecules in a specific and selective way. Since nature has perfectly fine-tuned these receptors in ways researchers in laboratories are not able to, we started integrating these natural receptors as such in sensors to obtain information about our environment. This way of working has resulted in many successful applications (Figure 1.1). The most famous example is the pregnancy test which determines if one is pregnant by measuring the concentration of the urinary β-subunit of hCG (human chorionic gonadotropin). This sensor uses hCG antibodies as sensing elements and a colorization method as read-out. When hCG is present in urine, it will bind to the hCG antibodies which are coupled to a gold nanoparticle. Subsequently, this mixture is flushed over a strip which contains immobilized hCG antibodies. The colloidal hCG –antibody – gold particle – complex will bind to one of the immobilized antibodies and a color change will be visible. Another well-known example is the glucose sensor which is used by patients with diabetes mellitus to monitor the blood glucose level. This was the first biosensor that reached the market in 1962.[1] By applying one drop of blood, the sensor was able to determine the glucose concentration in a few minutes based on an enzymatic reaction. The glucose oxidase enzyme metabolizes glucose into gluconolactone. During this conversion, oxygen is consumed. Using a Clarke electrode, this oxygen decrease (which is proportional to the initial glucose concentration) could be quantified. People who suffer from this disease have a pancreas that does not produce the hormone insulin which removes excess glucose in blood.[2] It is of relevance to frequently monitor the glucose level of such patients on a regular basis since long term hyperglycemia can lead to damage to the kidney, neurons, cardiovascular system, retina, feet and legs.[2] A relatively new example is the Idylla sensor developed by Biocartis which analyzes DNA and RNA to detect cancer genes and infectious diseases based on the real-time polymerase chain reaction in a fully automated way.[3]

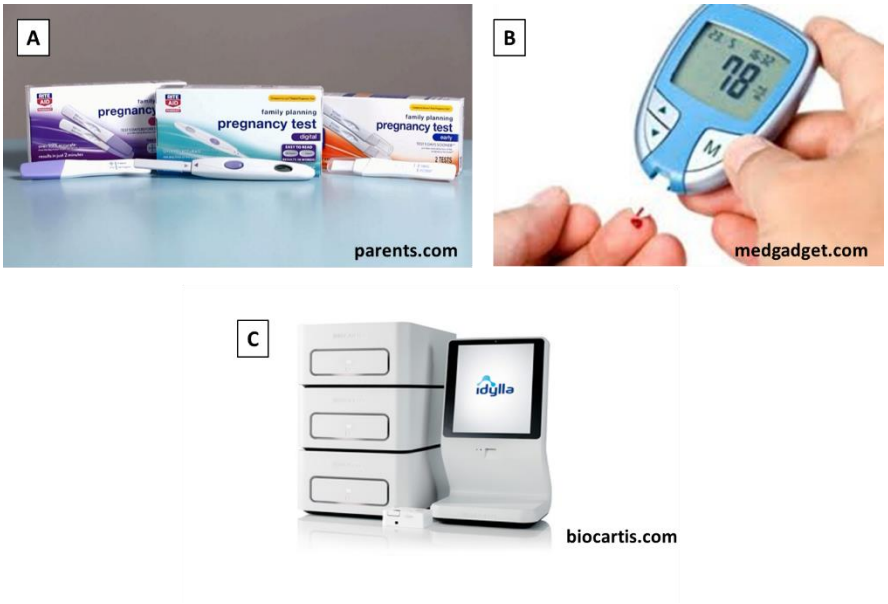

Figure 1.1. Various examples of biosensors that are commercially available: the pregnancy test (A), the glucose sensor (B) and the Idylla DNA and RNA analyzer of Biocartis (C).

Since several years, the curiosity of researchers motivated them to investigate the working principles of the natural receptors and unravel the essential information in order to mimic them. After all, as perfectly engineered as these natural receptors were, many of them were only designed to work at a physiological temperature and pH and therefore they were useless outside of the body. This means that the detection of most target molecules with natural receptors could only be done in specialized labs where specifically educated personnel could mimic the physiological conditions. This is one of the reasons why patient or environmental sample analysis based on biosensors takes so much time and costs so much money. Moreover, natural receptors are not readily available for all target molecules.

Imagine being able to perform drug detection, water pollution tests, full blood and urine analysis, etc. in the same setting as the glucose sensor or pregnancy test: user-friendly, fast, cheap, reliable and outside the laboratory, even at home. This would benefit industries like health care, food quality control, environmental safety, pharmaceutics, etc.

A highly interesting alternative to natural receptors, is to develop synthetic receptors that are robust and low-cost. In that regard, molecularly imprinted polymers (MIPs) [4-6] offer high stability and are a lot easier to handle which makes them ideal candidates to replace natural receptors for a user-friendly sensor that can be taken out of the lab. In addition, MIPs are relatively more easy and cost-efficient to obtain in comparison with their natural counterparts while still offering comparable affinity and specificity for the target molecule. In order to create a reliable and high performing sensor that is consistent in terms of target molecule quantification in various samples, it is of high importance to on the one hand reduce the variation of MIP material (amount and distribution) between different sensors to a minimum and on the other hand to find a way to couple the MIP on the sensor which ensures a stable attachment. Also a suitable read-out technique which is cost-efficient, small, sensitive and reliable should be chosen. Taking these aspects into account, usually an electronic read-out is preferred as it is straightforward, can be integrated in a hand-held device and provides a numeric read-out while no post processing of information is needed.

The focus of this thesis is to realize label-free, reliable, reproducible and reusable MIP based sensors for the detection of proof of concept target molecules testosterone and serotonin. To successfully achieve this goal, techniques such as the miniemulsion and microfluidics were studied as they offer the possibility to synthesize high performance MIPs in well-defined geometries in a highly reproducible way. To fixate the MIPs on the sensor substrate in a stable and reliable fashion, different immobilization techniques were investigated such as direct coupling or through the use of an adhesive layer. To take this one step further, proper coupling allows for regeneration of the substrate after a measurement which opens the possibility for reusable sensors. For MIPs in the form of particles, spray coating was studied as a scalable and controllable deposition technique. As electronic MIP sensor read-out techniques, both electrochemical impedance spectroscopy and the heat transfer method were implemented as they are cost-efficient and miniaturizable while still offering sufficient sensitivity in the relevant target molecule concentration ranges.

In this chapter, MIPs and different aspects of the sensors based on the molecularly imprinted polymer principle will be discussed.

1.1 Bio (chemical-) sensors

1.1.1 Basic components of a biosensor

A sensor is a device, used for the detection and quantification of a specific analyte in an environment.[7] In a typical sensor, receptor elements are immobilized on a suitable platform material (electrode). The binding between the target molecules and the receptors is transduced to a concentration-dependent signal which can be measured by using electronic or optical read-out techniques.[8, 9] When these receptor elements have a biological or synthetic origin, they are classified as bio or biomimetic sensor, respectively. The main components of a sensor are depicted in Figure 1.2.

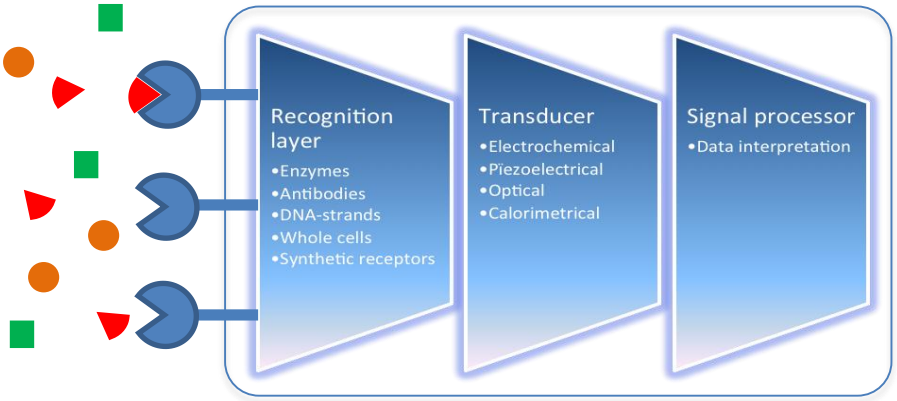

Figure 1.2. Schematic representation of a biosensor.

The choice of receptor and transducer type depend on the specific requirements of the application. For example: a biosensor based on enzymes, such as the glucose sensor, responds in 30 seconds while a biosensor based on antibodies, such as the pregnancy test, needs several minutes. In the next section, these aspects will be explained more in depth.

1.1.2 Recognition layer: natural and synthetic receptor elements

The recognition layer of a sensor consists out of receptor elements which are able to selectively recognize and bind the target molecule. These receptors can be of biological (natural) or synthetic origin. In a biosensor, the highly selective and efficient binding between the natural receptor and target molecule is based on non-covalent interactions such as hydrophobic interaction, hydrogen bonding, electrostatic interaction and van der Waals forces. However, because of the limited physical and chemical stability of these natural receptors and the fact that they are expensive and laborious to obtain, a compelling alternative which overcomes these drawbacks is a synthetic receptor.

Enzymes [10-13], antibodies [14-16], nucleic acids (DNA and RNA)[17-19] or whole cells[20, 21] can be used as natural receptors. A short overview of these receptors is given below:

- Enzymes are the most used biological receptors. As mentioned before, the glucose sensor falls in this category of enzymatic sensors. Enzymes cleave their target molecules into sub-units which are detected. Because one enzyme can decompose multiple targets without being consumed themselves, a sort of signal amplification takes place which permits lower limits of detection. Enzymes can be used in their pure form (extracted) but also in microorganisms or slices of tissue.[22] The advantage of using enzymes in tissue is that their stability is ensured since they are in their natural environment. In addition, the latter is also low cost since the enzymes do not need to be extracted. However, a disadvantage with using tissue is the longer sensor response time due to the physical transport barrier.[23]

- Antibodies are the receptors of the immune system. They are able to recognize and bind a specific pathogen so that it can be destroyed and eliminated from the body.[24, 25] Sensors based on antibody receptors are called immunosensors/assays.

- Sensors based on genetic nucleic acid receptors, are called genosensors. These DNA or RNA receptors are used in a short single strand form which can bind to complementary fragments. The less complementary the fragments, the weaker the bond will be. They are therefore able to detect genetic mutations in DNA or RNA sequences which are related to several genetic disorders, cancer and viral infections.[19]

- When cells are used as receptors in a biosensor, the target molecule is detected by the response of the cells to that molecule. These cell responses can be the release of membrane proteins, metabolism changes (oxygen or glucose consumption), cell adhesion to the sensor surface, etc. These kind of receptors are, amongst others, used to monitor the treatment effect of a certain drugs or to detect global parameters such as stress conditions or cell toxicity.[26, 27]

Examples of synthetic receptors are metal organic frameworks (MOFs), aptamers, dendrimers and MIPs. A short overview of these receptors is given below:

- MOFs are metal coordination complexes containing one or more transition metal cations coordinated in to rigid organic building blocks via self-assembly. The result is an open cage with cavities that are large enough to encapsulate molecular guests. MOFs are porous structures that are often used as synthetic receptors for electron rich molecules such as anionic biomolecules. The drawbacks of these MOFs are the high costs of the inorganic precursors and thermal instability.[28]

- Aptamers are single strand oligomers made from 15 - 50 ribonucleotide building units. This chain can be folded to form a tertiary structure which is able to bind a target molecule. Disadvantages of aptamers are the high production cost, thermal instability and fast degradation by nucleases in biological samples. In addition, generating aptamers is a laborious and time consuming process.[29]

- Dendrimers are monodisperse, symmetrical, branched polymers. As they grow larger, they adopt a spherical shape with a sterically crowded surface and pores which are able to bind a target molecule. However, to make

customized systems to detect a specific target molecule can be complex, time consuming and expensive.[28, 30]

- MIPs are crosslinked polymer materials which contain imprinted cavities that are complementary to the target molecule regarding size, shape and functional group distribution. Therefore, these imprints act as selective molecular recognition sites. MIPs are easy to produce and customize, very stable in many non-physiological environments, low cost and possess a long shelf life.[28] Due to their aforementioned characteristics, MIPs have been opted for SPE, affinity columns, sensors,…[31-33] As this thesis deals with MIP based sensors, a more detailed description about MIPs is provided in section 1.2.

1.1.3 Receptor immobilization on a sensor surface

The immobilization of receptor elements on a sensor transducer substrate can be done in several different ways depending on the type of receptor and sensor application. For example, an expensive immobilization technique would not be feasible to fabricate a disposable sensor while a reusable sensor requires the receptors to be more firmly attached to the substrate. Regardless of these aspects, in every case the immobilization strategy needs to be optimized so that the binding sites of the receptor are accessible for the target molecules. Additionally, to obtain a consistent sensor, it is of high importance that the amount and distribution of receptor material coupled to the sensor substrate is controlled and reproducible. In the following section, a short overview of the different immobilization techniques is given. Figure 1.3 illustrates the different immobilization methods that are used for both natural and synthetic receptors.[34]

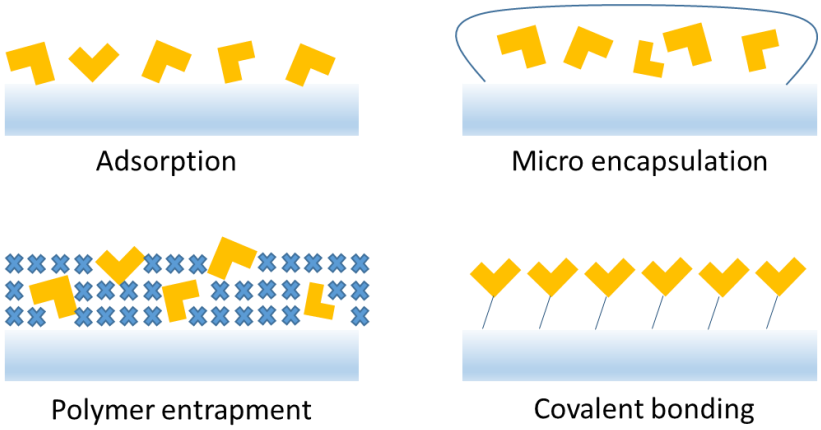

Figure 1.3. Different immobilization techniques.

- Adsorption: This technique is based on non-covalent bonding such as electrostatic interactions, van der Waals forces and hydrophobic effects. This technique is the simplest one since it involves minimal chemical preparation which ensures the conservation of receptor activity. The drawback is that the bonding is weak and will only last for a couple of days. In addition, using this immobilization technique, it is challenging to optimize the orientation of the receptors in such a way that the active site is accessible for the target molecule.

- Micro encapsulation: This method was used in the first enzymatic glucose biosensors. The receptor elements are held close to the transducer substrate by using a membrane which is permeable for the small target molecule and impermeable for the larger receptors. This technique ensures minimal receptor damage and degradation and is mostly used for the immobilization of enzymes.

- Polymer entrapment: In this technique, the receptors are mixed with a monomer solution which serves as a kind of adhesive glue. Subsequently these monomer molecules are polymerized on the transducer substrate, encapsulating the receptors. The drawback of this technique is that many receptor binding sites for the target molecule, will be blocked by the polymer.

- Covalent bonding: Here, the receptor molecules are covalently bound to the transducer substrate. The transducer is usually functionalized with functional groups such as for instance silanes which contain functional groups to which the receptors can be coupled via chemical bonds. This is the most reliable and stable immobilization technique which enhances the lifetime of the sensor but also requires the most optimization depending on the transducer material and receptor type.

1.1.4 The transducer layer and signal read-out techniques

When the target molecule is present in the sample that is being analyzed, it will bind to the receptors of the sensor. Upon this binding, several physical changes occur which are picked up by the transducing element. This element translates these physical changes into a signal that is proportional to the concentration of the analyte being sensed. In short, the transducer translates the binding events into a measurable signal. In Table 1.1, some commonly used sensing techniques are listed. Depending on the type of the transducer, a specific read-out technique can be chosen.

Table 1.1: Different types of sensing techniques.

Measurement technique	**Consequence of binding event**
Potentiometric (electrochemical)	change in charge distribution which causes an electrical potential
Amperometric (electrochemical)	redox reaction which produces electrons
Impedance spectroscopy (electrochemical)[15, 17]	change in the frequency dependent resistance behaviour of the interface and/or transducer
Capacitive	change in capacitive properties (dielectric constant, thickness, etc.)

Magnetic (magnetic beads attached to target)[35]	change in the magnetic field
Optical (i.e. surface plasmon resonance, fluorescence and absorption spectroscopy, etc.)[36-38]	change in the optical properties of the interface and/or transducer
Calorimetric (thermometers)[39]	thermal change
Microgravimetric (quartz crystal microbalance)[40, 41]	small mass change which causes a shift in the crystal oscillation

Depending on the chosen read-out technique, a suitable sensor substrate material should be used. Polymers [42], metals (gold [43] and aluminum [39]), silicon [44], diamond [45], etc. are all possible candidates. For instance, when QCM is used as a read-out technique, it is necessary that the substrate material offers piezoelectric properties. However, when impedimetric or calorimetric read-out techniques are used, the substrates need to be electrically or thermally conductive, respectively. Another important aspect is that the substrate material should not interfere during the measurement. For instance, during impedimetric measurements, bare silicon substrates would grow a silicon oxide layer. This process would cause a drift in the impedance signal due to increasing capacitive effects. Because of these conditions, there is no universal substrate material which is suitable for all purposes.

1.2 Molecularly imprinted polymers

As mentioned in previous sections, a limitation to the concept of biosensors, is imposed by the fact that there are target molecules for which natural receptors either do not exist or exhibit insufficient specificity and physical or chemical stability.[46, 47] For instance, it is difficult to obtain antibodies that bind immune suppressants or toxins because of their adverse effects on the immune response.[48] Natural receptors only operate at body conditions (aqueous media,

temperature and pH), are often difficult and expensive to isolate in sufficient quantities and have a limited shelf life.[34] Also, the binding between an antibody and the target molecule cannot be reversed without damaging the receptor, which makes immunosensors not reusable. Furthermore, the immobilization of antibodies is far from straightforward and their production against small molecules requires chemical coupling to a carrier hapten moiety.[49, 50]

In this regard, the development of so-called 'synthetic' or 'biomimetic' receptors is an intriguing choice. An especially promising approach towards these receptors is based on molecularly imprinted polymer principle.[51-53] MIPs mimic the recognition and binding behavior of natural receptors and are therefore also called 'plastic antibodies'.[54, 55] These synthetic receptors show more stability in many different environments (pH and temperature extremes) [47, 56-58], they are more inert towards acids, bases, metal ions and organic solvents and they have a long shelf life [59]. For the aforementioned reasons, they are far less demanding in terms of operating conditions in comparison with natural receptors. This allows MIP based sensors to be more user friendly and to be used outside of the lab. With MIPs, expensive and time consuming extraction steps which are necessary to obtain natural receptors are avoided. Additionally, these synthetic receptors can be readily generated in large quantities from cheap materials [60], are reusable [61] and can perform in both organic and aqueous solvents.[54, 62]

The first step towards the MIP knowledge we have today, was made by Frank Dickey in 1949, who polymerized sodium silicate in the presence of dye molecules.[63] After removing the dye molecules from the imprints, these silica materials were able to rebind the dye molecules in a selective way. Later, in 1971, Takagishi and Klotz, reported the first imprinted organic polymers after crosslinking linear polyethyleneimine in a dilute solution in the presence of methyl orange as a target molecule.[64] A few years later, the group of Wulff published their results on enantiomeric affinity for the D-form of glycerolic acid.[60, 65] Both Klotz and Wulff established a covalent bond between the polymer and the target molecule, however, the most common approach today is to use non-covalent linkage. This latter principle was introduced by the group of Mosbach in 1981.[66] Today, the molecular imprinting principle is a versatile and promising technique which is able to detect various chemicals as well as biological molecules including

metal ions [67], amino acids and proteins [68, 69], nucleotide derivatives [70], pollutants [71, 72] and food and drugs [73-78]. A more detailed description about possible target molecules is given in section 1.2.4.

In the following paragraphs the MIP applications, working principle, synthesis techniques, target molecules and deposition and immobilization methods for use in sensor platform will be discussed in more detail.

1.2.1 MIP applications

The ability of MIPs to be tailor-made for a spectrum of target molecules and in terms of geometries, offers a very wide range of applications. Below, a few examples are given.

MIP particles can be packed in columns as a chromatography stationary phase [79, 80] for the separation of target molecules in environmental [81] or food analysis [82, 83]. Also in the pharmaceutical industry, this application is very interesting since often only one optical isomer of a specific drug offers therapeutic properties. The first studies in this field were performed by the group of Mosbach. They realized a MIP which was used as a stationary phase in liquid chromatography to separate amino acid derivatives.[84] The main challenge with MIPs in chromatography columns, is the peak broadening and tailing. This effect is due to the heterogeneity of the binding sites in the polymer [85] and could be reduced by obtaining a higher degree of homogeneity between the MIP particles regarding size, shape and functional group distribution.

Another application for MIPs is drug delivery.[86-89] MIPs are able to carry a high load while ensuring a prolonged release time of the bound molecules which is a critical factor in dosage forms.[90] Water compatible molecular imprinting is still under development due to the weak hydrogen bonding and electrostatic interactions in aqueous media. Typically, this decreases the selectivity of the MIP for the target molecules.

Also the catalytic applications of MIPs have been investigated because of their high selectivity and stability even at elevated temperatures and pressures and in the presence of organic solvents, acids and bases.[91, 92] Catalytic functionalities

are introduced in the correct positions of the imprints in the polymer.[93, 94] Generally, biological antibodies or enzymes which are more fragile are used for these kinds of applications.

1.2.2 General working principle of MIPs

MIPs are obtained when the target/template molecule is present during polymerization, where the functional groups of the monomer are arranged around the template molecule. After polymerization, a highly cross-linked matrix is formed and the subsequent removal of the template leaves nano cavities that are complementary to the target molecule regarding size, shape and geometrical functional group arrangement. Therefore these cavities are capable of rebinding the target molecule with high specificity. A scheme illustrating the MIP concept is presented in Figure 1.4. As a negative control, a non-imprinted polymer (NIP) is also synthesized, following the same procedure but in the absence of the template molecule. Therefore the NIP will not possess any imprints and will not bind the target molecule in a specific way.

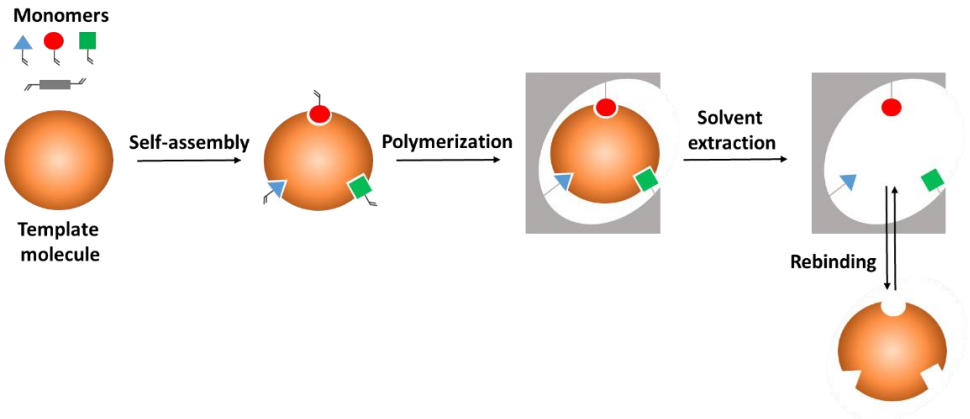

Figure 1.4. The molecular imprinting principle.

The functional monomers of the prepolymerization mixture interact with the template molecule through covalent, non-covalent or semi-covalent interactions.

- The covalent method is a preorganized approach in which covalent reversible bonds are established between the functional monomers and

the template molecule. This gives a homogeneous population of binding imprint sites after polymerization, which leads to a relatively high affinity and selectivity between the imprint and the target molecule. The drawback is that in order to remove the template from the polymer imprint, the covalent bond needs to be cleaved using chemical steps while still keeping the polymer structure intact. As a result, this method is limited to only a number of compound classes. Upon rebinding of the target, the covalent bonds are reformed.[95, 96]

- The non-covalent method is a self-assembling approach which is similar to the biological recognition systems.[66] In this approach, relatively weak non-covalent intermolecular interactions such as hydrogen bonding, π-π interactions, electrostatic and hydrophobic interactions are formed between the monomers and the template molecule leading to more heterogeneous imprint sites and therefore non selective target molecule rebinding as compared to the covalent method. This means that there is a range of different binding affinities towards the target molecule ranging from strong to very weak.[97-99] In Figure 1.5 some of these effects are visualized. Binding spot A is the most specific with the maximum number of hydrogen bonds between the polymer and the target molecule. Binding site B is also very specific but it is not physically accessible for the target molecule. Site C will be less specific since it can only bind with the target molecule using two or three hydrogen bonds. The careful selection of functional monomers (acidic, basic, neutral, hydrophilic and hydrophobic), which interact strongly with the template, is crucial to obtain a MIP with high affinity binding sites.[100, 101] Despite the fact that the covalent method generates MIPs that are more specific and selective towards the target molecule [102], the non-covalent approach is generally preferred due to simplicity of complex formation and dissociation and the flexibility with respect to the broad range of available functional monomers that can interact with many kinds of template molecules. Therefore, in this work only non-covalent binding was studied.

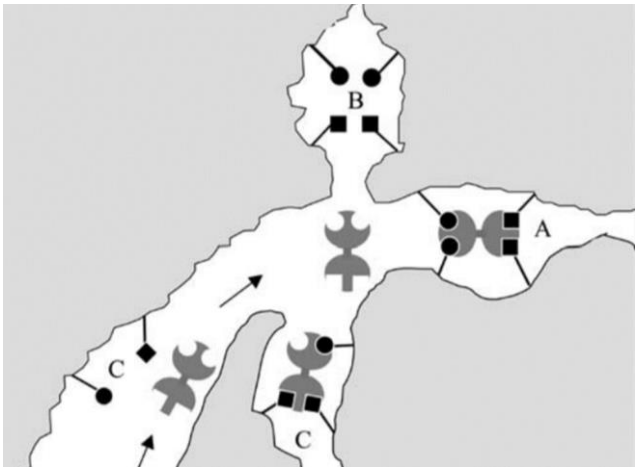

Figure 1.5. Schematic representation of the different binding sites present in imprinted polymers: high affinity sites associated with macropores (easy accessibility, fast mass transfer, A), high affinity sites associated with micropores (difficult accessibility, slow mass transfer, B) and binding sites with different stoichiometry and affinity (C).[103]

- In the semi-covalent approach, the template is covalently bound to the functional monomer (just like in the covalent approach), while the rebinding between the target molecule and the MIP is based on non-covalent bonds. The fact that there is a covalent binding during polymerization, can in principle result in imprint sites with a higher binding affinity in comparison with the non-covalent approach.[97, 104] However, the removal of template molecules from the imprints using chemical cleaving steps remains an issue.

Subsequently to the polymerization reaction, the template molecules should be extracted from the polymer imprints. This is done by performing a sequence of washing steps which are repeated until no template molecule is detected in the solvent waste anymore. It is important to keep the polymer exposure time to the washing solvents as short as possible as the polymer (prone to degradation) might start to degrade upon contact for a long period depending on the solvent(s) used. The latter can cause polymer swelling and the imprint cavities will no longer be functional as they lose their shape.

When the template molecules are removed from the imprint cavities, the simplest way to test the capability of the MIP to rebind a target molecule in a specific and

selective way is by using batch rebinding experiments. A certain fixed amount of MIP and NIP is mixed with a solvent containing a known target molecule concentration. After reaching the equilibrium state between bound and free target molecule, the polymer is separated from the solvent and the free target molecule concentration in the supernatants is determined by using for instance UV-VIS spectroscopy. It is expected that, in the supernatants of the MIP, less target molecule will be present since a large portion will be bound to the imprints of the polymer. From the initial and free target molecule concentrations, the concentration that is bound to the polymer can be calculated. A NIP is always needed as a negative control, since the target molecule will also bind aspecifically to the polymer to some extent. This amount of aspecific binding is subtracted from the MIP signal and what remains is only the specific binding of the target molecule. In order to check the selectivity of the MIPs, the same experiment is performed with a molecule that is structurally similar to the target molecule. When the MIP is very selective, it will not bind this structural analogue specifically.

1.2.3 MIP synthesis

1.2.3.1 MIP synthesis using free radical polymerization

MIPs are most commonly synthesized using free radical polymerization of monomers containing vinyl groups.[105] This reaction can be performed in both homogeneous and heterophase systems. This type of polymerization is a method by which a polymer forms by the successive addition of building blocks and it includes three steps:

- **Initiation**: In order to start a polymerization, free radicals need to be present. Radicals are formed when the initiator molecule decomposes upon heating or radiation with UV light. Subsequently, the radicals react with a vinyl group present in the monomers and new radicals are formed.

  In general: $I \rightarrow n\ R\cdot$

  $R\cdot + M \rightarrow M_i\cdot$

  With I = initiator and M = monomer/repeating unit

- **Propagation**: During this step, more monomers are added to the growing polymer chain.

  In general: $M_i\cdot + M \rightarrow M_{i+1}\cdot$

- **Termination:** The addition of monomers containing vinyl groups to the polymer chain can be stopped in various ways:
  - Recombination reactions: $M_n\cdot + M_m\cdot \rightarrow M_{n+m}$
  - Disproportionation reactions: $M_n\cdot + M_m\cdot \rightarrow M_n + M_m$

When no measures are taken to prevent a growing polymer chain from terminating, it is called a traditional radical polymerization. It can be carried out under mild reaction conditions, it is tolerant of protonic impurities like water and it can be used for a broad range of monomers.[106] When a growing polymer chain is controlled (for instance by controlling the termination or by degenerative transfer), it is called controlled/living radical polymerization (referred to as reversible deactivation radical polymerization). Examples of controlled polymerization methods are reversible addition–fragmentation chain transfer (RAFT) [107] and atom transfer radical polymerization (ATRP) [108, 109]. These systems have been used to obtain MIPs, as they ensure a high control with respect to the polymer chains and network structures.[109, 110] With controlled polymerization, the recognition sites are better defined leading to enhanced recognition of the target. This way, MIPs that possess faster binding kinetics and enhanced affinity and selectivity for the target molecule are obtained.[111, 112]

1.2.3.2 Factors influencing MIP characteristics

Numerous parameters such as prepolymerization mixture components (monomer choice, initiator, solvent and their relative ratios) and polymerization conditions (temperature and time) during synthesis, need to be considered as they influence the performance and morphology of the resulting MIP. Many scientists have investigated the influence of the various parameters in MIP synthesis. A full comprehension of these factors is still challenging to achieve. However, some aspects can be highlighted.[113]

For MIP synthesis, usually monomers containing a functional group (~ 10 – 20 %) that can interact with the template molecules are used in combination with a crosslinking monomer (~ 80 - 90 %) which fixates the structure and gives a rigid polymeric material. This crosslinker is often similar to the functional monomers in terms of structure and reactivity. This is necessary in order to obtain a matrix with a homogeneous distribution of functional groups to assure a high imprinting efficiency. Frequently used functional monomers are methacylic acid (MAA), 4-vinylpyridine (4-VPY) and acrylamide (AAM). Also the flexibility of the crosslinker plays a role in the selectivity of the resulting MIP. When the crosslinker monomer is too flexible, the cavities will not be sufficiently stabilized while when the crosslinker is too rigid, the accessibility of the cavities will be decreased significantly. As crosslinking monomer, divinylbenzene (DVB) trimethylolpropane trimethacrylate (TRIM) or ethylene glycol dimethacrylate (EGDMA) are often used as they offer an optimal balance between flexibility and rigidity.[100] Although the concept of MIP synthesis seems fairly straightforward, optimization of MIP formulation components is challenging. One has to choose the appropriate functional monomer with respect to the template/target molecule, together with an appropriate crosslinker. The quality of the final MIP also depends on the concentration ratios of these individual components. Alternatively, high performance MIPs were realized using a single bifunctional monomer (crosslinking and functional).[114-116] Imprinted polymers made with such a single monomer are called OMNiMIPs which stands for One MoNomer Molecularly Imprinted Polymers. With that concept, a simplified route to design MIPs was developed where the need for additional functional monomers and empirical optimization of the relative ratios of functional monomers, crosslinkers, and template in the formulation was eliminated. OMNiMIPs based on N,O-bismethacryloyl ethanolamine (NOBE) have been imprinted with a large variety of target molecules containing free hydroxyl or carboxyl groups and showed enhanced enantioselectivity in comparison with EDGMA-co-MAA MIPs except for template compounds with amine functionalities.[117]

Also the solvent type influences the molecular imprinting process. On the one hand, the solvent brings all components (initiator, monomers and template) into one phase to form the pre-polymerization complex and on the other hand it

creates pores in the polymer matrix to increase the accessibility of the imprint sites. A sponge-like structure ensures that not only the surface of the polymer but the whole volume is capable of rebinding the target molecule. Also, during polymerization, the porogen distributes the heat of the reaction to prevent side-reactions due to local heating. The best solvents for establishing non-covalent interactions, are the less polar ones. Most often, solvents such as toluene, chloroform, dichloromethane or acetonitrile are used. More polar solvents dissociate the hydrogen bonds leading to inefficient MIP imprints which limits their applicability. After polymerization, the rebinding performance is most optimal when carried out in the same solvent that was used for imprinting.[118-121] Therefore, interest rises in molecular imprinting in aqueous media for applications such as food and water analysis and drug delivery.

Generally, the preferred method to obtain MIPs is free radical polymerization since it is performed under mild reaction conditions such as ambient pressures and temperatures under 80 °C for thermally induced polymerization and at room temperature for light induced polymerization. This polymerization method is generally very fast and N-N'-bis isobutyronitrile (AIBN) is often the initiator of choice as it can be decomposed both thermally and photochemically. Photo-initiated polymerization at low temperatures decreases the kinetic energy of the prepolymerization complexes. This leads to stronger interactions between the functional monomer and the template molecule which results in a MIP with an increased binding capacity and specificity.[73, 119, 122]

Prolonged polymerization time results in a lower amount of unpolymerized vinyl groups and therefore an increased level of crosslinking, which makes the polymer more rigid. Therefore, the imprint cavities will be much more defined in shape which results in more selective MIPs.[123, 124] As a downside, polymers that are too rigid, display slow binding kinetics due to slow target molecule diffusion. A certain balance between the flexibility and rigidity of the polymer should be found but this aspect remains poorly understood.

The MIP network formed by using increased amounts of initiator also has a higher degree of crosslinking which leads to more MIP selectivity. On the other side, when an increased amount of initiator is used, the peak temperature during

polymerization will increase as more bonds are formed at the same time. Mijangos et.al. studied the influence of the amount of initiator on the recognition capacity of the MIPs.[124] Although the MIPs obtained using high amounts of initiator were more rigid, they were less selective in comparison with the less rigid MIPs prepared with less initiator. Apparently, the most important factor that determines the rebinding capacity of the MIPs is the reaction temperature that is reached during polymerization. The more initiator is used, the higher the developed reaction temperature during polymerization. Therefore the kinetic energy will be higher and the non-covalent bonds between the functional monomer and the template molecule will be less stable. This leads to a less selective MIP even when it has a more rigid structure.

1.2.3.3 Different MIP synthesis techniques

Depending on the application, MIPs require a different morphology to assure optimal performance. There are many different techniques to obtain different structural MIP geometries. In this section, an overview of methods using homogeneous and heterophase systems for MIP synthesis will be given.

1.2.3.3.1 Homogeneous systems

Bulk polymerization is the most common and straightforward MIP synthesis method. All components of the prepolymerization mixture (monomers, initiator and template molecule) are dissolved in a solvent/porogen. After polymerization, a polymer monolith is obtained. If a smaller size of MIP particles is desired, the monolith has to be crushed. As a result, these particles will have a broad size, shape and material distribution which limits their reproducibility and therefore also their applicability in sensor applications.[125] In Figure 1.6 an optical microscope image of bulk MIP particles is shown. If a particle size range within certain limits is desired, the material also needs to be sieved which leads to huge material losses. In addition, the complete extraction of the imprinted target molecules (especially larger molecules) is difficult, as some of the molecules stay trapped inside the network. This is very detrimental not only when expensive template molecules are employed but also during application in biosensors for detection of diseases where any uncontrolled release of target molecule can lead to false diagnosis. Although this production technique of MIPs has serious drawbacks with

respect to efficiency and control over synthesis parameters, it is widely used in separation columns due to the simplicity of the preparation.

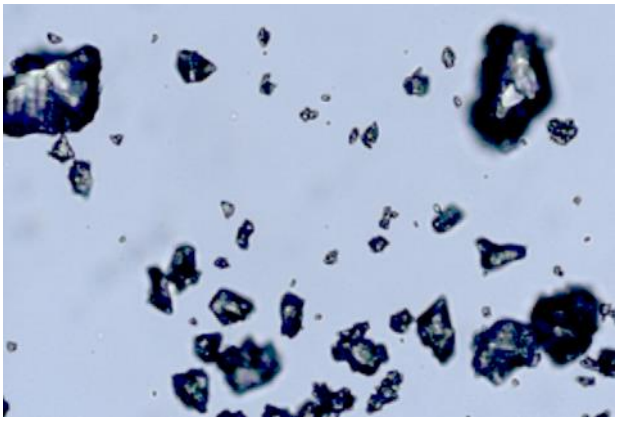

Figure 1.6. Light microscopy image of crushed MIP particles obtained by bulk polymerization

1.2.3.3.2 Heterophase systems

A heterogeneous system comprises of distinct immiscible compounds which are separated by boundaries. In a heterogeneous system that consists of two phases, one will be the dispersion medium or the continuous phase and the other compound will be the dispersed phase. In an emulsion, the two phases are both liquid while in a dispersion, solid particles are dispersed in a liquid. When solid particles or liquid droplets are mixed with a gas, it is called smoke or mist respectively. Examples from our everyday life are milk (which is an emulsion of fat droplets in water), fog (which is a mist of water droplets in air), paints (dispersion of solid particles in a solvent), etc.

When an emulsion in which the dispersed phase consists out of monomer and initiator molecules is subjected to heat or UV, a polymerization reaction takes place resulting in a polymer dispersion. In these kind of systems, a stabilizer to keep the droplets dispersed in the continuous phase is of critical importance. Surfactant (which is short for surface-active agent) is a substance that when present in low concentrations in a system, can absorb to the interfaces of the system and has the ability to alter the interfacial free energy.[126]

Two types of emulsions can be distinguished depending on the continuous phase being aqueous or an organic solvent, namely direct and inverse emulsions. In a direct emulsion, a lipophilic phase is dispersed in a hydrophilic continuous phase (oil/water emulsion). In an indirect or inverse emulsion, a hydrophilic phase is dispersed in a hydrophobic organic solvent as continuous phase (water/oil emulsion).

Emulsion polymerization can be classified further in to macroemulsion, miniemulsion and microemulsion based on their stability and formation mechanisms.

Macroemulsions are kinetically stabilized and contain large monomer droplets in the size range of 1 – 10 µm which are optionally stabilized with surfactants. A macroemulsion is an unstable system which returns rapidly to its two phase state when the mixing is stopped. During polymerization, the radical ends of the slightly water soluble monomer, which are formed by the water soluble initiator, are absorbed by the micelles. Inside these micelles the polymer particle grows by further diffusion of monomer from the large droplets to the micelles. The resulting particles are around 100 nm in size. After polymerization, the size of the polymer particles does not correspond with the size of the emulsion droplets due to the monomer exchange between the empty and monomer swollen micelles.[127]

Microemulsions are thermodynamically stable and are spontaneously formed with a droplet size range of 10 – 100 nm. This system demands a very high amount of surfactant and therefore the interfacial tension between the different phases is almost zero. Because of the surfactant excess, monomers are allowed to diffuse between empty and monomer containing micelles. This effect leads again to a thermodynamic non-equilibrium state resulting in a broad polymer particle size distribution.[126] Zeng et al. used inverse microemulsion to obtain spherical nano sized MIPs imprinted with a small hydrophillic peptide coupled to fatty acids of different lengths to serve as a surfactant.[54]

In miniemulsions the surfactant concentration is well below the critical micellar concentration (thus the interfacial tension is not zero). The droplet size can be tuned between 50 – 500 nm. A miniemulsion is thus known to be 'critically stable'.[128-130] This means that the droplet surface coverage by surfactants is

incomplete, and as a result of this, no micelle formation in the continuous phase occurs. Therefore, contrary to micro emulsion polymerization, the droplet size before and after the polymerization process in miniemulsions are identical.[129] This aspect makes miniemulsion polymerization highly interesting for a wide range of applications. In this work, the miniemulsion technique was used for MIP synthesis. Hence, in section 1.2.3.3.3, the latter will be further explained.

Another commonly used heterophase polymerization technique is in suspension. Also here, spherical polymer particles are obtained, but in the micron size range.[127, 131, 132] The monomer droplets are mixed in the continuous phase by using mechanical agitation. This method is widely used in the industry for the production of commercial resins and is also applicable in MIP synthesis. The particle size can be tuned by the mixing speed, amount of monomers and surfactant concentration.[133, 134]

Using the precipitation polymerization technique, regular imprinted beads are formed in an excess of solvent (monomer concentration 2% v/v) without any surfactant.[67, 135, 136] Growing polymer chains continue to capture mono- and oligomers from the solution. They will precipitate when their size is big enough to make them insoluble in the reaction medium. This technique is easy, provides good yields (80 – 90 %) and is not time-consuming. The diameter of the beads decrease with increasing solvent volume. However, the requirement of high dilutions has a negative impact on the automatization of this technique. In addition, polymerization in highly diluted conditions, decreases interaction between the template molecule and the monomer leading to less selectivity and sensitivity of the MIPs.

Finally, core-shell emulsion polymerization and grafting are popular techniques to synthesize MIP nanoparticles with complex architectures and controlled sizes.[108, 125, 137] The MIP layer is deposited on a preformed support such as a nanosphere composed of various materials such as silica, polymers or magnetite. This way it is possible to use a core which has specific properties.[138, 139] It can be magnetic [140], fluorescent [141], enhance Raman signal [142], enhance electrical conductivity [143], etc.

1.2.3.3.3 Miniemulsions

In an oil/water miniemulsion, a heterophase system is subjected to high shear forces in order to generate small, homogeneous, and stable droplets of an oil based phase in a continuous aqueous phase containing surfactants (ionic or non-ionic). Stable droplets can be created for instance by using a high power ultrasonifier or a high pressure homogenizer. During the homogenization process, the droplets are deformed and disrupted which increases the specific interfacial area of the emulsion. At the same time, the newly formed interfaces are stabilized by surfactant molecules.[127] Because the droplet surface coverage by surfactants is incomplete, no micelle formation in the continuous phase occurs. The miniemulsion technique relies on the nanoreactor concept, wherein the polymer particles formed are identical to the droplets (1:1 copy) prior to polymerization. The nanoparticle production using the miniemulsion process is shown in Figure 1.7 The size of droplets is tuneable from 50 – 500 nm and is mainly dependent on the type and the amount of the emulsifier used in the particular system.

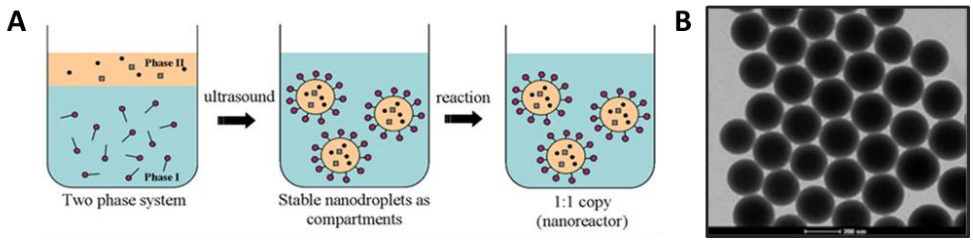

Figure 1.7. Principle of miniemulsion synthesis (A) and a transmission electron micrograph of poly(styrene-co-acrylic acid) polymer particles obtained via miniemulsion polymerization (B)[144].

1.2.3.3.3.1 Stability of miniemulsions

The purpose of the surfactant is to prevent coalescence of the dispersed droplets during collisions. Coalescence is the process in which two dispersed droplets merge. Usually, in addition to the surfactant, a costabilizer is required inside the dispersed droplets for the suppression of Ostwald ripening. This is the process in which inter droplet mass transfer takes place following the Laplace law. The smaller droplets will disappear, increasing the average droplet size.[145, 146] In the case of an oil/water emulsion, the co-stabilizer is an ultra-hydrophobic agent such as hexadecane. This costabilizer is highly insoluble in the continuous phase and is

therefore not able to diffuse from one droplet to another. This assures the emulsion stability by building up an osmotic pressure which counteracts the Laplace pressure.[147, 148]

1.2.3.3.3.2 Miniemulsion based MIPs

The reason why the miniemulsion technique is more interesting for the synthesis of MIPs in comparison with the other aforementioned techniques, lies in the fact that its working principle is based on the concept of a nanoreactor in which each of the droplets can be treated as an individual entity. This means that during the polymerization, no exchange of materials takes place between the droplets. For the miniemulsion colloidal MIP synthesis, a high homogeneity, solid content, and entrapment/encapsulation efficiency of the target molecule is decisive. The continuous phase used is water (in case of an oil soluble target molecule) or an organic solvent (in case of a water soluble target molecule) and the precursor material is a mixture of the monomer, initiator, porogen and the template molecule. Since each droplet acts as independent nanoreactor, high entrapment of template molecules inside the droplets is ensured.[149, 150] The colloidal size and stability of the nano MIPs offers another advantage as compared to bulk MIPs regarding access of the imprints for both target molecule extraction and rebinding.[151, 152] As the colloidal MIPs in this work are produced as water-based stable colloidal dispersions, it is simple to dose them reproducibly and conveniently for the immobilization onto sensor electrodes.[153]

Because of the aforementioned advantages of the miniemulsion technique, also other researchers focus on this method for MIP synthesis.[154-156] Vaihinger et al. successfully created miniemulsion MIPs based on EGDMA and MAA imprinted non-covalently with L- or D-Boc-phenylalanine anilid. Vaihinger synthesized this target molecule starting from L- or D-Boc-phenylalanine. The obtained particles showed enantioselective binding of the target molecules.[157] Later, Pluhar et al. synthesized selective surface imprinted miniemulsion MIPs imprinted with protein pepsin.[158] Curcio et al. synthesized semi-covalent MIP miniemulsion particles imprinted with glucopyranoside.[159] These MIP particles showed good rebinding capacity and selectivity compared to non-covalent imprinted MIPs. However,

complete extraction of the template molecule from the imprint sites was not achieved.

1.2.4 Target molecules

A very attractive feature of MIPs is that they can be imprinted with a broad range of analytes. MIPs are especially interesting for the detection of target molecules with a small size such as steroids [160-163], toxins [76-78], metal ions [67], drugs [164, 165] or amino acids [166] as they can easily move through the porous polymer network. The smaller the target molecule, the more binding imprint sites become accessible for rebinding. But also larger organic structures such as proteins [118, 167, 168], DNA [169], viruses [170, 171] and even cells [172, 173] have been successfully imprinted. Although for these target molecules adapted protocols have been proposed such as surface imprinted polymers, obtaining a MIP for large structures with high affinity capacity remains challenging. In this thesis, the focus was on two small molecules namely serotonin and testosterone.

Serotonin (Figure 1.8) is a biologically relevant metabolite which has a role in smooth muscle contraction [174], emotions, sleep and appetite [175]. An imbalance in serotonin body concentrations can be found in patients with hypertension [176], migraine, fibrotic syndrome, carcinoid tumors [177, 178] and mental disorders like anorexia, depression and schizophrenia.[175, 179] The concentration range of serotonin in the plasma of healthy individuals is 5 – 20 nM.[178, 180] For the detection of serotonin, usually high performance liquid chromatography is used.[181, 182] At the host institute, serotonin has been detected using MIP based sensors.[183, 184]

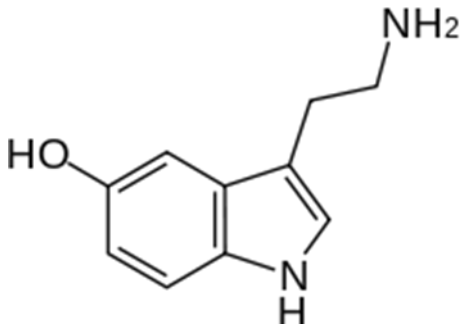

Figure 1.8. Chemical structure of serotonin.

The male sex hormone testosterone is of significant interest due to its role in several pathological conditions depending on its concentration.[185] For instance, increased testosterone levels are associated with a high risk for breast cancer in women [186] and has been related to the cause of prostate and lung cancer in men[187]. However, also low levels of testosterone can have profound effects on a man's health. Signs of a testosterone deficiency are: depression, fatigue, dementia, osteoporosis, heart disease, stroke, abdominal obesity and diabetes type 2.[188-191] Additionally, the quantification of testosterone blood levels is of particular interest in sports as its anabolic effects is associated with performance boosting.[192] Typically, in clinical laboratories, the testosterone analysis in plasma or urine is performed with immunoassays, high performance liquid chromatography or gas chromatography-mass spectrometry.[193] [194] The physiological testosterone concentration in the plasma of an adult male is 8.2 – 57.5 nM but differs with age.[195, 196] Because of the strong correlation between the free testosterone in blood plasma and the testosterone present in saliva and urine, non-invasive testosterone quantification is preferred. The concentration of testosterone in saliva and urine is approximately 0.66 nM and 88 nM respectively in men. In Figure 1.9, the chemical structure of testosterone is shown.

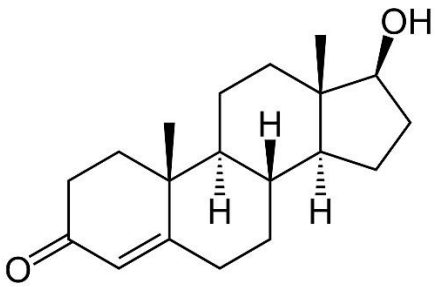

Figure 1.9. Chemical structure of testosterone.

1.2.5 MIPs in sensors

Due to the many advantages MIPs have to offer, scientists have been engaged in the development of imprinted sensors. In 1992, the first attempts to integrate bulk MIPs in sensors were made.[197] Since 2005, more than 1500 papers in which MIP based sensors are the main focus were published (mipdatabase.com) and the interest in this area is still increasing. In the following sections, the integration of MIPs in sensors and the read-out techniques will be discussed more in detail.

1.2.5.1 Deposition and immobilization

In order to guarantee a well performing reliable and reusable sensor, the receptor material needs to be attached to the sensor transducer substrate in a specific way. On the one hand, the receptors need to be deposited in a controllable and reproducible manner. If there is a variation in the material amount and distribution between different sensor substrates, the quantification of the target molecule in a specific sample will not be consistent. On the other hand, the receptors need to be firmly attached to the substrate. In case of insufficient coupling, the receptor will detach during the washing steps or during the measurement, leading to unreliable target molecule quantification results. Furthermore, the accessibility of the imprint sites for the analyte should always be assured.

MIPs can be used in the form of ex-situ prepared particles which are subsequently immobilized on the sensor substrate [183, 198] but also in the form of films or structures which are directly in-situ polymerized and grafted on the sensor substrate [199, 200].

MIPs in the form of ex-situ prepared particles are very interesting for sensor applications due to their high and controllable active sensing surface. These particles are implemented in a biosensor through covalent coupling or through embedding/entrapment using an adhesive polymer layer.[183, 198] In case of entrapment in an adhesive matrix, an additional layer (usually spin coated) on top of the transducer substrate is used.[201] When the substrate is heated above the glass transition temperature (T_g) of the adhesive polymer, the latter softens and the MIP particles can partially sink in. When the substrate is cooled down again, the MIPs are trapped in the adhesive matrix. The range of polymers usable as an adhesive is limited to the ones that contain a lower T_g in comparison with that of MIPs such as PVC or agarose.[39, 202] If the substrate is heated above the T_g of the MIPs, the imprint structure might be affected and the imprint cavities will no longer be functional. Although this entrapment method is very simple and efficient, an aspect that needs to be taken into account is that many imprint cavities get physically blocked by the adhesive polymer leading to a reduced sensor sensitivity. In addition, the MIP particles can loosen up during the measurement which might lead to unforeseen erroneous detection. In case of direct covalent MIP coupling, the transducer substrate is functionalized with certain chemical groups to which the displayed functionalities of the MIP particle can bind.[198] This way, a firm fixation of the MIP particles can be realized and the imprint sites are easily accessible for the target molecules.

Common techniques used to deposit MIP particles include: stamping, screen printing, spin coating and spray coating. Using the simple stamping technique, the MIP particles are pressed onto the substrate using an elastomer stamp. The deposition is therefore determined by the skill of the operator and large batch to batch variations can be observed.[39] Another MIP deposition technique is screen printing which is also simple and easily upscalable.[203] However, a high concentration slurry, special solvents, fillers and binders are needed which might encapsulate the MIP particles and block the imprint cavities leaving them unable to rebind any target molecule. Spin coating can be used as an efficient MIP deposition technique, however, a stable dispersion is required to obtain a homogeneous particle layer.[37] A method to deposit MIP particles in a controllable and reproducible way is spray coating. This technique gives a high surface

coverage, reduces the intra- and inter sample variation and allows a standardized way to create scalable solutions (spraying of large surfaces) for sensor array production with a high spatial resolution (100 µm) using specialized nozzles.

Apart from MIP particle based sensors, the direct in situ coupling of MIP films on the sensor surface has also been an interesting advance in the field. This way, always the same amount and geometries of imprinted polymer are present to act as molecular recognition layer and a superior attachment to the substrate was obtained.[110, 162, 204] However, due to the low sensor sensitivity obtained from a MIP film, patterning was introduced to increase the active MIP sensing interface. In this regard, for quite some time, photolithographic methods have been extensively employed. Later, advanced fabrication techniques have been developed such as scanning-beam, projection, and interference (holography) photography.[199, 205, 206] Also non-optical based approaches have been used including electrodeposition [207], self-assembly [208], and the use of microfluidic molds [209]. However, in this research area, there is still room for optimizations associated with the multi-step and time-consuming procedures and the use of expensive equipment.

1.2.5.2 Overview of MIP sensor read-out techniques

After the fabrication of a sensor substrate that contains immobilized receptors which can selectively bind the target molecule, its sensor performance is studied. The binding between the analyte and the receptor will induce physical or chemical changes which are detected using a specific read-out technique. In the following sections, the most popular read-out techniques are discussed.

A Quartz Crystal Microbalance (QCM) sensor uses two electrodes to apply an oscillating electric field to an AT-cut quartz crystal in which, as a consequence, an acoustic wave is induced. The resonant frequency of the crystal is dependent on its mass. This means that when target molecules bind to the MIPs on the surface of the crystal, this can be observed through the change in frequency. QCM can be used for the detection of molecules in the nanomolar range. By attaching labels to the analytes to increase the mass, a detection limit in the femtomolar range can be reached.[40, 162, 210-212]

A Surface Plasmon Resonance (SPR) sensor uses the change in refractive index at the sensor substrate surface (where the MIPs are immobilized) to detect interactions between molecules. Therefore, they are used to study label-free molecular interactions in the picomolar range. When the molecules are labeled, femtomolar concentrations can also be detected.[211] SPR is a fast and very sensitive technique, but it is also very expensive.[213, 214] Using this read-out technique, as sensor substrate usually metals such as aluminum, silver or gold are used.[38, 215, 216]

Both QCM and SPR are very popular in laboratories. However, the complexity of these set-ups limits their applicability for a low-cost hand held sensor device.

In general, as electronic read-out is the most straightforward one, it is desired and necessary to use techniques that are simple to use, inexpensive, fast, offer miniaturization possibilities, allow a numerical display of the result and require no post-processing of the signal. Therefore, in this work, impedance spectroscopy and the heat transfer method are used as sensor read-out techniques and are discussed more in detail in the following sections.

1.2.5.2.1 Impedance spectroscopy for MIP based sensors

Impedance (Z) is in this case the frequency dependent resistance of an electrochemical circuit. It is measured by applying a small alternating sinusoidal voltage U_0 of a given frequency and amplitude to a system and the response current I_0 is measured. The resulting current through the system is measured as a function of time, and the phase shift θ relative to the input is determined. This procedure is repeated at different frequencies, and the impedance Z is then calculated in accordance to Ohms law as:

$$\boldsymbol{Z} = \frac{\boldsymbol{U_0}}{\boldsymbol{I_0}} \qquad \text{Eq. 1.1}$$

The excitation signal, expressed as a function of time, has the form:

$$U_{(t)} = U_0 e^{i(\omega t)} \quad \text{Eq.1.2}$$

With U_t the potential time at time t, U_0 is the amplitude of the signal, and ω the radial frequency ω=2πf.(θ). In a linear system, the response signal, I_t is shifted in phase (θ) and has a different amplitude, I_0:

$$I_{(t)} = I_0 e^{i(\omega t - \theta)} \quad \text{Eq.1.3}$$

From these expressions the impedance, Z, as function of frequency ω of the system can be calculated. The impedance is thus expressed in terms of Z_0 and a phase shift as mentioned in the following equations:

$$Z = \frac{U_t}{I_t} = Z_0 e^{(-i\theta)} = Z_0(cos\theta + isin\theta) \quad \text{Eq.1.4}$$

The complex resistance includes a real and an imaginary part. Z_0 represents the magnitude of the impedance and the phase shift corresponds to θ. A Nyquist plot is obtained by plotting the real part of the impedance on the X-axis and the imaginary part on the Y-axis. During an experiment such plots typically have a semicircle shape which is shown in Figure 1.10. When the target molecule binds to the MIP, which is immobilized on the substrate surface, this semicircle will change in size depending on the variation in impedance caused by the binding events. Each point on the semicircle thus corresponds to the impedance at a given frequency and is represented by a vector with length Z. The angle between the X-axis and this vector Z represents the phase θ or the argument of Z. Time resolved measurements should be performed, in which Z at a given frequency is plotted as a function of time.[217]

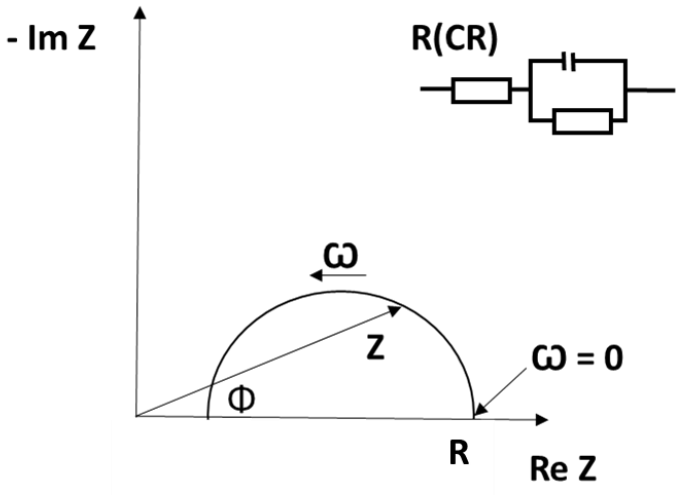

Figure 1.10. Nyquist plot for a typical R (CR) circuit.[218]

When an electrode is submerged in an electrolyte, a double layer capacitance is formed at the interface. When MIPs are immobilized at this electrode interface it will directly influence the equivalent elements representing the interface properties. In the model above a simplified Randles Cell is shown which has a R(CR) construction. The series resistor typically represents the liquid solution while the (CR) component is representing the double layer interface at the electrode and the corresponding charge transfer/polarization/absorption resistance. The binding between the target molecule and the MIP will theoretically influence the (CR) component due to: on the one hand a change in the dielectric properties of the double layer and/or on the other hand the charge transfer resistance changes.[33]

Time resolved impedance spectroscopy will reveal binding events in real time, and could also provide details about the target molecule binding kinetics to the MIPs. The various frequency domains (typically 100 Hz – 1 MHz) will represent the different elements of the equivalent circuit. Typically, the lowest frequencies reveal information about the double layer capacitance, and thus holding information about the binding events, while the higher frequencies show the dominant resistive components of the liquid.

Determination of unknown concentrations will be possible by the construction of a dose response curve for a specific target molecule. In this way, changes at the transducer surface can be detected and binding events can be observed in the pico- or nanomolar range (depending on the observed molecule).[33, 219] At the host institute, Peeters et al. developed bulk MIP based impedimetric sensors for the detection of serotonin and histamine using matrix entrapment.[201, 220] In Figure 1.11, a schematic representation of the custom designed and home built impedance flow cell set-up is shown.

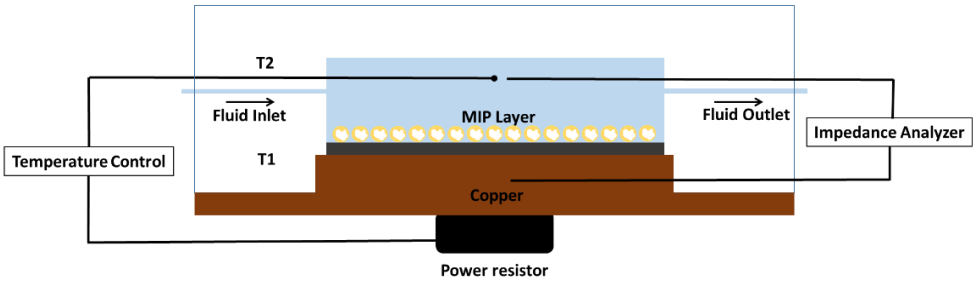

Figure 1.11. Schematic representation of the impedance flow cell for sensor substrate read-out.

Using impedance spectroscopy as a read-out technique, conductive sensor substrates with a diamond interface are especially interesting due to the unique properties of this material namely the large electrochemical potential window, chemical inertness, physicochemical stability and biocompatibility.[16, 45, 221-225] Polycrystalline diamond layers are grown on a conductive support substrate (doped silicon) by using chemical vapor deposition (CVD) from a carbon-containing process gas (usually methane). During this process, diamond is grown under relatively low pressure and temperature conditions by continuous and selective etching of the graphite deposit with hydrogen gas.[226] Diamond is a wide band-gap material and can be made conductive by introducing impurities such as phosphorus (n-doped, electron conduction) or boron (p-doped, hole conduction) during CVD synthesis.[227]

At the host institute, the coupling of biomolecules to diamond sensor substrates has been well-established.[19] In this work, diamond coated substrates are used for immobilizing MIPs.

1.2.5.2.2 Heat transfer method for MIP based sensors

The heat transfer method (HTM) [228] in the context of sensor read-out, was developed at the host institute. Using this concept, the thermal resistance of a substrate and part of its surroundings is measured at certain time intervals. As only two thermocouples, a copper plate and a power resistor heating element are needed, this simple set-up is very cost-effective and can be easily miniaturized. Van Grinsven et al. successfully used HTM as a denaturation-based method to detect single-nucleotide polymorphisms in DNA.[228] Later, Peeters et al. implemented HTM as a read-out technique for MIP based sensors for the detection of small molecules.[184] Subsequently, Wackers et al. succeeded in array formatting the HTM MIP based sensor for the simultaneous detection of three different target molecules.[39]

In general, for the HTM technique based MIP sensors (Figure 1.12), the transducer substrate is placed on top of a heating element (MIP particles facing up) of which the temperature is controlled.

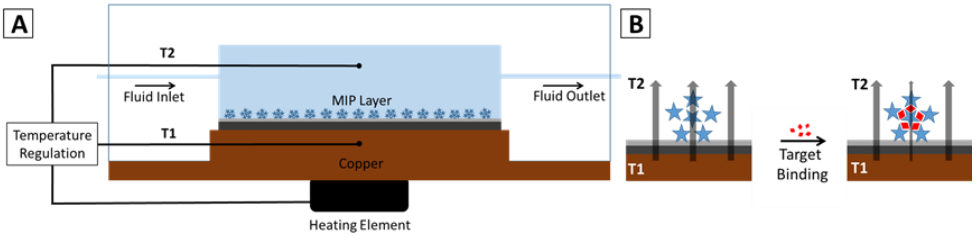

Figure 1.12. Schematic illustration of the heat transfer method set-up (A) and the visualization of the 'pore blocking model'[184] (B).

Both the temperature above the MIP layer (T2) and the temperature of the heating element (T1) are measured by using thermocouples. There will be a certain thermal resistance caused by the sensor substrate and the liquid above it. This means that the temperature measured in the liquid above the MIPs will be slightly lower in comparison with the temperature in the heater element. This difference in temperature originates from the initial thermal resistance. When a sample which contains the target molecule is added to the system, these molecules will bind to the MIPs. The liquid that was present in these binding cavities, is now

replaced with a target molecule which has a different thermal resistance. As a result the overall thermal resistance of the sensor substrate will change depending on how much target molecules are bound. This principle is shown by the pore blocking model in Figure 1.12 [184] (B). By using the temperature in the heater (T1) and the liquid (T2) and the power needed to keep T1 at the intended temperature, the thermal resistance (R_{th}) can be calculated using the following equation.

$$Rth = (T1 - T2)/\mathrm{P} \qquad \text{Eq.1.5}$$

In Eq. 1.5, P is the power in Watt (W), T1 is the temperature in degrees Celsius (°C) of the heating element (copper block) and T2 is the temperature of the fluid (°C).[39, 184]

For the HTM as a sensor read-out technique, it is necessary to use substrates that offer a good thermal conductivity such as aluminium, copper, etc.[39, 184]

1.3 Aims of the thesis

At the host institute, the concept of bulk MIP sensor for the detection of target molecules nicotine, histamine, caffeine and serotonin in aqueous samples has already been proven employing stamping and matrix entrapment as deposition and immobilization techniques, respectively. Impedance spectroscopy, the heat transfer method and quartz crystal microbalance were used as read-out techniques.[40, 184, 201] However, the variation between different sensor substrates should be reduced to a minimum to obtain consistent target molecule quantification results. As bulk MIPs suffer from inhomogeneities with respect to size, shape and material (within the batches as well as batch to batch), their applicability in sensor applications is limited. Also, the used deposition technique induces a significant amount of inter and intra sensor substrate variation in terms of MIP material amount and distribution as the stamping technique is a time consuming manual technique which is highly dependent on the skill of the operator. Moreover, using matrix entrapment to immobilize the MIP particles on the sensor substrates, physically blocks a significant amount of imprint binding sites which might reduce the sensor sensitivity. In addition, the embedded particles might loosen up or the adhesive layer might detach from the substrate

during a measurement which leads to false sensor results and limits the possibility for sensor regeneration.

To tackle the aforementioned problems, this thesis aims at developing several straightforward, reproducible and efficient strategies to obtain a cost-efficient, high performing and reusable sensor for the detection of physiologically relevant molecules in their natural concentration ranges in biological samples. In concise, the objectives can be summarized as follows:

- Development of high performing colloidal MIPs which display a large active sensing interface and are homogeneous regarding shape and material distribution for the recognition of testosterone in aqueous solutions.

- Fabrication of a reliable and reproducible impedimetric sensor based on the aforementioned colloidal MIPs using a straightforward, reliable, efficient and simple immobilization technique that relies on direct coupling to the transducer substrate and avoids the use of an interfacial adhesive polymer layer to detect testosterone in biological samples.

- Development of a cost-effective and straightforward technique to produce sensitive, high performance, reproducible, reliable, reusable and patterned in situ grafted and polymerized MIP based sensors for the electronic detection of (bio-) molecules in biological samples. The technique should also allow for straightforward design flexibility for tuning the dimensions of the MIP structures.

- Exploration of spray coating as a new MIP deposition technique in combination with a low-cost MIP immobilisation adhesive layer and sensor read-out technique, for the fabrication of cheap and scalable sensors. In here, spray coating allows for high reproducibility and automation for the large scale fabrication of sensor layers.

The sensors based on the fabrication methods developed in this work are foreseen to replace the more expensive and time consuming detection techniques such as immunosensors and liquid and gas chromatography in the laboratories while also being suitable for a broader public and personal usages.

1.4 Guide through the chapters

This thesis is organized as follows:

In **chapter 2**, a bifunctional crosslinking monomer - N,O-bismethacryloyl ethanolamine (NOBE) - based MIPs obtained via bulk and miniemulsion polymerization and imprinted with testosterone, are compared in terms of their ability to selectively rebind the target molecule.

Chapter 3 covers the direct immobilization of these miniemulsion MIP particles on a functionalized diamond coated transducer substrate. In here, a doped silicon substrate covered with a doped nanocrystalline diamond (NCD) layer was functionalized with amorphous carbon coating and then used as substrates for immobilization. Miniemulsion MIPs are especially interesting for sensor applications due to their high active sensing surface. The sensor performance to detect testosterone in buffer and urine samples is verified using electrochemical impedance spectroscopy as a read-out technique.

In **chapter 4**, patterned MIP structures on a functionalized diamond substrate are obtained by using a microfluidic system in conjunction with in situ photo-polymerization and –grafting of monomer. Also, in here, doped silicon substrates covered with a doped NCD layer are further functionalized with an amorphous carbon coating and then used as substrates. The MIP structures are tested as a selective sensor platform to detect testosterone in buffer, urine and saliva samples using electrochemical impedance spectroscopy.

Chapter 5 covers the comparison between two different MIP deposition techniques namely stamping and spray coating in terms of sensor coverage and sensor performance towards low-cost and large scale fabrication sensors. Bulk MIPs are fixed onto the sensor substrate using a cheap PVC adhesive layer. The ability of these sensor substrates to selectively detect the target molecule serotonin, is tested by using the cost-effective HTM as a read-out.

In **chapter 6**, the summary and future outlook are provided.

1.5 References

[1] L. C. Clark, C. Lyons, *Annals of the New York Academy of Sciences* **1962**, 102, 29.

[2] J. E. Shaw, A. J. Boulton, *Diabetes* **1997**, 46 Suppl 2, S58.

[3] L. Melchior, M. Grauslund, B. Bellosillo, C. Montagut, E. Torres, E. Moragon, I. Micalessi, J. Frans, V. Noten, C. Bourgain, R. Vriesema, R. van der Geize, K. Cokelaere, N. Vercooren, K. Crul, T. Rudiger, D. Buchmuller, M. Reijans, C. Jans, *Experimental and molecular pathology* **2015**, 99, 485.

[4] K. Mosbach, *Trends Biochem. Sci.* **1994**, 19, 9.

[5] B. Sellergren, *Molecularly Imprinted Polymers. Man-Made Mimics of Antibodies and their Application in Analytical Chemistry*, Elsevier Science, Amsterdam, The Netherlands **2000**.

[6] S. A. Piletsky, S. Alcock, A. P. F. Turner, *Trends Biotechnol.* **2001**, 19, 9.

[7] D. R. Thévenot, K. Toth, R. A. Durst, G. S. Wilson, *Biosensors and Bioelectronics* **2001**, 16, 121.

[8] A. P. Turner, *Biosensors & bioelectronics* **2015**, 65, A1.

[9] F.-G. Bănică, in *Chemical Sensors and Biosensors*, John Wiley & Sons, Ltd, **2012**, 1.

[10] J. Yang, S. Deng, J. Lei, H. Ju, S. Gunasekaran, *Biosensors & bioelectronics* **2011**, 29, 159.

[11] M. I. Prodromidis, M. I. Karayannis, *Electroanalysis* **2002**, 14, 241.

[12] J. Wang, Z. Liu, C. Hu, S. Hu, *Analytical Chemistry* **2015**, 87, 9368.

[13] C. A. Marquette, L. J. Blum, *Analytical and bioanalytical chemistry* **2008**, 390, 155.

[14] K. Bonroy, F. Frederix, G. Reekmans, E. Dewolf, R. De Palma, G. Borghs, P. Declerck, B. Goddeeris, *Journal of immunological methods* **2006**, 312, 167.

[15] P. Cooreman, R. Thoelen, J. Manca, M. vandeVen, V. Vermeeren, L. Michiels, M. Ameloot, P. Wagner, *Biosens Bioelectron* **2005**, 20, 2151.

[16] V. Vermeeren, L. Grieten, N. Vanden Bon, N. Bijnens, S. Wenmackers, S. D. Janssens, K. Haenen, P. Wagner, L. Michiels, *Sensors and Actuators B: Chemical* **2011**, 157, 130.

[17] V. Vermeeren, N. Bijnens, S. Wenmackers, M. Daenen, K. Haenen, O. A. Williams, M. Ameloot, M. vandeVen, P. Wagner, L. Michiels, *Langmuir* **2007**, 23, 13193.

[18] M. J. Schöning, A. Poghossian, *Electroanalysis* **2006**, 18, 1893.

[19] B. van Grinsven, N. Vanden Bon, L. Grieten, M. Murib, S. D. Janssens, K. Haenen, E. Schneider, S. Ingebrandt, M. J. Schoning, V. Vermeeren, M. Ameloot, L. Michiels, R. Thoelen, W. De Ceuninck, P. Wagner, *Lab Chip* **2011**, 11, 1656.

[20] E. Akyilmaz, I. Yasa, E. Dinckaya, *Analytical biochemistry* **2006**, 354, 78.

[21] K. Eersels, B. van Grinsven, M. Khorshid, V. Somers, C. Püttmann, C. Stein, S. Barth, H. Diliën, G. M. J. Bos, W. T. V. Germeraad, T. J. Cleij, R. Thoelen, W. De Ceuninck, P. Wagner, *Langmuir : the ACS journal of surfaces and colloids* **2015**, 31, 2043.

[22] L. Lu, Z. Qian, Y.-D. Cai, Y. Li, *Computational Biology and Chemistry* **2007**, 31, 226.

[23] M. Campàs, R. Carpentier, R. Rouillon, *Biotechnology Advances* **2008**, 26, 370.

[24] R. M. Lequin, *Clinical chemistry* **2005**, 51, 2415.

[25] S. Missailidis, K. Brady, in *Antibody Engineering: Methods and Protocols*, (Ed: B. K. C. Lo), Humana Press, Totowa, NJ **2004**, 431.

[26] S. P. Desai, J. Voldman, *Integrative Biology* **2011**, 3, 48.

[27] S. Belkin, *Current opinion in microbiology* **2003**, 6, 206.

[28] B. Smith, *Synthetic Receptors for Biomolecules : Design Principles and Applications*, Royal Society of Chemistry, Cambridge, UK **2015**.

[29] A. V. Lakhin, V. Z. Tarantul, L. V. Gening, *Acta Naturae* **2013**, 5, 34.

[30] J. Satija, V. V. R. Sai, S. Mukherji, *Journal of Materials Chemistry* **2011**, 21, 14367.

[31] B. Y. Guo, S. Wang, B. Ren, X. Li, F. Qin, J. Li, *Journal of separation science* **2010**, 33, 1156.

[32] J. Haginaka, *Journal of Chromatography B* **2008**, 866, 3.

[33] R. Thoelen, R. Vansweevelt, J. Duchateau, F. Horemans, J. D'Haen, L. Lutsen, D. Vanderzande, M. Ameloot, M. vandeVen, T. J. Cleij, P. Wagner, *Biosens. Bioelectron.* **2008**, 23, 913.

[34] B. Eggins, ***Biosensors An Introduction***, Wiley, **1996**.

[35] R. De Palma, G. Reekmans, C. Liu, R. Wirix-Speetjens, W. Laureyn, O. Nilsson, L. Lagae, *Anal Chem* **2007**, 79, 8669.

[36] G. R. Marchesini, W. Haasnoot, P. Delahaut, H. Gerçek, M. W. F. Nielen, *Analytica Chimica Acta* **2007**, 586, 259.

[37] B. K. Lavine, D. J. Westover, N. Kaval, N. Mirjankar, L. Oxenford, G. K. Mwangi, *Talanta* **2007**, 72, 1042.

[38] Y. Tan, L. Jing, Y. Ding, T. Wei, *Appl. Surf. Sci.* **2015**, 342, 84.

[39] G. Wackers, T. Vandenryt, P. Cornelis, E. Kellens, R. Thoelen, W. De Ceuninck, P. Losada-Perez, B. van Grinsven, M. Peeters, P. Wagner, *Sensors (Basel, Switzerland)* **2014**, 14, 11016.

[40] J. Alenus, A. Ethirajan, F. Horemans, A. Weustenraed, P. Csipai, J. Gruber, M. Peeters, T. J. Cleij, P. Wagner, *Anal. Bioanal. Chem.* **2013**, 405, 6479.

[41] K. Reimhult, K. Yoshimatsu, K. Risveden, S. Chen, L. Ye, A. Krozer, *Biosensors and Bioelectronics* **2008**, 23, 1908.

[42] K. A. Marx, *Biomacromolecules* **2003**, 4, 1099.

[43] F. Frederix, K. Bonroy, W. Laureyn, G. Reekmans, A. Campitelli, W. Dehaen, G. Maes, *Langmuir : the ACS journal of surfaces and colloids* **2003**, 19, 4351.

[44] Z. Gao, A. Agarwal, A. D. Trigg, N. Singh, C. Fang, C.-H. Tung, Y. Fan, K. D. Buddharaju, J. Kong, *Analytical chemistry* **2007**, 79, 3291.

[45] S. Wenmackers, V. Vermeeren, M. vandeVen, M. Ameloot, N. Bijnens, K. Haenen, L. Michiels, P. Wagner, *physica status solidi (a)* **2009**, 206, 391.

[46] K. Yano, I. Karube, *TrAC Trends in Analytical Chemistry* **1999**, 18, 199.

[47] P. K. Owens, L. Karlsson, E. S. M. Lutz, L. I. Andersson, *TrAC Trends in Analytical Chemistry* **1999**, 18, 146.

[48] J. L. Urraca, M. C. Moreno-Bondi, G. Orellana, B. Sellergren, A. J. Hall, *Analytical chemistry* **2007**, 79, 4915.

[49] N. Lavignac, C. J. Allender, K. R. Brain, *Analytica Chimica Acta* **2004**, 510, 139.

[50] J. Omersel, U. Zager, T. Kveder, B. Bozic, *Journal of immunoassay & immunochemistry* **2010**, 31, 45.

[51] B. Sellergren, *Molecularly imprinted polymers: man-made mimics of antibodies and their application in analytical chemistry*, Vol. 23, Elsevier, Amsterdam, The Netherlands **2000**.

[52] S. A. Piletsky, S. Alcock, A. P. Turner, *Trends in Biotechnology* **2001**, 19, 9.

[53] K. Mosbach, *Trends in biochemical sciences* **1994**, 19, 9.

[54] Z. Zeng, Y. Hoshino, A. Rodriguez, H. Yoo, K. J. Shea, *ACS Nano* **2010**, 4, 199.

[55] K. Haupt, K. Mosbach, *Trends in biotechnology* **1998**, 16, 468.

[56] L. Ye, K. Mosbach, *Journal of inclusion phenomena and macrocyclic chemistry* **2001**, 41, 107.

[57] L. Ye, K. Haupt, *Analytical and bioanalytical chemistry* **2004**, 378, 1887.

[58] S. A. Piletsky, N. W. Turner, P. Laitenberger, *Medical engineering & physics* **2006**, 28, 971.

[59] G. Vlatakis, L. I. Andersson, R. Muller, K. Mosbach, *Nature* **1993**, 361, 645.

[60] G. Wulff, *Trends in biotechnology* **1993**, 11, 85.

[61] D. Spivak, *Adv. Drug Deliv. Rev.* **2005**, 57, 1779.

[62] C. Esen, M. Andac, N. Bereli, R. Say, E. Henden, A. Denizli, *Materials Science and Engineering: C* **2009**, 29, 2464.

[63] F. H. Dickey, *Proceedings of the National Academy of Sciences of the United States of America* **1949**, 35, 227.

[64] T. Takagishi, I. M. Klotz, *Biopolymers* **1972**, 11, 483.

[65] G. Wulff, W. Vesper, R. Grobe-Einsler, A. Sarhan, *Die Makromolekulare Chemie* **1977**, 178, 2799.

[66] R. Arshady, K. Mosbach, *Die Makromolekulare Chemie* **1981**, 182, 687.

[67] Z.-p. Yang, C.-j. Zhang, *Sensors and Actuators B: Chemical* **2009**, 142, 210.

[68] A. Bossi, F. Bonini, A. P. Turner, S. A. Piletsky, *Biosensors & bioelectronics* **2007**, 22, 1131.

[69] S. Scorrano, L. Mergola, R. Del Sole, G. Vasapollo, *Int J Mol Sci* **2011**, 12, 1735.

[70] L. Longo, G. Vasapollo, *Mini-Rev Org Chem.* **2008**, 5, 163.

[71] V. Pichon, F. Chapuis-Hugon, *Anal Chim Acta* **2008**, 622, 48.

[72] F. G. Tamayo, J. L. Casillas, A. Martin-Esteban, *Analytical and bioanalytical chemistry* **2005**, 381, 1234.

[73] F. Puoci, G. Cirillo, M. Curcio, F. Iemma, U. G. Spizzirri, N. Picci, *Analytica Chimica Acta* **2007**, 593, 164.

[74] C. Baggiani, L. Anfossi, C. Giovannoli, *Anal Chim Acta* **2007**, 591, 29.

[75] P. Lenain, J. Diana Di Mavungu, P. Dubruel, J. Robbens, S. De Saeger, *Analytical chemistry* **2012**, 84, 10411.

[76] D. De Smet, S. Monbaliu, P. Dubruel, C. Van Peteghem, E. Schacht, S. De Saeger, *Journal of chromatography. A* **2010**, 1217, 2879.

[77] T. Mausia, D. De Smet, Q. Guorun, C. Van Peteghem, D. Zhang, A. Wu, S. De Saeger, *Analytical Letters* **2011**, 44, 2633.

[78] D. D. Smet, P. Dubruel, C. V. Peteghem, S. D. Saeger, *World Mycotoxin Journal* **2011**, 4, 375.

[79] V. T. Remcho, Z. J. Tan, *Analytical chemistry* **1999**, 71, 248A.

[80] K. Balamurugan, K. Gokulakrishnan, T. Prakasam, *Saudi Pharmaceutical Journal : SPJ* **2012**, 20, 53.

[81] T. Alizadeh, M. Zare, M. R. Ganjali, P. Norouzi, B. Tavana, *Biosensors & bioelectronics* **2010**, 25, 1166.

[82] H. Sun, Z. H. Mo, J. T. S. Choy, D. R. Zhu, Y. S. Fung, *Sensors and Actuators B: Chemical* **2008**, 131, 148.

[83] D. De Smet, P. Dubruel, C. Van Peteghem, E. Schacht, S. De Saeger, *Food additives & contaminants. Part A, Chemistry, analysis, control, exposure & risk assessment* **2009**, 26, 874.

[84] B. Sellergren, B. Ekberg, K. Mosbach, *Journal of Chromatography A* **1985**, 347, 1.

[85] W. C. Lee, C. H. Cheng, H. H. Pan, T. H. Chung, C. C. Hwang, *Analytical and bioanalytical chemistry* **2008**, 390, 1101.

[86] G. Cirillo, F. Iemma, F. Puoci, O. I. Parisi, M. Curcio, U. G. Spizzirri, N. Picci, *Journal of drug targeting* **2009**, 17, 72.

[87] G. Ciardelli, B. Cioni, C. Cristallini, N. Barbani, D. Silvestri, P. Giusti, *Biosensors & bioelectronics* **2004**, 20, 1083.

[88] F. Puoci, G. Cirillo, M. Curcio, F. Iemma, O. I. Parisi, M. Castiglione, N. Picci, *Drug delivery* **2008**, 15, 253.

[89] J. P. Schillemans, C. F. van Nostrum, *Nanomedicine (London, England)* **2006**, 1, 437.

[90] F. Puoci, F. Iemma, N. Picci, *Current drug delivery* **2008**, 5, 85.

[91] G. Wulff, *Chemical reviews* **2002**, 102, 1.

[92] A. Strikovsky, J. Hradil, G. Wulff, *Reactive and Functional Polymers* **2003**, 54, 49.

[93] A. Leonhardt, K. Mosbach, *Reactive Polymers, Ion Exchangers, Sorbents* **1987**, 6, 285.

[94] J. V. Beach, K. J. Shea, *Journal of the American Chemical Society* **1994**, 116, 379.

[95] F. Shen, X. Ren, *RSC Advances* **2014**, 4, 13123.

[96] T. Ikegami, W. S. Lee, H. Nariai, T. Takeuchi, *Journal of chromatography. B, Analytical technologies in the biomedical and life sciences* **2004**, 804, 197.

[97] M. J. Whitcombe, M. E. Rodriguez, P. Villar, E. N. Vulfson, *Journal of the American Chemical Society* **1995**, 117, 7105.

[98] M. J. Whitcombe, C. Alexander, E. N. Vulfson, *Trends in Food Science & Technology* **1997**, 8, 140.

[99] T. Takeuchi, J. Matsui, *Acta Polymerica* **1996**, 47, 471.

[100] M. Komiyama, T. Takeuchi, T. Mukawa, H. Asanuma, in *Molecular Imprinting*, Wiley-VCH Verlag GmbH & Co. KGaA, **2004**.

[101] D. Kriz, O. Ramström, K. Mosbach, *Analytical chemistry* **1997**, 69, 345A.

[102] S. N. N. S. Hashim, R. I. Boysen, L. J. Schwarz, B. Danylec, M. T. W. Hearn, *Journal of Chromatography A* **2014**, 1359, 35.

[103] E. Turiel, A. Martin-Esteban, *Analytical and bioanalytical chemistry* **2004**, 378, 1876.

[104] V. P. Joshi, S. K. Karode, M. G. Kulkarni, R. A. Mashelkar, *Chemical Engineering Science* **1998**, 53, 2271.

[105] B. Sellergren, in *Techniques and Instrumentation in Analytical Chemistry*, Vol. Volume 23 (Ed: S. Börje), Elsevier, **2001**, 113.

[106] A. R. Wang, S. Zhu, *Polymer Engineering & Science* **2005**, 45, 720.

[107] C.-H. Lu, W.-H. Zhou, B. Han, H.-H. Yang, X. Chen, X.-R. Wang, *Analytical chemistry* **2007**, 79, 5457.

[108] C.-H. Lu, Y. Wang, Y. Li, H.-H. Yang, X. Chen, X.-R. Wang, *Journal of Materials Chemistry* **2009**, 19, 1077.

[109] X. Wei, X. Li, S. M. Husson, *Biomacromolecules* **2005**, 6, 1113.

[110] M.-M. Titirici, B. Sellergren, *Chemistry of Materials* **2006**, 18, 1773.

[111] G. Pan, B. Zu, X. Guo, Y. Zhang, C. Li, H. Zhang, *Polymer* **2009**, 50, 2819.

[112] B. Zu, G. Pan, X. Guo, Y. Zhang, H. Zhang, *Journal of Polymer Science Part A: Polymer Chemistry* **2009**, 47, 3257.

[113] E. V. Piletska, A. R. Guerreiro, M. J. Whitcombe, S. A. Piletsky, *Macromolecules* **2009**, 42, 4921.

[114] M. Sibrian-Vazquez, D. Spivak, *J. Am. Chem. Soc.* **2004**, 126, 7827.

[115] J. LeJeune, D. Spivak, *Biosens. Bioelectron.* **2009**, 25, 604.

[116] M. Sibrian-Vazquez, D. A. Spivak, *Macromolecules* **2003**, 36, 5105.

[117] J. LeJeune, D. A. Spivak, *Anal. Bioanal. Chem.* **2007**, 389, 433.

[118] M. Kempe, *Anal. Chem.* **1996**, 68, 1948.

[119] D. Spivak, M. A. Gilmore, K. J. Shea, *J. Am. Chem. Soc.* **1997**, 119, 4388.

[120] C. Yu, O. Ramström, K. Mosbach, *Anal. Lett.* **1997**, 30, 2123.

[121] C. Yu, K. Mosbach, *J. Chromatogr. A* **2000**, 888, 63.

[122] J. M. Lin, T. Nakagama, K. Uchiyama, T. Hobo, *Biomedical chromatography : BMC* **1997**, 11, 298.

[123] Z. Zhang, H. Li, H. Liao, L. Nie, S. Yao, *Sensors and Actuators B: Chemical* **2005**, 105, 176.

[124] I. Mijangos, F. Navarro-Villoslada, A. Guerreiro, E. Piletska, I. Chianella, K. Karim, A. Turner, S. Piletsky, *Biosensors and Bioelectronics* **2006**, 22, 381.

[125] N. Perez-Moral, A. G. Mayes, *Langmuir : the ACS journal of surfaces and colloids* **2004**, 20, 3775.

[126] M. J. Rosen, J. T. Kunjappu, in *Surfactants and Interfacial Phenomena*, John Wiley & Sons, Inc., **2012**.

[127] K. Landfester, *Macromolecular Rapid Communications* **2001**, 22, 896.

[128] Y. J. Chou, M. S. El-Aasser, J. W. Vanderhoff, *Journal of Dispersion Science and Technology* **1980**, 1, 129.

[129] K. Landfester, N. Bechthold, F. Tiarks, M. Antonietti, *Macromolecules* **1999**, 32, 5222.

[130] K. Landfester, *Macromolecular Symposia* **2000**, 150, 171.

[131] N. Pérez-Moral, A. G. Mayes, *Analytica Chimica Acta* **2004**, 504, 15.

[132] N. Perez-Moral, A. G. Mayes, *Bioseparation* **2001**, 10, 287.

[133] R. J. Ansell, K. Mosbach, *J. Chromatogr. A* **1997**, 787, 55.

[134] A. G. Mayes, K. Mosbach, *Anal. Chem.* **1996**, 68, 3769.

[135] L. Ye, R. Weiss, K. Mosbach, *Macromolecules* **2000**, 33, 8239.

[136] Y. Hoshino, H. Koide, T. Urakami, H. Kanazawa, T. Kodama, N. Oku, K. J. Shea, *Journal of the American Chemical Society* **2010**, 132, 6644.

[137] W.-H. Zhou, C.-H. Lu, X.-C. Guo, F.-R. Chen, H.-H. Yang, X.-R. Wang, *Journal of Materials Chemistry* **2010**, 20, 880.

[138] C. J. Tan, Y. W. Tong, *Analytical and bioanalytical chemistry* **2007**, 389, 369.

[139] N. P. Moral, A. G. Mayes, *MRS Proceedings* **2011**, 723.

[140] S. Azodi-Deilami, M. Abdouss, D. Kordestani, Z. Shariatinia, *Journal of materials science. Materials in medicine* **2014**, 25, 645.

[141] C. I. Lin, A. K. Joseph, C. K. Chang, Y. D. Lee, *Biosensors and Bioelectronics* **2004**, 20, 127.

[142] J. Q. Xue, D. W. Li, L. L. Qu, Y. T. Long, *Anal Chim Acta* **2013**, 777, 57.

[143] D. Yu, Y. Zeng, Y. Qi, T. Zhou, G. Shi, *Biosensors & bioelectronics* **2012**, 38, 270.

[144] E. Kellens, in *Biomedical Sciences*, Hasselt University, Diepenbeek **2012**, 1

[145] W. Ostwald, *Z. Phys. Chem.* **1900**, 34, 495

[146] N. A. Mishchuk, S. V. Verbich, S. S. Dukhin, Ø. Holt, J. Sjöblom, *Journal of Dispersion Science and Technology* **1997**, 18, 517.

[147] M. Postel, J. G. Riess, J. G. Weers, *Artificial cells, blood substitutes, and immobilization biotechnology* **1994**, 22, 991.

[148] K. C. Lowe, *Artificial cells, blood substitutes, and immobilization biotechnology* **2000**, 28, 25.

[149] L. P. Ramirez, K. Landfester, *Macromol. Chem. Phys.* **2003**, 204, 22.

[150] A. Ethirajan, A. Musyanovych, A. Chuvilin, K. Landfester, *Macromol. Chem. Phys.* **2011**, 212, 915.

[151] S. Tokonami, H. Shiigi, T. Nagaoka, *Anal Chim Acta* **2009**, 641, 7.

[152] D. Gao, Z. Zhang, M. Wu, C. Xie, G. Guan, D. Wang, *J Am Chem Soc* **2007**, 129, 7859.

[153] Y. Ge, A. P. Turner, *Chemistry (Weinheim an der Bergstrasse, Germany)* **2009**, 15, 8100.

[154] N. Zhang, X. Hu, P. Guan, C. Du, J. Li, L. Qian, X. Zhang, S. Ding, B. Li, *Chemical Engineering Journal* **2017**, 317, 356.

[155] P. Yu, Q. Sun, J. Li, Z. Tan, Y. Yan, C. Li, *Journal of Environmental Chemical Engineering* **2015**, 3, 797.

[156] E. Asadi, S. Azodi-Deilami, M. Abdouss, D. Kordestani, A. Rahimi, S. Asadi, *Korean J. Chem. Eng.* **2014**, 31, 1028.

[157] D. Vaihinger, K. Landfester, I. Kräuter, H. Brunner, G. E. M. Tovar, *Macromol. Chem. Phys.* **2002**, 203, 1965.

[158] B. Pluhar, U. Ziener, B. Mizaikoff, *J. Mater. Chem. B* **2013**, 1, 5489.

[159] P. Curcio, C. Zandanel, A. Wagner, C. Mioskowski, R. Baati, *Macromol Biosci* **2009**, 9, 596.

[160] B. Tse Sum Bui, K. Haupt, *J. Mol. Recognit.* **2011**, 24, 1123.

[161] S. H. Cheong, S. McNiven, A. Rachkov, R. Levi, K. Yano, I. Karube, *Macromolecules* **1997**, 30, 1317.

[162] C. J. Percival, S. Stanley, A. Braithwaite, M. I. Newton, G. McHale, *Analyst* **2002**, 127, 1024.

[163] A. Rachkov, S. McNiven, A. El'skaya, K. Yano, I. Karube, *Analytica Chimica Acta* **2000**, 405, 23.

[164] J. Yin, G. Yang, Y. Chen, *Journal of chromatography. A* **2005**, 1090, 68.

[165] D. De Smet, V. Kodeck, P. Dubruel, C. Van Peteghem, E. Schacht, S. De Saeger, *Journal of chromatography. A* **2011**, 1218, 1122.

[166] S. Scorrano, L. Mergola, R. Del Sole, G. Vasapollo, *International Journal of Molecular Sciences* **2011**, 12, 1735.

[167] H. Shi, W.-B. Tsai, M. D. Garrison, S. Ferrari, B. D. Ratner, *Nature* **1999**, 398, 593.

[168] C. H. Lu, Y. Zhang, S. F. Tang, Z. B. Fang, H. H. Yang, X. Chen, G. N. Chen, *Biosensors & bioelectronics* **2012**, 31, 439.

[169] M. Ogiso, N. Minoura, T. Shinbo, T. Shimizu, *Biosensors & bioelectronics* **2007**, 22, 1974.

[170] L. D. Bolisay, J. N. Culver, P. Kofinas, *Biomaterials* **2006**, 27, 4165.

[171] F. L. Dickert, O. Hayden, R. Bindeus, K. J. Mann, D. Blaas, E. Waigmann, *Analytical and bioanalytical chemistry* **2004**, 378, 1929.

[172] F. L. Dickert, P. Lieberzeit, S. G. Miarecka, K. J. Mann, O. Hayden, C. Palfinger, *Biosensors & bioelectronics* **2004**, 20, 1040.

[173] O. Hayden, R. Bindeus, C. Haderspöck, K.-J. Mann, B. Wirl, F. L. Dickert, *Sensors and Actuators B: Chemical* **2003**, 91, 316.

[174] V. Erspamer, G. Boretti, *Archives internationales de pharmacodynamie et de therapie* **1951**, 88, 296.

[175] I. P. Kema, E. G. E. de Vries, F. A. J. Muskiet, *Journal of Chromatography B: Biomedical Sciences and Applications* **2000**, 747, 33.

[176] P. M. Vanhoutte, in *Serotonin and the Cardiovascular system*, (Ed: R. Press), New York **1985**.

[177] D. G. Grahame-Smith, *The American Journal of Cardiology* **1968**, 21, 376.

[178] A. N. M. Wymenga, W. T. A. van der Graaf, I. P. Kema, E. G. E. de Vries, N. H. Mulder, *The Lancet* **1999**, 353, 293.

[179] J. E. Blundell, *The American journal of clinical nutrition* **1992**, 55, 155s.

[180] G. M. Anderson, J. M. Stevenson, D. J. Cohen, *Life Sciences* **1987**, 41, 1777.

[181] G. M. Anderson, in *Kynurenine and Serotonin Pathways: Progress in Tryptophan Research*, (Eds: R. Schwarcz, S. N. Young, R. R. Brown), Springer New York, Boston, MA **1991**, 51.

[182] B. A. Patel, M. Arundell, K. H. Parker, M. S. Yeoman, D. O'Hare, *Journal of Chromatography B* **2005**, 818, 269.

[183] M. Peeters, F. Troost, B. van Grinsven, F. Horemans, J. Alenus, M. S. Murib, D. Keszthelyi, A. Ethirajan, R. Thoelen, T. Cleij, *Sensors and Actuators B: Chemical* **2012**, 171, 602.

[184] M. Peeters, P. Csipai, B. Geerets, A. Weustenraed, B. van Grinsven, R. Thoelen, J. Gruber, W. De Ceuninck, T. J. Cleij, F. J. Troost, P. Wagner, *Analytical and bioanalytical chemistry* **2013**, 405, 6453.

[185] D. Thieme, P. Hemmersbach, *Springer* **2009**.

[186] J. Cauley, F. Lucas, L. Kuller, K. Stone, W. Browner, S. Cummings, *Ann. Intern. Med.* **1999**, 130, 270.

[187] Z. Hyde, L. Flicker, K. McCaul, O. Almeida, G. Hankey, S. Chubb, B. Yeap, *Canc. Epidemiol. Biomarkers Prev.* **2012**, 21, 1319.

[188] M. Hoffman, W. DeWolf, A. Morgentaler, *J. Urol.* **2000**, 163, 824.

[189] M. Akishita, M. Hashimoto, Y. Ohike, S. Ogawa, K. Iijima, M. Eto, Y. Ouchi, *Atherosclerosis* **2010**, 210, 232.

[190] M. Schubert, F. Jockenhövel, *Der Urologe* **2010**, 49, 47.

[191] U. Srinivas-Shankar, S. Roberts, M. Connolly, M. O'Connell, J. Adams, J. Oldham, F. Wu, *J. Clin. Endocrinol. Metab.* **2010**, 95, 639.

[192] C. Saudan, N. Baume, N. Robinson, L. Avois, P. Mangin, M. Saugy, *Br J Sports Med* **2006**, 40 Suppl 1, i21.

[193] J. Taieb, B. Mathian, P. Boudou, F. Millot, J. Y. Badonnel, I. Lacroix, E. Mathieu, N. Queyrel, C. Somma-Delpero, M. C. Patricot, *Immuno. Anal. Biol. Spé.* **2001**, 16, 338.

[194] F. Gasser, N. Jeandidier, S. Doffoel, F. Klein, R. Sapin, *Immuno. Anal Biol. Spé.* **2003**, 18, 98.

[195] J. Taieb, B. Mathian, F. Millot, M. C. Patricot, E. Mathieu, N. Queyrel, I. Lacroix, C. Somma-Delpero, P. Boudou, *Clin. Chem.* **2003**, 49, 1381.

[196] J. Dana-Haeri, J. Oxley, A. Richens, *British Medical Journal (Clinical research ed.)* **1982**, 284, 85.

[197] S. A. Piletsky, I. A. Butovich, V. P. Kukhar, *Zh. Anal. Khim.* **1992**, 47, 1681.

[198] T. Kamra, S. Chaudhary, C. Xu, N. Johansson, L. Montelius, J. Schnadt, L. Ye, *Journal of Colloid and Interface Science* **2015**, 445, 277.

[199] Y. Fuchs, O. Soppera, A. G. Mayes, K. Haupt, *Advanced Materials* **2013**, 25, 566.

[200] Y. Chen, Y. Liu, X. Shen, Z. Chang, L. Tang, W.-F. Dong, M. Li, J.-J. He, *Sensors* **2015**, 15, 29877.

[201] M. Peeters, F. J. Troost, R. H. Mingels, T. Welsch, B. van Grinsven, T. Vranken, S. Ingebrandt, R. Thoelen, T. J. Cleij, P. Wagner, *Analytical chemistry* **2013**, 85, 1475.

[202] D. Kriz, K. Mosbach, *Analytica Chimica Acta* **1995**, 300, 71.

[203] N. Kirsch, J. P. Hart, D. J. Bird, R. W. Luxton, D. V. McCalley, *Analyst* **2001**, 126, 1936.

[204] C.-H. Weng, W.-M. Yeh, K.-C. Ho, G.-B. Lee, *Sensors and Actuators B: Chemical* **2007**, 121, 576.

[205] B. D. Gates, Q. Xu, J. C. Love, D. B. Wolfe, G. M. Whitesides, *Annual Review of Materials Research* **2004**, 34, 339.

[206] A. V. Linares, A. Falcimaigne-Cordin, L. A. Gheber, K. Haupt, *Small* **2011**, 7, 2318.

[207] R. B. Pernites, S. K. Venkata, B. D. B. Tiu, A. C. C. Yago, R. C. Advincula, *Small* **2012**, 8, 1669.

[208] D. C. Apodaca, R. B. Pernites, F. R. Del Mundo, R. C. Advincula, *Langmuir : the ACS journal of surfaces and colloids* **2011**, 27, 6768.

[209] K. M. Choi, *Bio-chemical sensors based on molecularly imprinted polymers; soft lithography, microfabrication and microfluidic synthesis*, One Central Press **2014**.

[210] N. Vo Ke Thanh, N. Dang Giang, N. Hoang Phuong Uyen, T. Van Man, N. Thi Khoa My, H. Trong Phat, L. Quang Vinh, H. Thanh Dat, T. Thi Ngoc Lien, *Advances in Natural Sciences: Nanoscience and Nanotechnology* **2014**, 5, 045004.

[211] J. L. Arlett, E. B. Myers, M. L. Roukes, *Nat Nano* **2011**, 6, 203.

[212] J. Alenus, P. Galar, A. Ethirajan, F. Horemans, A. Weustenraed, T. J. Cleij, P. Wagner, *Phys. Status Solidi A* **2012**, 209, 905.

[213] G. Ertürk, H. Özen, M. A. Tümer, B. Mattiasson, A. Denizli, *Sensors and Actuators B: Chemical* **2016**, 224, 823.

[214] A. P. Turner, *Chemical Society reviews* **2013**, 42, 3184.

[215] M. Mitsushio, K. Watanabe, Y. Abe, M. Higo, *Sensors and Actuators A: Physical* **2010**, 163, 1.

[216] Z. Wang, Z. Cheng, V. Singh, Z. Zheng, Y. Wang, S. Li, L. Song, J. Zhu, *Analytical chemistry* **2014**, 86, 1430.

[217] S. Grimmes, O. G. Martinsen, *Bioimpedance and bioelectricity basics*, **2000**.

[218] A. Bonanni, A. H. Loo, M. Pumera, *TrAC Trends in Analytical Chemistry* **2012**, 37, 12.

[219] A. Betatache, F. Lagarde, C. Sanglar, A. Bonhommé, D. Léonard, N. Jaffrezic-Renault, *Sensors & Transducers Journal* **2014**, 27, 92.

[220] M. Peeters, F. J. Troost, B. van Grinsven, F. Horemans, J. Alenus, D. Keszthelyi, A. Ethirajan, R. Thoelen, T. J. Cleij, P. Wagner, *Sens. Actuators B Chem.* **2012**, 171-172, 602.

[221] G. M. Swain, A. B. Anderson, J. C. Angus, *MRS Bulletin* **1998**, 23, 56.

[222] M. Shen, L. Martinson, M. S. Wagner, D. G. Castner, B. D. Ratner, T. A. Horbett, *J Biomater Sci Polym Ed* **2002**, 13, 367.

[223] A. Hartl, E. Schmich, J. A. Garrido, J. Hernando, S. C. Catharino, S. Walter, P. Feulner, A. Kromka, D. Steinmuller, M. Stutzmann, *Nat Mater* **2004**, 3, 736.

[224] J. Rubio-Retama, J. Hernando, B. López-Ruiz, A. Härtl, D. Steinmüller, M. Stutzmann, E. López-Cabarcos, J. Antonio Garrido, *Langmuir* **2006**, 22, 5837.

[225] K. Bakowicz-Mitura, G. Bartosz, S. Mitura, *Surface and Coatings Technology* **2007**, 201, 6131.

[226] J. C. Angus, H. A. Will, W. S. Stanko, *Journal of Applied Physics* **1968**, 39, 2915.

[227] H. Young, R. Freedman, *University physics with modern physics*, Addison-Wesly publishing company, New York **2000**.

[228] B. van Grinsven, N. Vanden Bon, H. Strauven, L. Grieten, M. Murib, K. L. Jiménez Monroy, S. D. Janssens, K. Haenen, M. J. Schöning, V. Vermeeren, M. Ameloot, L. Michiels, R. Thoelen, W. De Ceuninck, P. Wagner, *ACS Nano* **2012**, 6, 2712.

2 Improved molecular imprinting based on colloidal particles made from miniemulsion: a case study on testosterone and its structural analogues

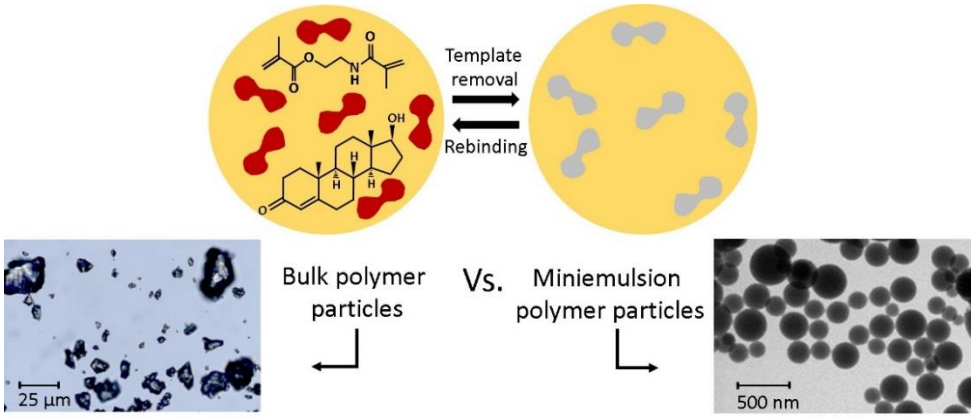

2.1 Abstract

Molecularly imprinted polymers (MIPs) in the micron and sub-micron scale based on the bifunctional cross-linker N,O-bismethacryloyl ethanolamine (NOBE) have been synthesized using bulk and miniemulsion polymerization, respectively. MIPs with distinct selectivity for the template testosterone were obtained. Colloidal MIP particles made using the miniemulsion technique have significant advantages compared to bulk MIP counterparts owing to their small size, homogeneity and increased surface, as is demonstrated by optical batch rebinding studies using a non-imprinted polymer (NIP) as a negative control. Affinity and selectivity studies were also performed with the miniemulsion colloidal MIPs. These MIPs display largely increased imprint factors (6.8 vs 2.2) when compared to their bulk MIP counterparts. Further, selectivity studies by using analogue steroids show that colloidal MIPs also display a higher selectivity. In summary, miniemulsion MIPs show much better performance with regards to molecular recognition in aqueous

solution, while providing at the same time the possibility for a water-based MIP synthesis.

2.2 Introduction

Molecularly imprinted polymers (MIPs) are tailor made recognition materials that can bind specific target molecules with high affinity and selectivity.[1-5] MIPs are made of cross-linked polymer matrices obtained usually by polymerization of functional monomer(s) and cross-linkers in the presence of a template molecule. The functional groups in the monomer(s) have the possibility to be arranged around the template molecule through non-covalent or covalent interactions in a so-called prepolymerization complex, which is fixed in its conformation during cross-linking polymerization. After MIP formation, the subsequent removal of the template molecule leaves nanocavities that can act as binding sites for the target molecule.[2] These recognition sites are complementary in size, shape and arrangement of functional groups to the target molecule, thereby making these cavities capable of rebinding the latter with a high specificity. Unlike natural receptors such as proteins or enzymes, these artificial MIP receptors are low-cost, robust with respect to physical stability and chemical inertness, possess long shelf life and offer the ease of mass production. Therefore, MIPs are highly interesting for use in stationary phase extractions, sensor applications, membranes, affinity chromatography, drug delivery systems and pseudo-immunoassays.[6-11]

Over the last years significant interest arose on the detection of steroid compounds. In this regard, the male sex hormone testosterone is of significant interest due to its role in several pathological conditions depending on its concentration.[12] For instance, increased testosterone levels are associated with a high risk for breast cancer in women [13] and has been related to the cause of prostate and lung cancer in men.[14] However, also low levels of testosterone can have profound effects on a man's health. The normal value of total testosterone in an adult male is 0.03 µM,[15] but differs with age. Signs of a testosterone deficiency are: depression, fatigue, dementia, osteoporosis, heart disease, stroke, abdominal obesity and diabetes type 2.[16-19] Additionally, the quantification of testosterone blood or urine levels is of particular interest in sports as its anabolic effects is associated with performance boosting by doping.[20] In clinical

laboratories, the general testosterone analysis in serum and plasma is performed with immunoassays and optionally a chromatography preconcentration step with a limit of detection in the pg/mL range.[21, 22] Although this method is sensitive, the specificity is rather low because of high cross-reactivity between the antibodies and other steroids.[23] Therefore, MIPs with high binding affinity for testosterone are highly desirable for use in clean-up and preconcentration steps in samples and for the absolute quantification of testosterone. Several methods of synthesis of MIPs for testosterone have already been reported using usually MAA and EGDMA as monomers. The capacity of the MIPs to rebind the target molecule with high affinity and specificity is also very much dependent on the choice of the solvent used during imprinting (porogen) and detection. For instance, using acetonitrile (ACN) as a porogen as well as solvent for rebinding, imprint factors in the range of 2 to 4 have been obtained.[24, 25] While using chloroform as a porogen, imprinting factors of about 1.4 and 3.6 were reported, where acetonitrile and chloroform were used as rebinding solvents respectively.[26, 27] Also, a number of reports have been published about MAA/EGDMA MIP films (formed using a non-aqueous porogen) directly immobilized on the substrate for the detection of testosterone in aqueous media (buffer/deionized water) using different read-out techniques such as surface plasmon resonance, impedance and microring resonance where they reached a limit of detection of 2.88 pg/mL, 103 pg/mL and 48.7 pg/mL, respectively.[28-30]

MIPs are commonly synthesized using bulk polymerization resulting in polymer monoliths, which are then subsequently grounded and sieved to yield micron sized particles.[9, 10, 31] While the crushing usually leads to irregular shapes and a broad size distribution, the sieving step to obtain particles by size selection results in a huge loss of valuable materials.[32] The still relatively large size in conjunction with their broad size distribution, leads in consequence to a low surface area and renders bulk MIPs inefficient for several applications where a low particle dispersity and efficient packing of particles are desired, such as in chromatographic columns or immobilization on sensor platforms.[33, 34] In addition, with bulk MIPs, the complete extraction of the imprinted target molecules (especially larger molecules such as proteins) is difficult, as some of the molecules stay trapped inside the network.[35] In this regard, MIPs prepared using colloidal

methods such as precipitation, suspension and emulsion techniques are a compelling alternative as they offer uniformity in shape, better control over the particle size and a largely increased surface area.[36-43]

Although the concept of MIP synthesis seems simple, irrespective of the exact production method, the optimization of MIP formulation is challenging and tedious. The performance of the MIP is highly dependent on the stoichiometry of the used components. Usually, one has to choose the appropriate functional monomer (~ 10 – 20 %) with respect to the template/target molecule together with a suitable cross-linker monomer (~ 80 – 90 %) that allows to create imprinting sites.[44] To ease the cumbersome trial and error efforts in formulation, alternatively, a high performance MIP for template molecules containing free hydroxyl or carboxyl groups based on bulk polymerization was realized using single functional-cross-linking monomer, N,O-bismethacryloyl ethanolamine (NOBE).[45] With this concept, coined "one monomer MIPs (OMNiMIPs)", a straightforward route to design MIPs was developed where the need for additional functional monomers and empirical optimization of the relative ratios of different monomers, and template in the formulation was eliminated.[46] The self-association ability of NOBE via hydrogen bond interactions in the solution phase prior to polymerization was indicated as reason for its enhanced performance for instance, over the widely employed methacrylic acid/ethyleneglycol dimethacrylate MIPs.[2, 9] Apart from bulk MIPs, NOBE based peptide-imprinted microspheres using precipitation polymerization employing acetonitrile as solvent were successfully obtained.[39] With these imprint materials, however, the recognition studies were performed under non-aqueous conditions. The synthesis of MIPs in aqueous media poses significant challenge especially if the recognition is governed by hydrogen bonding interactions as water can potentially interfere in H-bonding interactions between the template and the monomer/polymer matrix. To the best of our knowledge, NOBE MIPs have not been synthesized so far using any heterophase polymerization technique employing aqueous continuous media. As many real-life samples like biological fluids are water based, such an approach can enhance the recognition of MIPs as the conditions under which molecular recognition is desired mimic the environment used during the imprinting process.[47-50]

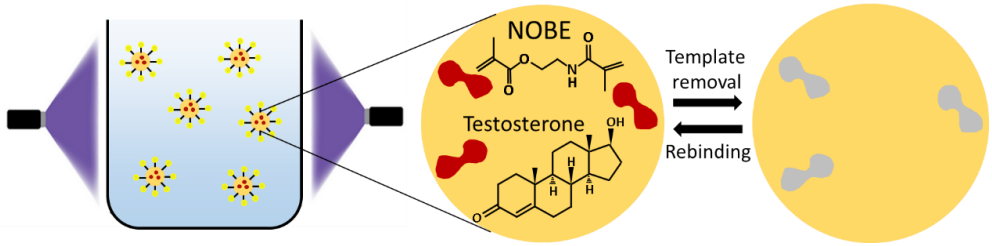

Figure 2.1. Schematic representation of the MIP concept using colloidal MIP particles alongside the structures of NOBE and the template molecule testosterone.

The colloidal MIPs (see Scheme in Figure 2.1) were prepared as water based dispersions using the miniemulsion technique.[40, 51] The latter allows for the effective encapsulation of both hydrophobic as well as hydrophilic compounds and for obtaining dispersions with high solid content.[52-54] To the best of our knowledge, the synthesis of NOBE based MIPs – for the recognition of target molecule containing free hydroxyl group via non-covalent interactions – in aqueous media is reported for the first time. As testosterone has limited solubility in water, it will be retained within the organic droplet phase in dispersed media. To systematically compare the conventional bulk monolith MIP concept with the miniemulsion MIP synthesis technique, both bulk and miniemulsion polymerized NOBE MIPs were formulated employing the same relative ratios of target molecule, monomer, initiator and porogen. The molecular recognition capacity of the different MIPs were studied using equilibrium binding analysis. As recognition in aqueous media is more relevant for applications in separation or sensing, the batch rebinding studies using different initial concentrations of testosterone were performed using a mixture of buffer/ethanol solution. The binding properties of the bulk MIPs were tested first at various pH values against a non-imprinted polymer (NIP) prepared in an identical way as a control. After selecting the optimal pH, batch rebinding studies were performed with the miniemulsion colloidal MIPs. Further, the selectivity of the bulk and colloidal MIPs in a sample containing other small molecule impurities was evaluated in order to simulate the relevance of the MIP performance in sensing testosterone in biologically relevant samples.

As a next step, the MIP particles were also tested for their versatility in recognizing structural analogues. Apart from testosterone, other steroid compounds belonging

to the family of estrogenic endocrine compounds are also of great interest owing to their impact on the aquatic environment.[55, 56] Both the bulk and miniemulsion polymerized NOBE MIPs templated with testosterone were tested for their selectivity against the different structural analogues of testosterone (see Figure 2.2).

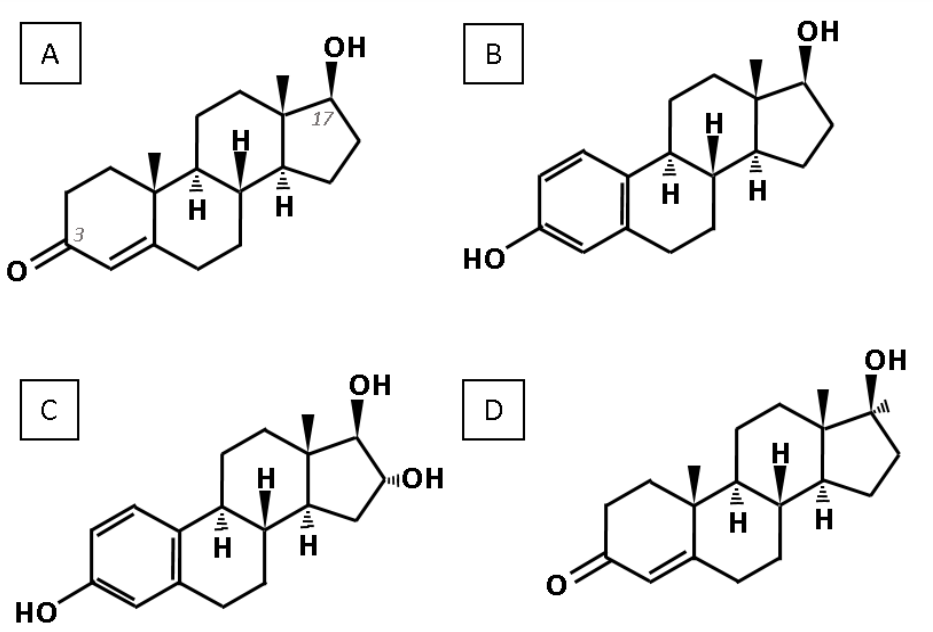

Figure 2.2. Chemical structures of the target molecule testosterone (A) and its structural analogues: 17β-estradiol (B), estriol (C) and 17α-methyltestosterone (D).

2.3 Experimental section

2.3.1 Materials

Methacryloyl chloride, ethanolamine, triethylamine, dimethylformamide, $NaHCO_3$, NH_4Cl, NaCl, magnesium sulphate powder, basic alumina, testosterone, cetyltrimethylammonium chloride, hexane, butanol, cyclohexanone and hydroquinone were obtained from Sigma Aldrich. 2,2'azobis(isobutyronitrile) was purchased from Fluka. Ethyl acetate, petroleum spirit, ethanol, methanol,

chloroform, and acetic acid were obtained from VWR. Phosphate buffered saline (PBS) solution was purchased from Thermo Scientific.

2.3.2 N,O-bismethacryloyl ethanolamine (NOBE) monomer synthesis

For the synthesis of NOBE, a previously reported literature procedure was adapted.[45] 1.125 mol (109.89 mL, 117.59 g, 2.5 equivalents) of methacryloyl chloride was mixed drop-wise with a solution of 0.450 mol (27.15 mL, 27.48 g, 1 equivalent) of ethanolamine and 0.900 mol (125.61 mL, 91 g, 2.5 equivalents) of triethylamine (TEA) in dry dimethylformamide under anhydrous nitrogen conditions at 0 °C in a 2 L round bottom flask equipped with a magnetic stir bar. After stirring for 24 h at 40 °C under nitrogen atmosphere conditions, the solution was quenched, the formed ammonia salts were filtered off and the product was washed with 500 mL aqueous $NaHCO_3$, aqueous NH_4Cl and brine (saturated NaCl solution), followed by drying of the organic phase with magnesium sulphate powder. The crude product was then passed over a basic alumina column to filter out acrylic acid. Final purification was achieved by column chromatography (GraceResolve Silica Cartridges) using ethyl acetate/petroleum spirit (5/95 ratio) as a mobile phase. The monomer yield before and after purification are 85 % and 35 % respectively. Since the monomer is prone to self-polymerization, a significant amount of material is lost during purification. The NMR data are presented in the supporting information (Figure S2.1, Supporting Information). ^{1}H-NMR ($CDCl_3$, 400 MHz) δ = 6.33 (br s, ^{1}H, NH), 6.09 (m, ^{1}H, =C**H**H), 5.67 (m, ^{1}H, =CH**H**), 5.57 (m, ^{1}H, =C**H**H), 5.31 (m, ^{1}H, =CH**H**), 4.27 (m, ^{2}H, CH_2-O-), 3.60 (m, ^{2}H, CH_2-N-), 1.91 (m, ^{6}H, CH_3).

2.3.3 Synthesis of micron sized bulk MIPs

In a standard glass container (250 x 500 mm) chloroform (2.1 g, 17.61 mmol), testosterone (17.6 mol % of monomer target molecule mix, 1.032 g, 3.58 mmol), radical initiator 2,2’ azobisisobutyronitrile (AIBN, 0.12 g, 0.730 mmol) and the monomer NOBE (4 g, 20.2 mmol) were mixed. This homogeneous mixture was purged with nitrogen for 5 minutes and polymerized in a UV chamber connected with a UV lamp. An OMNICURE Series 1000 lamp system with four-arm setting

was used as a UV light source: the system was equipped with a 100 W high-pressure mercury vapor short arc lamp (320 – 500 nm). An iris setting of 20 % for the first 25 min and subsequently reduced to 3 % for 16 h (overnight) was used. While one of the UV lamp arms illuminated the sample from the top, the other three arms were used for illumination from different sides of the vial. After polymerization, the polymer was grounded (pulverisette 7, Fritsch) at 500 rpm for 300 s to obtain microparticles with a size ranging from 1 – 50 µm. To use as control, NIP particles were prepared in an identical way as MIP particles except for the inclusion of the target molecule.

2.3.4 Synthesis of colloidal MIPs

In a standard glass container (250 x 500 mm) all elements of the dispersed phase were mixed: NOBE (0.5 g, 2.535 mmol), testosterone (17.6 mol % of monomer target molecule mix, 0.129 g, 0.447 mmol), AIBN (0.015 g, 91.3 µmol) and chloroform (0.26 g, 2.18 mmol) were mixed. As the monomer is highly reactive, to avoid polymerization during sonication, a small amount of hydroquinone (1.46 µg, 13.3 nmol), was also added. Separately, water (10 g, 0.555 mol) was mixed with cetyltrimethylammonium chloride (CTMA, cationic surfactant, 0.052 g, 0.163 mmol) to prepare the continuous phase. Both phases were mixed together and ultrasonicated (Branson sonifier W450 Digital; 1/8 " tip) in two steps using the following conditions with ice-cooling: 30 % amplitude for 120 s using a 30 s pulse and 20 s pause regime followed by a second sonication step using 65 % amplitude for 120 s using a 30 s pulse, and 20 s pause regime. The sample was then stirred at 750 rpm, purged with nitrogen and polymerized using the same Omnicure series lamp with four-arms illuminating the samples from different sides as before with the following settings: an iris setting of 20 % for the first 2 h and then 3 % for 16 h. After polymerization, the samples were passed through paper filters (Whatman filters, 4 - 7 µm pore size) to remove any large aggregates and then the solid contents of the resulting dispersions were determined thermogravimetrically. Subsequently, the surfactant was removed from the particles by diafiltration (Amicon solvent resistant ultrafiltration cell) using regenerated cellulose membranes (Ultracel 30 kDa Ultrafiltration discs). To use as

control, colloidal NIP particles were prepared in an identical way as MIP particles except for the inclusion of the target molecule.

2.3.5 Template removal

For target extraction of the bulk MIPs, the particles were purified by Soxhlet extraction with a mixture of acetic acid/methanol (10/90) during the first 72 h (6 x solvent change) and pure ethanol during the last 16 h. The MIP particles were extracted until no template molecules were observable by UV-Vis spectroscopy (characteristic absorbance at 245 nm for testosterone, (Figure S2.2, Supporting Information) anymore in the solvent. The NIP particles were treated identically as the MIP particles. All washed MIP and NIP particles were dried on a vacuum pump overnight.

In case of the colloidal particles, both the MIP and NIP samples were subjected to multiple centrifugation (15 min, 9000 rpm) and redispersion in a pre-heated mixture of acetic acid/methanol (10/90 v/v %, 50 °C, mixing for 30 min). Totally, 5 cycles of resdispersion were performed. At the end of these washing cycles (lasting less than 4 h), no trace of template molecule was observable anymore by UV-Vis spectroscopy. The samples were then finally washed with ethanol to remove the acid. Subsequently, both MIP and NIP were dried on a vacuum pump overnight.

2.3.6 Characterization techniques

The size and morphology of the bulk MIP and NIP particles were characterized using the Axiovert 40 MAT optical microscope (ZEISS) equipped with a digital camera and using the Axiovision AC software. The diameter and polydispersity of the colloidal MIPs and NIPs in water were characterized using the particle analyzer ZetaPALS, Brookhaven Instruments Corporation (90 ° laser detector angle). Visualization of the colloidal particles was carried out with a transmission electron microscope (TEM) from Tecnai Spirit, FEI operating at an accelerating voltage of 120 kV (bright field imaging mode).

2.3.7 Batch rebinding studies

For binding studies, 30 mg of dried MIP and NIP polymer particles were suspended in 1.9 mL of PBS/ethanol solution (50/50 v/v %) containing different amounts (0; 0.1; 0.2; 0.4; 0.6; 0.8; 1.0; 1.2; 1.4; 1.6; 1.8 mM) of testosterone. Due to its low solubility in PBS, testosterone was first dissolved in ethanol and PBS was added subsequently. In case of micron sized MIP and NIP particles, the target molecule rebinding was performed at a pH of 4, 7 and 10 in order the find the best conditions. The optimal pH was then used for the rebinding studies using sub-micron sized MIPs and NIPs. After shaking overnight (16 h) at room temperature, the MIP and NIP particles were centrifuged down (15000 rpm, 40 min) and the supernatants were passed through a filter (0.2 µm Chromafil PTFE syringe filters). Calibration solutions containing testosterone were also treated via these filters to ascertain negligible retention by the filter. The amount of testosterone in the supernatant was quantified by measuring the UV absorbance (UV-Vis-NIR Spectrophotometer Cary 500 Scan from Varian) in a 10 mm quartz cuvette. These measurements were done with testosterone concentrations within the linear range of the calibration curve (Figure S2.3, Supporting Information), therefore the supernatants were diluted accordingly. For the blank measurement, the MIPs and NIPs were suspended in 50/50 ethanol/PBS without testosterone and subsequently centrifuged and filtered in the same way as the samples containing testosterone. All experiments were performed in triplicates; averaged values are discussed later. To test the response to testosterone of both bulk and miniemulsion polymer particles in the presence of other small molecule impurities, a batch rebinding experiment with a concentration of 0.8 mM testosterone in 1, 1, 1, 48.5, 48.5 v/v % butanol (109.25 mM), hexane (76 mM), cyclohexanone (96.5 mM), 1x PBS, ethanol respectively at pH 7 was performed.

2.3.8 Selectivity studies

The selectivity studies using different structurally analogue molecules, namely, β-estradiol, estriol and 17α-methyltestosterone were performed at pH 7 employing the same procedure used for the batch rebinding studies. For this, 30 mg of dried MIP and NIP polymer particles weighed in different containers were suspended in

1.9 mL of 50/50 ethanol/PBS buffer solution containing 0.8 mM of the respective test molecules. In each case, the amount of unbound molecules in the supernatant was then quantified by measuring the characteristic UV absorbance as before (Figure S2.2, Supporting Information). All experiments were performed in triplicates; average values are discussed later.

2.4 Results and discussion

As discussed above, MIP particles on the micron (bulk MIPs) and sub-micron scale (colloidal MIPs) were prepared using testosterone as template and NOBE as bifunctional cross-linker. As the latter has been previously shown to be suitable for imprinting small organic molecules especially containing hydroxyl or carboxyl groups [57], it is expected that the template molecule testosterone containing a significant hydroxyl group at C-17 can selectively bind via H-bonding to the polymer MIP matrix. While the micron sized MIPs were prepared by crushing and grinding the polymer monoliths obtained by bulk polymerization, the sub-micron sized colloidal MIPs were obtained via the miniemulsion technique as water based dispersions. In order to be able to directly compare the effectiveness of the MIPs produced under the different conditions (both employ free radical polymerization), the ratio of the active ingredients in the formulation was kept the same in both synthesis methods. The bulk MIPs require generally mechanical processing steps, thus there was inherent loss of material before characterization. In case of miniemulsion MIPs, as the hydrophobic cross-linking monomer is highly reactive, the reaction conditions (emulsion formulation and the reaction time) were optimized to yield coagulate-free stable dispersions. The optimized formulations used in the synthesis procedures are given in the experimental part. As polymerization using elevated temperature resulted in coagulation in the emulsion, UV polymerization was used for both synthesis approaches. This is also in agreement with previous findings where uniform microsphere MIPs were successfully prepared by UV initiation from NOBE rather than from thermal initiation.[58] For both production methods, non-imprinted polymer (NIP) particles were prepared as controls in an identical way as the MIP particles by following precisely the same procedures just in absence of the target molecules.

2.4.1 Characterization of bulk and colloidal MIP particles

The individual MIP particles were characterized using the techniques relevant to their respective scales. The size and the morphology of the synthesized MIPs were characterized using an optical microscope in case of bulk MIPs and using TEM for colloidal MIPs (Figure 2.3). As there were no characteristic differences in morphology between MIP and NIP particles produced using the respective methods, only images from NIPs are shown here and the MIP data are presented in Figure S2.4 in the Supporting Information. As can be seen in Figure 2.3 and S2.4, the crushed bulk MIPs and NIPs have irregular shapes with a very broad size range (1 - 50 µm), while the colloidal MIPs and NIPs have a spherical morphology and a size in the sub-micron range (as synthesized without any size selection). The colloidal MIPs were further analyzed for their size and size distribution (polydispersity index, PDI) using dynamic light scattering. The average hydrodynamic diameter was about 539 ± 49 nm (PDI 0.20) and 435 ± 20 (PDI 0.19) nm for the MIP and NIP, respectively.

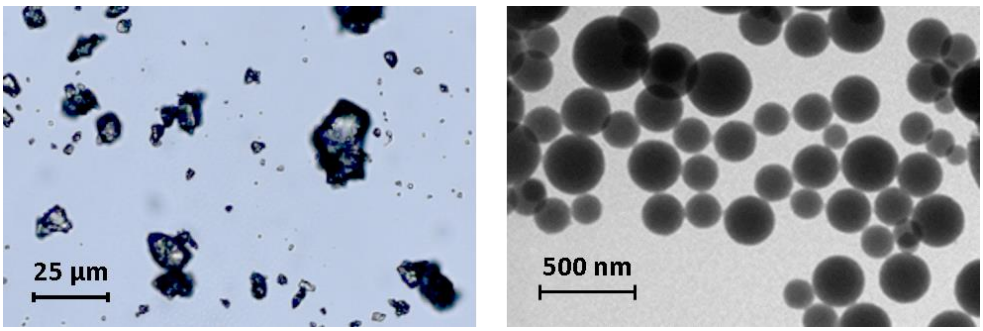

Figure 2.3. Optical microscope image of crushed bulk NIP (left) and a TEM image of the colloidal NIP (right) particles.

From these values, it can be inferred that the presence of the template molecule influences the size of the MIP particles. Previously, it has been shown that the presence of template influences the size distribution of the imprinted microspheres prepared by precipitation polymerization. Although the exact reasoning was

lacking, the molecular complexation between the template and the monomer was attributed as a difference towards the non-templated reaction system.[58] In case of miniemulsions, depending on the hydrophobicity the template molecules might also act as osmotic control agents.[52] However, as testosterone is slightly soluble in water, it will not fulfill this function effectively. In addition, the monomer used here can self-associate due to hydrogen bonds. Therefore, for a specific target-monomer combination, the hydrogen bonds between the monomer units will be influenced by the presence of the target molecules. The latter might affect the compactness of the resulting particles after polymerization. Concomitantly, in case of NIP particles where there are no target molecules involved, the size of the particles were indeed smaller as compared to MIP particles.

The size and the size distribution determined by DLS are in agreement with the observations made using TEM characterization. Though a narrow size distribution is expected for miniemulsion polymerized particles, the use of cross-linker can have an influence on the particle sizes.[41] Nevertheless, the sizes obtained here are similar to the values reported by *Vaihinger et al.* previously.[40] After polymerization, the conversion efficiency in case of the colloidal particles was determined in terms of solid content of the dispersion (containing only particulates, excluding any large aggregates/bulk material formed during the reaction) gravimetrically. Both the colloidal MIP and NIP particle formulations resulted in coagulate-free stable polymer dispersions with a conversion efficiency above 85 %. Despite the high reactivity of the cross-linking monomer, this significantly high conversion value clearly indicates the successful polymerization in the droplet phase and only very little loss incurred likely due to interparticle cross-linking leading to larger aggregate formation. Evidently, the presence of template molecule had no impact on the conversion efficiency as both MIP and NIP formulations resulted in high yields.

2.4.2 Batch rebinding studies

The molecular recognition capacity of the different MIPs was studied using equilibrium binding analysis. Due to the practical significance of the specific binding of the target molecule in the aqueous media, the batch rebinding studies were performed using a mixture of buffer/ethanol solution. The binding properties

of the bulk MIPs were first analyzed using batch rebinding experiments at various pH values and the NIP particles were used as control. The optimal pH value for recognition was evaluated and further used for batch rebinding studies using miniemulsion colloidal MIP and NIP particles. The rational behind using bulk MIPs for testing at all pHs is to evaluate the performance of the given monomer-template combination as a function of pH as this combination has never been reported in the literature. The miniemulsion particles were synthesized using surfactant that might interfere with the binding. Therefore, the evaluation using bulk MIP/NIP particles was opted as they will reflect the inherent performance of the used monomer (polymer)-template combination. For the batch rebinding studies, a fixed amount of washed and dried MIP and NIP particles were resuspended in a PBS/ethanol solution (50/50 v/v %) and incubated with a known concentration (ranging from 0.1 – 1.8 mM) of the template molecule testosterone. After the separation of the polymer particles by centrifugation, the free target molecule concentration (C_f) in the supernatant was analyzed using UV-Vis spectrophotometry. From the free concentration, the amount of testosterone molecule bound to both MIPs and NIPs (S_b) was determined. Figure 2.4 illustrates the binding isotherms obtained for both bulk MIP and NIP samples at pH 4, 7 and 10 by using different concentrations of testosterone. There are several models available to describe binding isotherms. Since both bulk and miniemulsion MIPs contain a heterogeneous distribution of binding sites and affinity constants, the Freundlich model is applied.[59, 60] The data were fitted by non-linear least square fitting ($S_b = AC_f^v$, where S_b is the amount of target molecule bound to the polymer particles, A is the Freundlich constant, C_f is the free concentration of target molecule and v is the Freundlich heterogeneity parameter).[4] As it can be seen, for any pH, there is a clear increase in the amount of bound testosterone with increasing concentration of testosterone. With increasing pH, also a clear trend is observed towards higher binding affinities. Although the binding of testosterone is not via electrostatic interactions, during the template washing procedure, the MIP-NIP particles made using only the crosslinking monomer NOBE (containing hydrolysis susceptible functionalities) can be affected by polymer hydrolysis. In some likelihood, pH dependent non-specific binding to the MIP-NIP pair can be anticipated for this template-polymer combination. With some of the hydrolyzed

ester groups, electrostatic interaction can prevail where with higher pH values a pronounced effect due to deprotonated carboxyl group can be expected.

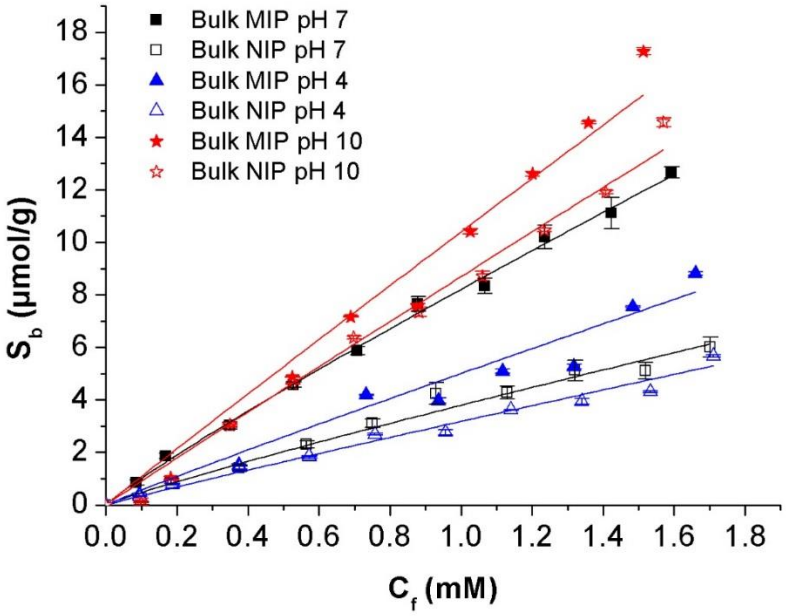

Figure 2.4. Non-linearly fitted binding isotherm with the target molecule concentration ranging from 0.1 – 1.8 mM for bulk MIP and NIP particles at pH 4, 7 and 10.

Also, during the batch rebinding studies, with incubation for several hours at pH conditions especially favouring hydrolysis, more damage to the polymer chains leading to swelling of the polymer matrix and thereby altering the cross-linked network is plausible. The latter can indeed significantly reduce the selective binding of the target molecules. The results in Figure 2.4 are in line with the above-mentioned points where at pH 10 an increased non-specific binding prevails via the electrostatic interaction as both MIP and NIP show substantial binding as compared to pH 4 and 7. It is apparent that basic conditions are quite detrimental due to accelerated hydrolysis for this polymer-template combination. However, at pH 7, the interaction of the solvent with the polymer matrix is likely enhanced due to the slightly swollen polymer matrix as compared to pH 4. Consequently, the hydrophobic interactions that might be responsible for aspecific binding can also

be minimized. The improved performance of MIP as compared to NIP at pH 7 reflects the latter arguments and indicates clearly that pH 7 is optimal for this polymer-template combination.

In all cases, a higher affinity of the MIPs for testosterone was observed compared to the NIPs indicating the existence of favourable interaction between the imprinted binding site and the template. In order to evaluate the specificity, the imprint factor, which is the ratio of the amount of target molecules bound per gram of the MIP to that of the NIP (S_b MIP/S_b NIP), was determined. As the aspecific binding is more pronounced for higher concentrations of the template molecule, the imprint factor was analyzed at a free concentration (C_f) of 0.8 mM. At this C_f, the imprint factors obtained were 1.6, 2.2 and 1.2 for pH 4, 7 and 10, respectively. A similar IF has been reported for testosterone templated MAA/EGDMA MIPs using chloroform as a porogen but ACN for the rebinding studies.[26] It is important to note that a strict comparison of the performance of the MIPs is difficult, as the solvent choice plays a crucial role in binding experiments. From the general trend of the binding isotherms (Figure 2.4) and the calculated imprint factors, a significant difference in binding between the MIP and NIP exists at pH 7 as compared to pH 4 and 10. From these findings, it was ascertained that a neutral pH was optimal for evaluating the performance of the miniemulsion based colloidal MIP particles.

Figure 2.5 illustrates the binding isotherms of colloidal MIP and NIP particles synthesized using the miniemulsion technique (ME MIP and ME NIP). For the sake of comparison and convenience, binding isotherms of bulk polymerized MIP and NIP particles are also included in the same graph. The distribution of the affinity sites is provided in the supporting information (Figure S2.5, Supporting Information). From the plot, it is clearly evident that the colloidal MIPs have a much higher binding affinity compared to the associated NIP particles, even though the bulk MIP particles display the highest absolute affinity. At C_f = 0.8 mM, the imprint factor is determined to be 6.8, which is higher in comparison to the previously reported values and approximately three times better compared to the bulk MIP-NIP combination.[24-27] The high imprint factor demonstrates that the template molecule has specific interaction owing to the imprinting sites within the polymer matrix. This enhanced performance of the colloidal MIP particles hints

towards the existence of well-defined recognition sites as a result of highly organized template-monomer interactions in the solution phase prior to polymerization. Although chloroform was used as the choice of porogen for both the MIP types, it is worth to note that despite water being used as continuous phase for the synthesis in case of the colloidal MIPs, the interaction (H-bonding) between the template and the monomer is largely uninterrupted.

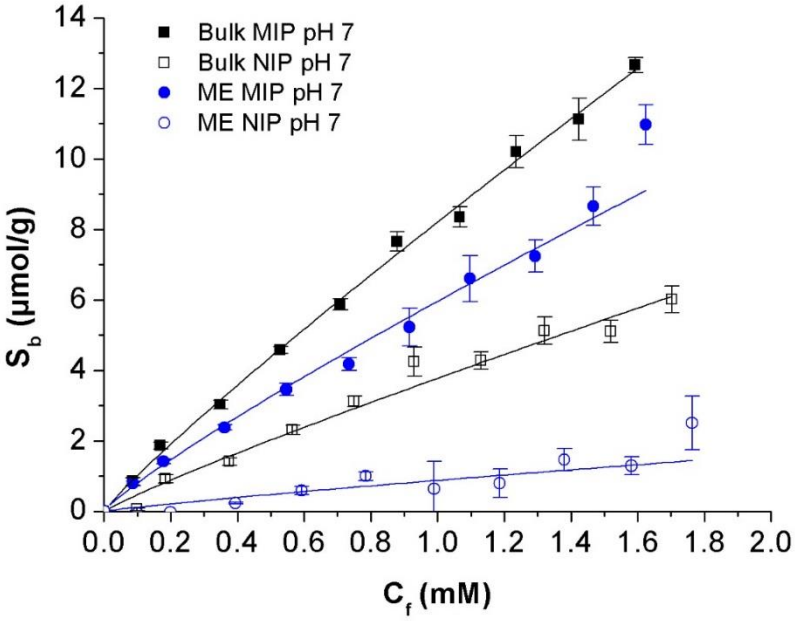

Figure 2.5. Non-linearly fitted binding isotherm with a target molecule concentration ranging from 0.1 – 1.8 mM performed for bulk and colloidal MIP and NIP particles at pH 7.

Also, the presence of the surfactant layer during the synthesis impedes the surface imprinting possibility, which might explain why the colloidal MIPs display significantly improved imprint factors, but not necessarily the highest absolute binding capacity. As the residual surfactants are present in both MIP and NIP samples (same procedure was applied), the influence of the former during rebinding can be safely neglected for the analysis. Regardless, it can be directly concluded that the miniemulsion NIP particles show significantly less aspecificity as compared to the bulk NIP particles.

As the rebinding studies were performed in aqueous solutions, it might be that the performance of the bulk MIP-NIP duo is affected. The polymers perform the best when analyzed using the solvent they were polymerized in as only in this way the interactions existing prior to and during the polymerization are matched.[48, 61] It has been previously suggested that H-bonding plays a predominant role in organic solvents and both hydrophobic interactions as well as H-bonding can contribute in case of hydro-organic phases.[62, 63] Since the solubility of testosterone is limited in water, hydrophobic interactions are very likely to occur between the polymer and the template molecule.
This is also in accordance to other studies involving chromatographic evaluations, where the retention of templates of moderate to low polarity in aqueous phase has been attributed to hydrophobic effects.[49, 64] Therefore, rebinding in the aqueous mixture can lead to unanticipated aspecific interactions in case of bulk MIP and NIP particles. In all likelihood, the non-mimicking interactions due to the change of solvent (as compared to the one used during the polymerization) might be the plausible explanation for the increased non-specific adsorption in case of bulk MIP and NIP samples. By the same token, in case of colloidal MIPs, the aforementioned reasons do not play a role as the particles were produced in water phase. This aspect makes these colloidal MIPs very attractive as imprinting and recognition can both be performed using aqueous media.

To test the response to testosterone of both bulk and miniemulsion polymer particles in the presence of other small molecule impurities, a batch rebinding experiment with a concentration of 0.8 mM testosterone in the presence of butanol, hexane and cyclohexanone in PBS/ethanol solution at pH 7 was performed. The results are shown in Figure S2.6 in the Supporting Information. Both the bulk and miniemulsion MIP – NIP pairs show specific binding for testosterone in the presence of the small molecule impurities. Also in accordance to the previous observation, the miniemulsion NIPs show relatively less aspecific binding than the bulk counterpart.

2.4.3 Selectivity studies

In here, the bulk and the colloidal MIPs synthesized using testosterone as template molecule were tested for the binding of structurally similar molecules. As

structural analogues of the template molecule, *β*-estradiol, estriol and 17*α*-methyltestosterone were chosen and subsequently tested using batch rebinding studies employing fixed amounts of the respective molecules (see Figure 2.2). The structural analogues all differ only marginally from testosterone, and thus provide – even though very interesting steroid targets themselves for recognition – a very sensitive probe for the selectivity of the MIP binding sites. The performance of bulk and colloidal MIP-NIP samples for the specific recognition of structurally similar analytes tested using an initial concentration of 0.8 mM at pH 7 are shown in Figure 2.6. The values presented in this graph are the bound concentrations (S_b) of the analyte to the MIP, corrected for the aspecific binding to the NIP (S_b MIP – S_b NIP). Figure S2.7 in the supporting information presents the bound concentrations to the MIP and NIP separately. In Figure 2.6, it can be seen that both the bulk and the miniemulsion particles show – unsurprisingly – the highest affinity for testosterone as compared to the other molecules (tested at pH = 7 using 0.8 mM initial concentration). Of the structural analogues, both types of MIP particles show a distinct affinity to 17*α*-methyl testosterone and *β*-estradiol. With estriol molecules, the colloidal MIPs show no significant affinity. Estriol is from the list of tested substances the molecule which contains the largest variation compared to testosterone. Thus, the general trend seen (decreasing affinity for bulk and colloidal MIPs from testosterone over methyl testosterone, estradiol to estriol) can be well reasoned based on the variation in (polar) chemical functionality in the molecules.

Testosterone is a tetracyclic steroid molecule with a sterically demanding C-18 methyl group and has a ketone and a hydroxyl functionality at C-3 and C-17 positions, respectively. From the structures depicted in Figure 2.2, it can be seen that 17*α*-methyl testosterone can fit well in the imprints created by testosterone molecules due to its close resemblance to the latter. A decreasing affinity trend can be observed with *β*-estradiol. Despite the hydroxyl group at C-17 position, this reduced affinity indicates that this functionality alone is not sufficient for the binding.

Among the structural analogues, estriol has the least resemblance to the template molecule with an excess hydroxyl group at the C-16 position. Apart from sterical hindrance, the latter can potentially interfere via additional H-bonding with the

polymer matrix resulting in less affinity to the imprints. From these observations, it can be directly inferred that the ability of a MIP to bind a structurally analogous molecule is strongly dependent on the laters' structural resemblance to the imprinted molecule in terms of shape and number as well as positioning of the functional groups that allows to dock efficiently within the receptor cavity.

Evidently, in case of bulk MIPs, the effect is predominantly governed by aspecific binding as also bulk NIP particles show increased affinities. The colloidal MIPs show generally lower affinity to the template variation, and with the slight exception of methyl testosterone also only insignificant higher binding of the MIPs compared to the NIPs.

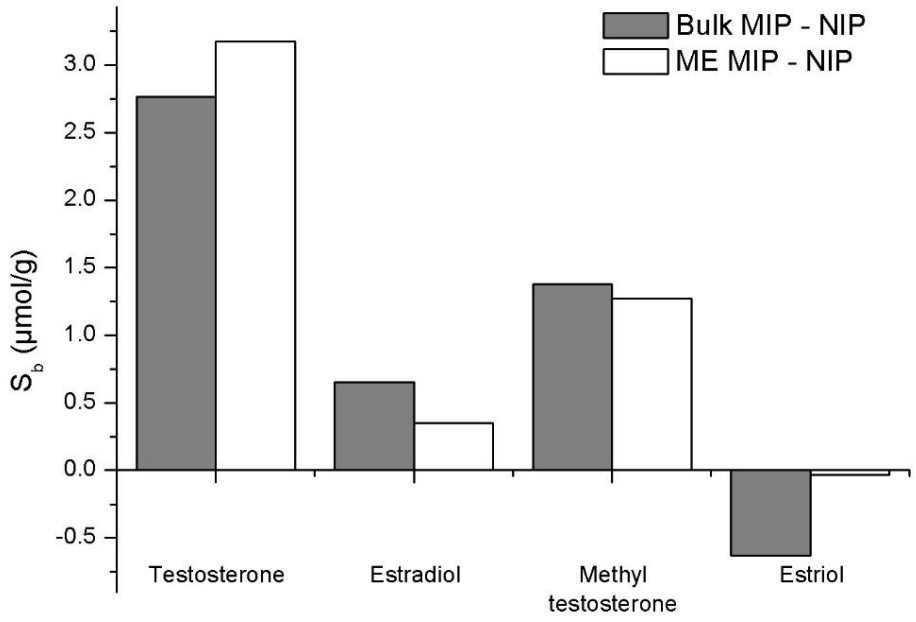

Figure 2.6. Graphical representation of the performance of bulk and colloidal MIP-NIP samples for the specific recognition of structurally similar analytes tested using an initial concentration of 0.8 mM at pH 7. The Y-axis represents the bound concentrations (Sb) of the analyte to the MIP corrected for aspecific binding (Sb MIP – Sb NIP).

The enhanced aspecific binding of testosterone as compared to the other structural analogues (seen more clearly in Figure S2.7) might be attributed to the C19 methyl group that might play a critical role in the hydrophobic interaction of

testosterone with the polymer matrix. As the latter type of interaction is more pronounced in case of hydro-organic phases, the aspecific binding of testosterone to the MIP-NIP duo via the methyl group can be expected. This is also in accordance to the fact that while 17α-methyltestosterone, which also has a C19 methyl group, shows a higher aspecificity whereas estriol and 17β-estradiol, which are both lacking the C19 methyl group, exhibit relatively less aspecific binding. Despite the C19 methyl group, the sterical hindrance provided by the C17 methyl group in case of 17α-methyl testosterone might be a plausible reason for the reduced non-specific binding of the latter as compared to testosterone.

2.5 Conclusions and outlook

NOBE based micron sized MIP and sub-micron sized colloidal MIP particles templated with testosterone were successfully prepared employing bulk and miniemulsion polymerizations, respectively. Equilibrium binding analysis in aqueous solution was performed to evaluate the molecular recognition capacity of the different MIPs. Both bulk MIP and colloidal MIPs showed higher affinity for the target molecule as compared to their respective non-imprinted counterparts. The selectivity of the MIPs in the presence of small molecule impurities was also tested successfully. The imprint factor determined for the colloidal MIP-NIP duo was superior to the bulk MIP-NIP combination. The colloidal NIP showed significantly less aspecificity as compared to the bulk NIP. The same trend was also observed in the presence of small molecule impurities. The use of different solvent (in here solvent mixtures) during rebinding as compared to the one used during polymerization might be the plausible explanation for the increased non-specific adsorption in case of bulk MIP and NIP samples. Both bulk and the colloidal MIPs imprinted with testosterone as template molecule were tested for the binding of structurally similar molecules. It was found that the recognition of the structural analogues is strongly dependent on the extent of their structural resemblances to the imprinted molecule in terms of shape and number as well as positioning of the functional groups for efficient docking within the receptor cavity. The selectivity findings clearly point out once again the need for understanding the functional group interactions between the monomers and target molecules for pre-determined selectivity. In concise, for the first time colloidal MIPs using the

simplified synthesis protocol employing single monomer for the recognition of testosterone and its structural analogues in aqueous solution are made available. As compared to the traditional MIPs (w.r.t. monomer mixtures), the developed materials with regular shapes are highly interesting for use in affinity columns as well as sensing elements in bioanalytical detection applications. Detailed competitive assays and cross-reactivity studies are currently in progress in our laboratories. As these water based stable MIP dispersions can be readily transferred to substrates efficiently by simple deposition methods (spin coating, drop casting) [65], currently they are also being tested for the fabrication of sensors in our labs employing various electrical read-out techniques.

2.6 Supporting information

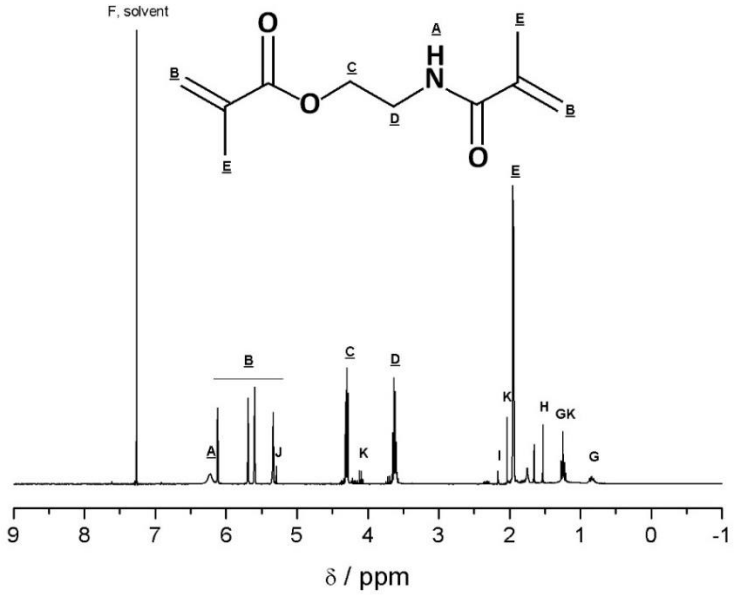

Figure S2.1. 1H-NMR (CDCl3, 400 MHz) spectrum of N,O-bismethacryloyl ethanolamine NOBE as used for MIP synthesis. The peaks F, G, H, I, J and K correspond to chloroform (δ= 7.26), petroleum spirit (δ= 1.26, 0.88), water (δ= 1.56), acetone (δ= 2.17), dichloromethane (δ= 5.30) and ethyl acetate (δ= 1.26, 2.05, 4.12) respectively. NOBE polymerizes spontaneously when kept unrefrigerated, thus residual solvents were not fully removed in vacuum to keep exposure to light and temperature as short as possible.

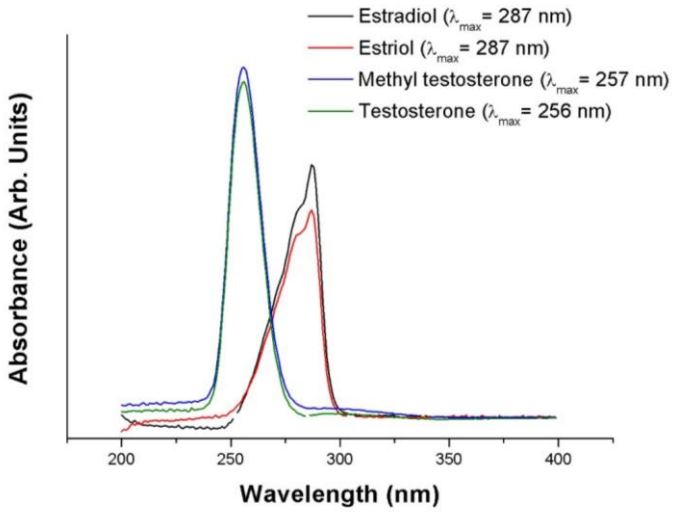

Figure S2.2. UV-Vis absorption spectra of 17β-estradiol, estriol, 17α-methyl testosterone and testosterone measured in PBS/ethanol solution (50/50 v/v %).

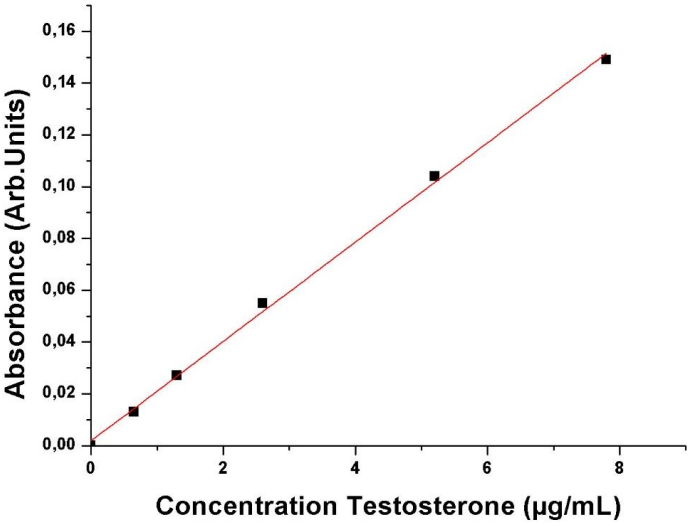

Figure S2.3. Calibration curve (linear fit R2 = 0.99) used for estimating the concentration of testosterone in PBS/ethanol solution (50/50 v/v %) using UV-Vis spectroscopy (employing Beer-Lambert law).

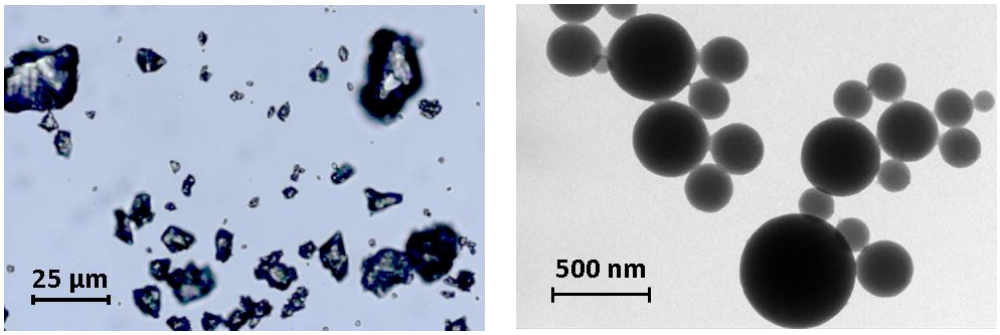

Figure S2.4. Optical microscope image of crushed bulk MIP (left) and a TEM image of the colloidal MIP (right) particles.

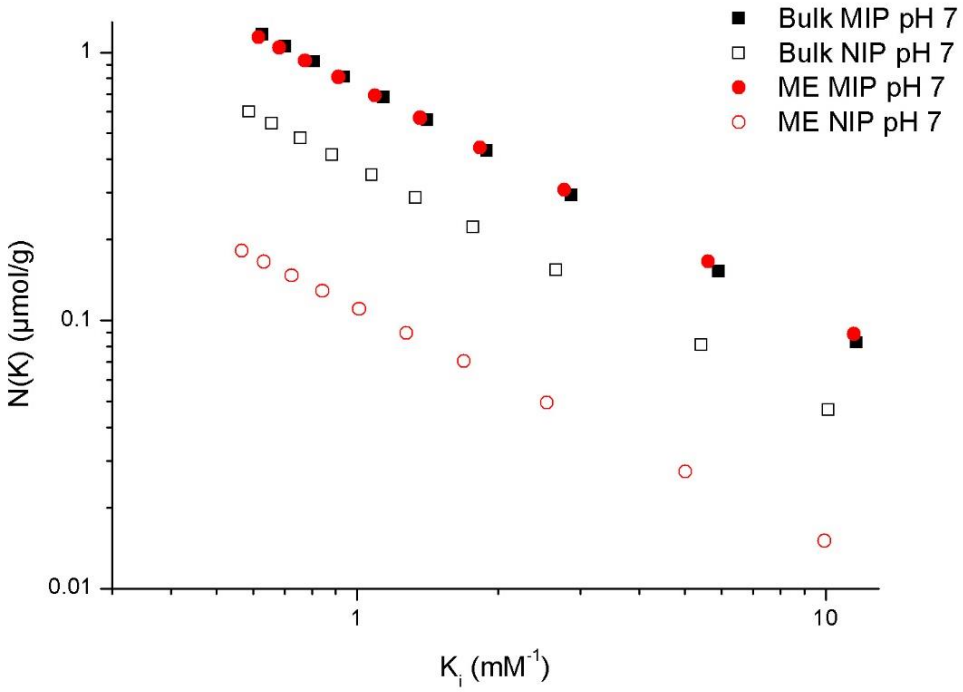

Figure S2.5. Distribution of the affinity sites: Freundlich isotherm in which the amount of binding sites (N) is presented as a function of a given binding constant (Ki) for both the bulk and miniemulsion MIPs and NIPs at pH 7 upon exposure to various testosterone concentrations (0.1 – 1.8 mM).

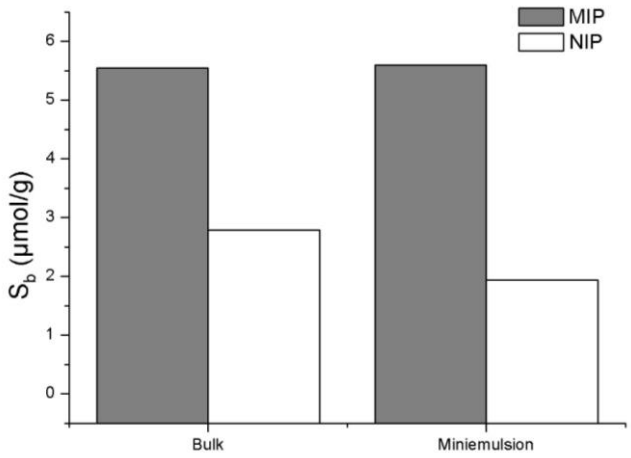

Figure S2.6. Graphical representation of the performance of bulk and colloidal MIP-NIP samples for the recognition of testosterone tested using an initial concentration of 0.8 mM at pH 7 in the presence of small impurities (butanol, hexane and cyclohexanone).

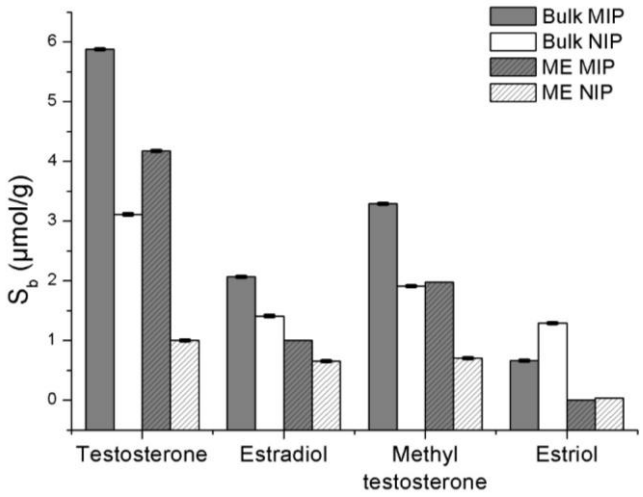

Figure S2.7. Graphical representation of the performance of bulk and colloidal MIP-NIP samples for the recognition of structurally similar analytes tested using an initial concentration of 0.8 mM at pH 7.

2.7 References

[1] K. Mosbach, *Trends Biochem. Sci.* **1994**, 19, 9.

[2] B. Sellergren, *Molecularly Imprinted Polymers. Man-Made Mimics of Antibodies and their Application in Analytical Chemistry*, Elsevier Science, Amsterdam, The Netherlands **2000**.

[3] G. E. M. Tovar, I. Kräuter, C. Gruber, *Top. Curr. Chem.* **2003**, 227, 125.

[4] D. Spivak, *Adv. Drug Deliv. Rev.* **2005**, 57, 1779.

[5] C. Alexander, H. S. Andersson, L. I. Andersson, R. J. Ansell, N. Kirsch, I. A. Nicholls, J. O'Mahony, M. J. Whitcombe, *J. Mol. Recognit.* **2006**, 19, 106.

[6] R. J. Ansell, *J. Chromatogr. B: Anal. Technol. Biomed. Life Sci.* **2004**, 804, 151.

[7] S. Wei, B. Mizaikoff, *J. Sep. Sci* **2007**, 30, 1794.

[8] M. Abdouss, E. Asadi, S. Azodi-Deilami, N. Beik-mohammadi, S. Amir Aslanzadeh, *J. Mater. Sci. Mater. Med.* **2011**, 22, 2273.

[9] M. Peeters, F. J. Troost, B. van Grinsven, F. Horemans, J. Alenus, D. Keszthelyi, A. Ethirajan, R. Thoelen, T. J. Cleij, P. Wagner, *Sens. Actuators B Chem.* **2012**, 171-172, 602.

[10] J. Alenus, A. Ethirajan, F. Horemans, A. Weustenraed, P. Csipai, J. Gruber, M. Peeters, T. J. Cleij, P. Wagner, *Anal. Bioanal. Chem.* **2013**, 405, 6479.

[11] E. Asadi, S. Azodi-Deilami, M. Abdouss, D. Kordestani, A. Rahimi, S. Asadi, *Korean J. Chem. Eng.* **2014**, 31, 1028.

[12] D. Thieme, P. Hemmersbach, *Doping in sports*, Vol. 195, Springer Science & Business Media, **2009**.

[13] J. Cauley, F. Lucas, L. Kuller, K. Stone, W. Browner, S. Cummings, *Ann. Intern. Med.* **1999**, 130, 270.

[14] Z. Hyde, L. Flicker, K. McCaul, O. Almeida, G. Hankey, S. Chubb, B. Yeap, *Canc. Epidemiol. Biomarkers Prev.* **2012**, 21, 1319.

[15] H. Jin, J. Lin, L. Fu, Y.-F. Mei, G. Peng, X. Tan, D.-M. Wang, W. Wang, Y.-G. Li, *Biochem. Cell Biol.* **2007**, 85, 246.

[16] M. Hoffman, W. DeWolf, A. Morgentaler, *J. Urol.* **2000**, 163, 824.

[17] M. Akishita, M. Hashimoto, Y. Ohike, S. Ogawa, K. Iijima, M. Eto, Y. Ouchi, *Atherosclerosis* **2010**, 210, 232.

[18] M. Schubert, F. Jockenhövel, *Der Urologe* **2010**, 49, 47.

[19] U. Srinivas-Shankar, S. Roberts, M. Connolly, M. O'Connell, J. Adams, J. Oldham, F. Wu, *J. Clin. Endocrinol. Metab.* **2010**, 95, 639.

[20] C. Saudan, N. Baume, N. Robinson, L. Avois, P. Mangin, M. Saugy, *Br J Sports Med* **2006**, 40 Suppl 1, i21.

[21] J. Taieb, B. Mathian, P. Boudou, F. Millot, J. Y. Badonnel, I. Lacroix, E. Mathieu, N. Queyrel, C. Somma-Delpero, M. C. Patricot, *Immuno. Anal. Biol. Spé.* **2001**, 16, 338.

[22] F. Gasser, N. Jeandidier, S. Doffoel, F. Klein, R. Sapin, *Immuno. Anal Biol. Spé.* **2003**, 18, 98.

[23] J. Taieb, B. Mathian, F. Millot, M. C. Patricot, E. Mathieu, N. Queyrel, I. Lacroix, C. Somma-Delpero, P. Boudou, *Clin. Chem.* **2003**, 49, 1381.

[24] S. Mirmahdieh, A. Mardihallaj, Z. Hashemian, J. Razavizadeh, H. Ghaziaskar, T. Khayamian, *J. Sep. Sci.* **2011**, 34, 107.

[25] Y. Long, J. Y. Philip, K. Schillen, F. Liu, L. Ye, *J. Mol. Recognit.* **2011**, 24, 619.

[26] S.-H. Cheong, A. E. Rachkov, J.-K. Park, K. Yano, I. Karube, *J. Polym. Sci. A Polym. Chem.* **1998**, 36, 1725.

[27] K. R. Noss, A. D. Vaughan, M. E. Byrne, *J. Polym. Sci. A Polym. Chem.* **2008**, 107, 3435.

[28] Y. Tan, L. Jing, Y. Ding, T. Wei, *Appl. Surf. Sci.* **2015**, 342, 84.

[29] A. Betatache, F. Lagarde, C. Sanglar, A. Bonhomme, D. Leonard, N. Jaffrezic-Renault, *Sensors and Transducers* **2014**, 27, 92.

[30] Y. Chen, Y. Liu, X. Shen, Z. Chang, L. Tang, W.-F. Dong, M. Li, J.-J. He, *Sensors* **2015**, 15, 29877.

[31] J. Alenus, P. Galar, A. Ethirajan, F. Horemans, A. Weustenraed, T. J. Cleij, P. Wagner, *Phys. Status Solidi A* **2012**, 209, 905.

[32] O. Brueggemann, K. Haupt, L. Ye, E. Yilmaz, K. Mosbach, *J. Chromatogr. A* **2000**, 889, 15.

[33] F. Svec, J. M. J. Frechet, *Anal. Chem.* **1992**, 64, 820.

[34] R. Thoelen, R. Vansweevelt, J. Duchateau, F. Horemans, J. D'Haen, L. Lutsen, D. Vanderzande, M. Ameloot, M. vandeVen, T. J. Cleij, P. Wagner, *Biosens. Bioelectron.* **2008**, 23, 913.

[35] H. Yan, K. Row, *Int. J. Mol. Sci.* **2006**, 7, 155.

[36] A. G. Mayes, K. Mosbach, *Anal. Chem.* **1996**, 68, 3769.

[37] K. Hosoya, K. Yoshizako, Y. Shirasu, K. Kimata, T. Araki, N. Tanaka, J. Haginaka, *J. Chromatogr. A* **1996**, 728, 139.

[38] R. J. Ansell, K. Mosbach, *J. Chromatogr. A* **1997**, 787, 55.

[39] L. Ye, R. Weiss, K. Mosbach, *Macromolecules* **2000**, 33, 8239.

[40] D. Vaihinger, K. Landfester, I. Kräuter, H. Brunner, G. E. M. Tovar, *Macromol. Chem. Phys.* **2002**, 203, 1965.

[41] B. Pluhar, U. Ziener, B. Mizaikoff, *J. Mater. Chem. B* **2013**, 1, 5489.

[42] B. Pluhar, B. Mizaikoff, *Macromol. Biosci.* **2015**, 15, 1507.

[43] Z. Adali-Kaya, B. Tse Sum Bui, A. Falcimaigne-Cordin, K. Haupt, *Angew. Chem. Int. Ed. (English)* **2015**, 54, 5192.

[44] H. Kim, D. A. Spivak, *J. Am. Chem. Soc.* **2003**, 125, 11269.

[45] M. Sibrian-Vazquez, D. A. Spivak, *Macromolecules* **2003**, 36, 5105.

[46] J. LeJeune, D. A. Spivak, *Analytical and bioanalytical chemistry* **2007**, 389, 433.

[47] M. Kempe, *Anal. Chem.* **1996**, 68, 1948.

[48] D. Spivak, M. A. Gilmore, K. J. Shea, *J. Am. Chem. Soc.* **1997**, 119, 4388.

[49] C. Yu, O. Ramström, K. Mosbach, *Anal. Lett.* **1997**, 30, 2123.

[50] C. Yu, K. Mosbach, *J. Chromatogr. A* **2000**, 888, 63.

[51] A. Ethirajan, L. Baeten, M. Conradi, K. Ranieri, B. Conings, H.-G. Boyen, T. Junkers, *Polym. Chem.* **2013**, 4, 4010.

[52] K. Landfester, *Angew. Chem. Int. Ed.* **2009**, 48, 4488.

[53] A. Ethirajan, K. Landfester, *Chem. Eur. J.* **2010**, 16, 9398.

[54] A. Ethirajan, A. Musyanovych, A. Chuvilin, K. Landfester, *Macromol. Chem. Phys.* **2011**, 212, 915.

[55] H. M. Kuch, K. Ballschmiter, *Environ. Sci. Technol.* **2001**, 35, 3201.

[56] P. Lucci, O. Núñez, M. T. Galceran, *J. Chromatogr. A* **2011**, 1218, 4828.

[57] M. Sibrian-Vazquez, D. A. Spivak, *J. Polym. Sci. Part A: Polym. Chem.* **2004**, 42, 3668.

[58] K. Yoshimatsu, J. LeJeune, D. Spivak, L. Ye, *Analyst* **2009**, 134, 719.

[59] H. Freundlich, *Z. Phys. Chem.* **1906**, 57, 385.

[60] I. R. Umpleby, S. Baxter, A. Rampey, G. Rushton, Y. Chen, K. Shimizu, *J. Chromatogr. B* **2004**, 804, 141.

[61] M. Kempe, K. Mosbach, *Anal. Lett.* **1991**, 24, 1137.

[62] V. Pichon, K. Haupt, *J. Liq. Chrom. Relat. Tech.* **2006**, 29, 989.

[63] B. Tse Sum Bui, K. Haupt, *J. Mol. Recognit.* **2011**, 24, 1123.

[64] C. Yu, K. Mosbach, *J. Mol. Recognit.* **1998**, 11, 69.

[65] A. Zeller, A. Musyanovych, M. Kappl, A. Ethirajan, M. Dass, D. Markova, M. Klapper, K. Landfester, *ACS Appl. Mater. Interfaces* **2010**, 2, 2421.

3 Molecularly imprinted polymer nanoparticles on a functionalized diamond sensor interface: A simple and robust sensor platform for the electronic detection of testosterone in biological samples

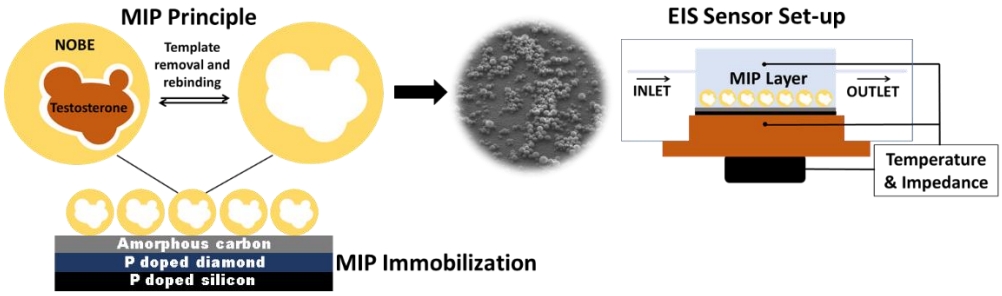

3.1 Abstract

Molecularly imprinted polymers (MIPs) can be used as a replacement for the fragile and expensive natural receptors (e.g., antibodies) in sensor applications. One of the many challenges in this field includes the reliable immobilization of MIPs on the transducer substrate. In this work, the direct covalent coupling of miniemulsion based colloidal MIP particles containing vinyl surface groups to an amorphous carbon functionalized transducer substrate was studied. Using a direct carbon based conjugation avoids the impairment in the function of the MIP particles and reduces the sample preparation steps while still offering a strong and reliable coupling. Bifunctional cross-linker N,O-bismethacryloyl ethanolamine (NOBE) based miniemulsion MIPs were used as they offer great advantages due to their inherent physical characteristics and improved recognition of target molecules in comparison with the widely employed bulk MIP counterparts. In addition, owing to their large surface to volume ratio, MIP nanoparticles display an increased active sensing surface that is crucial for the performance of the sensor. The sensor substrates were characterized using scanning electron

microscopy which shows a uniform MIP particle distribution on the surface. As a proof of concept, the sensor performance to detect hormone disruptor testosterone in urine samples in the physiological concentration range is successfully verified using electrochemical impedance spectroscopy as a read-out technique. The simple and efficient method for the direct particle immobilization on the transducer surface described in this work can be easily extended to detect other target molecules and can generally be applied in the development of low-cost and robust colloidal MIP based sensing devices.

3.2 Introduction

Recognition of molecules with high affinity and selectivity are crucial for the detection of (bio-) molecules. The development of a sensor which is low-cost, accurate and user-friendly is highly interesting in the field of point-of-care medical diagnostics and food- and environmental safety in general. In these sensors, biological receptors such as antibodies, enzymes, DNA and aptamers can be used as a sensing receptor element as they offer highly specific molecular recognition for their target molecules.[1-5] However, these natural receptors are laborious and expensive to obtain. In addition, they offer insufficient physical and chemical stability when physiological conditions such as temperature and pH are deviating, resulting in decreased selectivity towards the target molecule.[6] Therefore, the use of a synthetic receptor based on the molecular imprinting principle is a compelling alternative. Molecularly imprinted polymers (MIPs) are produced by polymerization in the presence of a template molecule. Subsequently, these templates are removed using several washing steps thereby leaving behind empty imprint sites. MIPs, have gained interest rapidly as they offer a high selectivity and affinity towards the target molecule while at the same time being robust and low-cost.[7, 8]

Testosterone is a marker for certain health conditions. Low concentrations of this steroid hormone can lead to uncommon skeletal and muscle growth and reduced masculinity.[9] High testosterone concentrations are related with increased chances of breast cancer in women [10] and prostate and lung cancer in men.[11] In order to avoid invasive procedures, which are risky and require specialized equipment, quantification in urine or saliva instead of blood is preferred. Today,

the techniques to quantify testosterone in the pg/mL range include high performance liquid chromatography [12], enzyme-linked immunosorbent assays [13, 14], radioimmunoassay [15], gas chromatography-mass spectrometry [16] and liquid chromatography-mass spectrometry [17]. The latter techniques are time consuming, expensive and require specialized personnel and equipment which makes them unsuitable for scalability, fast screening and point-of-care applications. In this regard, MIPs targeted for testosterone recognition is a highly intriguing choice as receptor element in a sensor platform.

In the development of a sensor device, a MIP layer can be polymerized directly in situ on the transducer substrate in order to provide a reliable immobilization. Chen et al. created a MIP film based on thermo polymerization for the detection of testosterone using micro ring resonance as a read-out and reached a limit of detection of 48.7 pg/mL.[18] Because of the large portion of physically inaccessible binding sites in the volume of a MIP film, researchers have been focussing on increasing the active sensing surface by patterning. Fuchs et al. designed a micro patterned MIP film based on photo polymerization with interfering laser beams for testosterone quantification.[19] In general, it is highly desired to design MIPs with a high active sensing surface area which are at the same time, efficiently immobilized on the transducer substrate.

The ex situ prepared micro- and nano- MIP particles are interesting due to their increased surface-to-volume ratio and many techniques have been successfully used for their production. Bulk polymerization is the most widely established MIP synthesis technique because of its simplicity. The obtained polymer monolith is crushed into irregularly shaped micron-sized particles with a broad size distribution.[20] In addition, the grinding step destroys some recognition sites which results in a reduced binding capacity [21, 22] while the size selection - for instance by sieving - leads to huge material losses.[23] Moreover, the high degree of inhomogeneity in size, shape and material distribution in bulk MIPs limits their applicability in sensor applications.

The latter mentioned restrictions can be circumvented by MIP synthesis techniques which offer more control over the physical geometries and sizes. Colloidal methods such as precipitation, suspension and emulsion techniques offer

spherical beads with a size in the micro- and nano meter range and therefore, a tremendously increased active sensing surface.[24-28] In our previous work, where we compared the bulk with the miniemulsion polymerization technique, we showed that the colloidal MIPs showed significantly improved recognition of the target molecule and the synthesis in aqueous media also resulted in decreased aspecific binding.[20] Moreover, we used the bi-functional crosslinking monomer N,O-bismethacryloyl ethanolamine (NOBE) employing the concept of a "one monomer MIP" (OMNiMIPs), thereby eliminating the need for empirical optimization of monomer combinations and ratios.[29-31] As the use of different crosslinking and functional monomers might also lead to inhomogeneous material, aspecific binding might be a consequence depending on the temple molecule - monomer combinations. NOBE has proven to be suitable for the non-covalent imprinting of hydroxyl and/or carboxyl containing small organic molecules such as testosterone.[30] The afore-mentioned properties make NOBE based miniemulsion MIP particles highly interesting for sensor applications.

For the use in sensor devices, the colloidal MIP particles need to be immobilized on the sensor transducer substrate. This can be obtained either through covalent coupling or through embedding/entrapment using an adhesive polymer layer.[32-35] However, the latter option can reduce the target molecule binding capacity of the MIP particles as part of the binding sites get physically blocked by the adhesive. In addition, a thick adhesive polymer might also interact with the target molecule causing unwanted aspecific binding. Also, the embedding of particles by physical entrapment might loosen up during the measurement and can lead to unforeseen erroneous detection. By using a direct covalent coupling, a firm fixation of the MIP particles can be realized and the imprint sites are easily accessible for the target molecules. Kamra et al. used perfluorophenylazide mediated photoconjugation chemistry to obtain a direct covalent coupling between MIP particles and the transducer. Despite a dense coverage of MIP particles, as the morphology was too rough and difficult to control, the applicability in sensors was limited.[36, 37] Later, they reported another approach to obtain covalent coupling resulting in smooth and homogeneous MIP particle layers by using epoxy silanes.[32] However, for the coupling with the silane epoxy terminal groups, the MIP particles need to be functionalized with amine functionalities. Alternatively,

immobilization of MIPs via electrostatic interactions using molecules with suitable ionic groups has also been reported.[38] However, the need for complimentary groups on the MIP particle surface and the influence of the electrolyte solution (pH, ionic strength) on the electrostatic binding impedes this approach. In general, the presence of the linker molecules in the final assembly reduces the proximity of the receptor element to the transducer surface. This aspect can impact the sensitivity and the performance of the sensor, especially when surface sensitive detection techniques are employed. In this regard, a direct coupling between a MIP particle and the sensor transducer without a linker molecule is highly desired.

In this work, we report a convenient and an effective method for covalent immobilization of ex-situ formed MIP particles directly on an electrochemically inert substrate without the need for a linker molecule. A conducting P-type (boron) doped bio-inert nano-crystalline diamond (NCD) coated silicon substrate was used as a transducer substrate and electrochemical impedance spectroscopy (EIS) was used as the read-out tool. Diamond substrates have been used previously as sensor interface for biosensing applications as they offer large electrochemical potential window, chemical inertness, physicochemical stability and biocompatibility.[39-45] Immobilization of (bio-) molecules using physical or chemical adsorption methods already exist and were established.[41, 46-48] Recently, we have developed a simple and elegant functionalization of diamond substrates by coating a thin (20 nm) homogeneous amorphous carbon layer by means of carbon evaporation (Chapter 4). The amorphous carbon displays binding sites to which the vinyl surface groups of the MIP particles can bind covalently via photografting.[49, 50] As vinyl functionalities are inherently present on the particles formulated using crosslinking monomers, no additional surface functionalization of the MIP particle is necessary. In Figure 3.1 a schematic representation is shown.

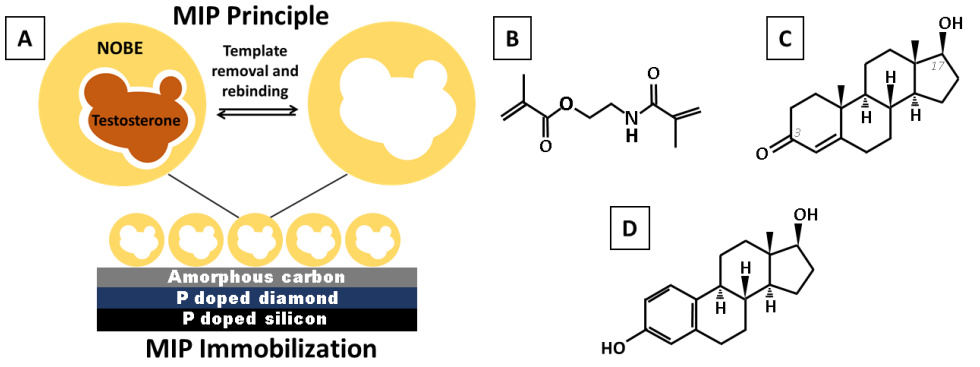

Figure 3.1. Schematic representation of the colloidal MIP principle and the immobilization of the latter on amorphous carbon functionalized boron (P-type) doped nano-crystalline diamond which was grown on boron doped silicon substrates (A) and the chemical structures of NOBE (B), testosterone (C) and β-estradiol (D).

Colloidal MIP particles based on NOBE for the detection of testosterone were obtained as stable dispersions in water by using the miniemulsion technique based on the previously established procedure.[20] As a negative control, non-imprinted polymers (NIPs) were obtained which were synthesized and handled in an identical way as the MIP particles but without the presence of template molecule during polymerization. To prove the rebinding capacity of the washed MIPs, equilibrium binding analysis experiments were performed. The particles were immobilized covalently on the functionalized NCD substrates and were tested for their performance using a home-built sensor set up for impedimetric sensing. The colloidal MIP based sensor platform was tested for the detection of testosterone and its structural analogue β-estradiol (see Figure 3.1 C and D) using spiked buffer and urine solutions. β-estradiol is an endocrine disruptor and is also of relevance because of its impact on the aquatic environment.[51, 52] To the best of our knowledge, so far the colloidal MIPs based on miniemulsion technique have not been used for impedimetric sensing and colloidal MIPs-transducer interface via the direct immobilization of the particles on the transducer substrate without a linker molecule has not been reported. The method presented in this work is simple and convenient and can be generally applied in the development of low-cost and robust sensing devices based on ex situ prepared MIP particles.

3.3 Experimental section

3.3.1 Materials

Solvents were obtained from VWR and other chemicals and materials were purchased from Sigma Aldrich unless noted otherwise. 2,2'-Azobis(2-methylpropionitrile) (AIBN) and phosphate buffered saline (PBS) solution were purchased from Fluka and Thermo Scientific, respectively. Column chromatography was conducted on silicon dioxide (EcoChrom) and 80 g silica cartridges (Grace Davison Discovery Sciences) using a Büchi automatic column chromatography device. Testosterone, β-estradiol and 2,2'azobis(isobutyronitrile)were purchased from Fluka Analytical. Filters (4 – 7 µm pore size) were purchased from Whatman. Silicon wafers (resistivity 10-20 kΩ, P-type doping) were obtained from Institute of Electronic Materials Technology. Membrane tubes (Amicon Ultracel 30 K, regenerated cellulose), were purchased from Merck). Throughout the work, MilliQ water (Sartorius) was used.

3.3.2 Synthesis procedure of N,O-bismethacryloyl ethanolamine (NOBE) monomer

Our previously reported NOBE synthesis protocol which was adapted from Sibrian-Vazquez et al. was followed.[20, 29] Under anhydrous nitrogen conditions at 0 °C, 1.125 mol of methacryloyl chloride was mixed with 0.450 mol of ethanolamine and 0.900 mol of triethylamine in dry dimethylformamide. This reaction was allowed to proceed at 40 °C with mechanical stirring for 24 h. Subsequently, the ammonia salts were removed and the product was washed with aqueous $NaHCO_3$, NH_4Cl and NaCl solutions. Subsequently, the product was dried by using magnesium sulfate powder and passed over a basic alumina column. The side products were removed by using chromatography (80 g silica cartridges of GraceResolve Silica and a Büchi automatic column device) with ethyl acetate/petroleum spirit (5/95 %) as a mobile phase. The monomer yield was about 35 % as a relatively large amount of it polymerizes in the column due to its high reactivity. For the NMR data, chapter 2 is referred to.

3.3.3 Synthesis of miniemulsion MIPs

The particles were prepared in accordance to our previously reported work.[20] 2.535 mmol (0.5 g) NOBE, 13.3 nmol (1.46 µg) hydroquinone, 0.447 mmol (0.129 g) testosterone, 91.3 µmol (0.015 g) AIBN and 2.18 mmol (0.26 g) chloroform were mixed to obtain the dispersed phase. For the continuous phase, 0.555 mol (10 g) water was mixed with 0.163 mmol (0.052 g) cetyltrimethyl ammonium chloride (cationic surfactant). Subsequently both phases were added together and ultrasonified (Branson sonifier W450 Digital; 1/8 in. tip) at 0 °C using the following steps: 30 % amplitude, 30 s pulse and 20 s pause during a total time of 120 s and 65 % amplitude, 30 s pulse and 20 s pause during a total time of 120 s. The obtained emulsion was purged with nitrogen for 2 min and stirred at 750 rpm. For polymerization, the system was illuminated with UV light (Omnicure series lamp with 4 arms) with an iris setting of 20 % for the first 2 h and then 3 % for 16 h. NIP particles were prepared the same way but without the presence of the target molecule during polymerization. As a following step, the obtained dispersion was filtered to remove large aggregates and the solid content was analysed gravimetrically. To analyse the diameter and the polydispersity of the miniemulsion particles in water, the dynamic light scattering (DLS, Zeta PALS analyser of Brookhaven Instruments Corporation, 90° laser detector angle) was used. Transmission electron microscopy (TEM, Tecnai Spirit, FEI, operating at an accelerating voltage of 120 kV in the bright-field imaging mode) was used to visualize the colloidal particles by drop casting them on a carbon coated copper TEM grid (Quantifoil).

3.3.4 Equilibrium binding analysis

To study the capability of the MIP particles to selectively rebind the target molecules, batch rebinding experiments are performed. Firstly, to remove the surfactants from the system, diafiltration (Amicon solvent resistant ultrafiltration cell) was used together with regenerated cellulose membranes (Ultracel 30 kDa discs). Next, the target molecules are removed from the imprints by 5 centrifugation and redispersion cycles in a heated mixture of acetic acid / methanol (10/90 v/v %, 50 °c). At the end of the washing procedure, no target

molecules are detected by UV-VIS spectroscopy in the supernatants anymore. Then, the samples were washed with ethanol to remove any residual acid and dried on a vacuum pump.

For the batch rebinding experiment, 30 mg of dried MIP and NIP particles was mixed with 1.9 mL of PBS/ethanol (50/50 v/v %) spiked with different concentrations of testosterone (0, 0.1, 0.2, 0.4 and 0.6 mM) at pH 7. Due to its low solubility in PBS, testosterone was first mixed with ethanol before adding the PBS. After an incubation time of 16 hours on a shaking plate, the particles were separated from the supernatants by centrifuging and filtration steps. The quantity of the free testosterone molecules present in the supernatants was determined using a UV-VIS-NIR spectrophotometer (Cary 500 Scan from Varian) and a 10 mm quartz cuvette. Testosterone has its characteristic absorption peak at a wavelength of 256 nm. For further details we refer to our previous work.[20]

3.3.5 Functionalization of the sensor substrate

On top of a P-type doped silicon wafer (10 – 20 kΩ resistivity), a 200 nm NCD layer (%CH_4 = 4, PPM $_{Boron}$ = 4800) was grown. Subsequently, the wafers were washed using a mixture of KNO_3 and sulphuric acid (1:10 ratio) at 100 °C for 30 min followed with a rinsing step with water. These substrates were hydrogenated using a microwave generator (2.45 GHz ASTeX reactor) for 2 min at 3500 W, 30 Torr, 500 sccm H_2 and 5 min at 2500 W, 15 Torr, 500 sccm H_2. Next, an amorphous carbon layer of 20 nm was deposited by evaporation at 40 A (Leica EM ACE600, carbon thread evaporation).

3.3.6 Coupling of the polymer particles to the functionalized substrates

In order to obtain a homogeneous coverage of polymer particles on the functionalized substrates, MIP and NIP particles were redispersed in water and washed with membrane tubes using centrifugation (18 cycles, 2000 rpm, 20 min) to remove the surfactant. Subsequently, the water was replaced by DMSO and the solid content was set to 2 wt. %. This dispersion was then sandwiched between the carbon functionalized NCD substrates and a quartz glass which were separated

by a 0.1 mm polydimethylsiloxane spacer. The quartz glass side of this setup was illuminated with UV light (24 h, in nitrogen conditions, Lawtronics ME5E UV-Lamps, 254 nm, 265 mW/cm^2) to couple the surface vinyl groups of the polymer particles to the carbon layer on the substrate. After coupling, in order to remove both the target molecules from the imprints of the particles together with any remaining uncoupled particles, the sensor substrates were washed by shaking them in a mixture of 1:1 ethanol/ultrapure water (7.5 h, 5 times), 1:19 acetic acid/methanol (4 h, 2 times) and 1:1 ethanol/ultrapure water (1 h, 4 times). To study the polymer particle distribution on the sensor substrate, scanning electron microscopy (SEM, FEI Quanta 200F) was used.

3.3.7 EIS sensor measurements

The capability of the MIP sensor substrate to detect testosterone is studied using electrochemical impedance spectroscopy. In Figure 3.2, a schematic representation of the home-made flow cell used for sensor experiments is shown.

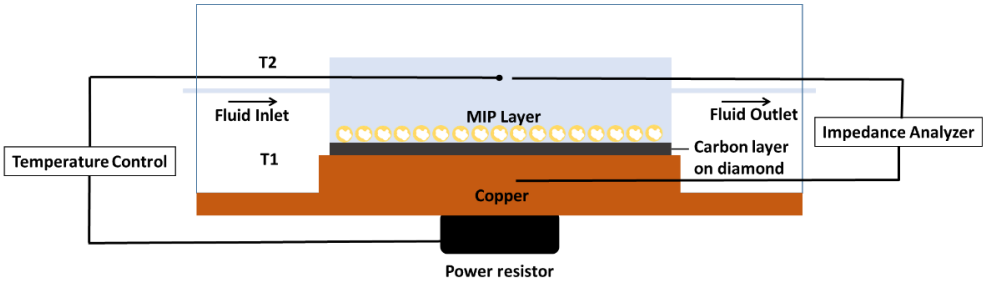

Figure 3.2. Schematic representation of the impedance flow cell for sensor substrate read-out.

This sensor set-up consists out of polymethyl methacrylate and the measuring chamber has a volume of 300 µL. The active sensing area of the MIP or NIP substrate is kept constant by using an O-ring with a surface of 28 mm^2 for every measurement. The impedance signal was measured using gold electrodes at a frequency range of 100 Hz to 100 kHz (10 frequencies per decade, a scanning speed of 5.69 s per sweep and an amplitude of the AC voltage of 10 mV). For every measurement, the temperature was kept constant at 25 ± 0.02 °C using a

proportional integral derivative (P = 1, I = 8, D = 0), thermocouples (TC-Direct) and a power resistor.

For the measurement, a mix of ethanol and 1 x PBS solution or filtered urine (1 µm pore size for polar media, Chromafil) in a 20/80 wt. % ratio at a pH of 7 was prepared. These solutions were spiked with testosterone to obtain the following concentrations: 0, 0.5, 2, 8, 20, 50, 100, 300 and 500 nM. Subsequently, the sensor substrate was installed in the sensor set-up and the impedance signal was allowed to stabilize under static conditions with an ethanol/ PBS or urine solution (blank) containing no target molecule. Next, 0.5 mL of spiked testosterone solutions are added from the lowest to the highest concentration with 15 minute stabilization intervals. To obtain a dose-response curve, the mean impedance signal at a frequency of 50118 Hz of the last 90 data points was normalized with the stabilization impedance value (blank) and plotted against the concentration of the target molecule that was administered. To test the selectivity of the sensor substrates, the same experiment in buffer was performed with β-estradiol which is structurally similar to testosterone.

3.4 Results and discussion

Using miniemulsion polymerization, coagulate free dispersions of NOBE based MIP (imprinted with testosterone) and NIP particles were obtained with a conversion efficiency of about 85 %. This value was calculated by determining the solid content of the filtered dispersion gravimetrically and is in accordance to the previously reported value.[20] To visualize the morphology and size of the polymer MIP particles, TEM was used (Figure 3.3 A). As the NIP particles exhibited similar morphology, the respective image is shown in the supporting information Figure S3.1.

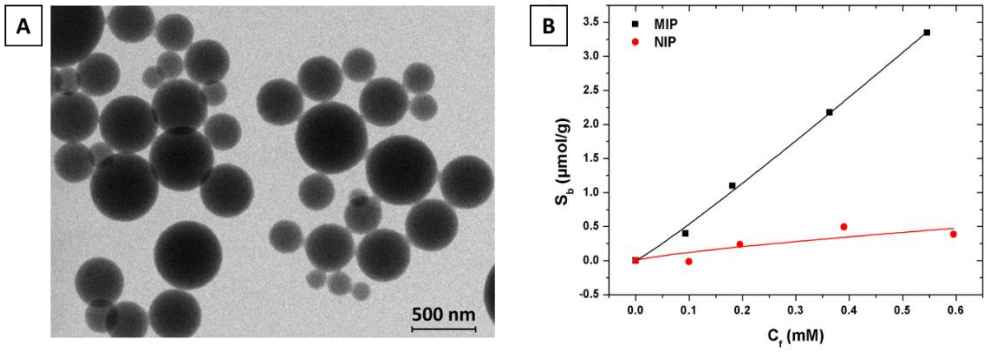

Figure 3.3. TEM image of the miniemulsion MIP particles (A) and a nonlinearly fitted binding isotherm with a target molecule concentration between 0.1 to 0.6 mM measured at pH 7 (B).

In Figure 3.3 A and Figure S3.1, it can be observed that the polymer particles have a spherical shape in the submicron size range. In order to further study the particle size and polydispersity index (PDI), dynamic light scattering (DLS) was used. For the NIP and MIP particles, a hydrodynamic radius of 501 ± 30 nm and 524 ± 32 nm and a PDI of 0.023 and 0.012 were detected respectively. These results are in agreement with previously reported work.[20, 26] The size difference between the MIP and NIP can be attributed to the compactness of the particles due to the self-associating nature of the monomer that is dominating in case of NIP particles and due to complexation of the target molecule with the monomer in case of MIP particles.[20, 53]

To study the capacity of the MIP particles to specifically bind the target molecules, both the surfactant and template molecules were removed by several washing steps and batch rebinding experiments were performed. As a negative control, the NIP particles were used. As biological samples are water based, these analyses were performed in PBS buffer. Because of the low solubility of testosterone in water, ethanol was also added to the system. In our previous work we obtained the best molecular recognition at a neutral pH of 7 for this particular monomer-template combination.[20] A set amount of dry MIP and NIP particle powder was dispersed in a testosterone spiked buffer/ethanol (50/50 v/v %, pH 7) mixture with a concentration between 0.1 and 1 mM. After reaching an equilibrium between bound and free target molecules overnight, the polymer particles were

separated from the supernatant by centrifugation and filtration. Using UV-VIS spectroscopy, the free target molecule concentration (C_f) of the supernatant was determined. From this value, the amount of testosterone which is bound to the MIP and NIP polymer (S_b) particles was calculated. In figure 3.3 B, the obtained binding isotherm is shown.

Since the interaction between the NOBE polymer and the testosterone target molecule is based on non-covalent interactions, the MIP particles contain a heterogeneous distribution of binding sites and affinity constants. Therefore, the Freundlich model is applied and the binding isotherms were fitted by a nonlinear least-squares model ($S_b = A\ C_f^v$) where S_b represents the bound target molecule concentration, A is the Freundlich constant, C_f is the concentration of target molecule that is free and v is the Freundlich heterogeneity parameter.[54-56] From this graph, it can be seen that the MIP particles have a higher affinity towards the target molecule in comparison with the NIPs which is caused by the imprinted binding sites. To estimate how specific this binding is, the concentration of bound testosterone per gram of MIP is divided by that of the NIP (S_b MIP/S_b NIP). This value is called the imprint factor. For a C_f of 0.3 mM, an imprint factor of 6.3 is obtained.

3.4.1 MIP immobilization

Subsequent to the washing steps to remove the surfactant molecules from the polymer particle dispersion, the water phase was replaced by DMSO and the solid content was set to 2 wt. %. The particles were then immobilized on the carbon functionalized diamond substrate by means of UV light induced coupling. Next, the sensor substrates were washed to remove any unattached particles together with the testosterone template molecules in the imprints. To visualize the miniemulsion MIP particles coupled to a sensor substrate, SEM was used (Figure 3.4). In the supporting information (Figure S3.2), also a SEM image is shown of the coupled NIP particles.

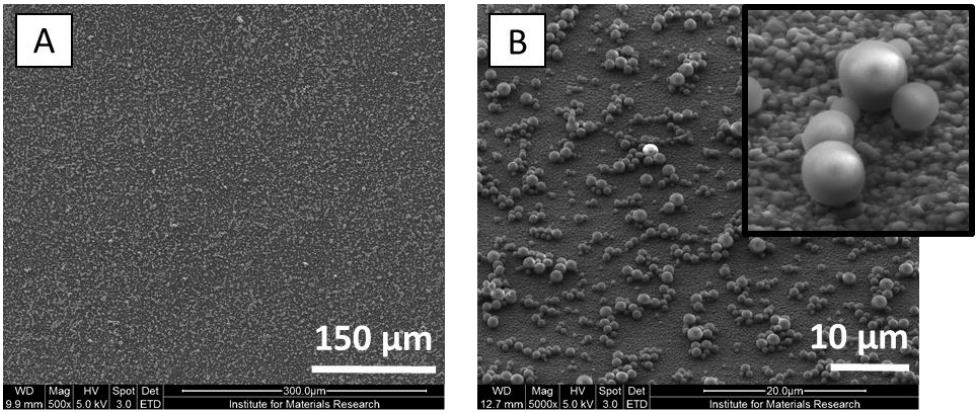

Figure 3.4. SEM images of the miniemulsion MIP particles coupled to a carbon coated diamond substrate at different magnifications (A and B). A magnified image of a region from the substrate is shown in inset (B).

In figure 3.4 A, a SEM image on a large area is shown to depict the homogeneous distribution of particles on the substrate. In figure 3.4 B, a higher magnification image is provided in order to visualize individual polymer particles. In the inset of figure 3.4 B, the nano crystalline diamond grains of the underlying substrate are clearly observable in between the polymer particles. From the latter image it can also be seen that most of the polymer particle surface is accessible for target molecule rebinding.

3.4.2 EIS sensor measurements in different fluids

To test the performance of the obtained MIP based sensor substrates, they were installed in the flow through cell which is discussed in the experimental section. The signal was allowed to stabilize in a 20/80 wt. % EtOH/PBS solution (blank) for around 1 h. Subsequently, increasing concentrations (0.5 – 500 nM) of the target molecule were added with 15 minute intervals. To test the selectivity of the sensor, testosterone was replaced with the structural analogue molecule β-estradiol. As the highest impedance signal-to-noise ratio was found at 50118 Hz, the dose-response curves are plotted at this frequency. To evaluate the sensor performance in real physiological samples, the PBS was replaced with urine (from a healthy volunteer) as it contains a wide range of different molecules such as proteins, salts, small molecules and cells. The urine was filtered as a precaution

to remove mainly the larger impurities as it might block the polymer imprint cavities causing a reduced sensor sensitivity.

In Figure 3.5 the normalized dose-response curve of a MIP and NIP sensor in EtOH/PBS spiked with different testosterone and β-estradiol concentrations is presented. In the supporting information (Figure S3.3), the dose-response curve with a logarithmic plotted concentration range is shown.

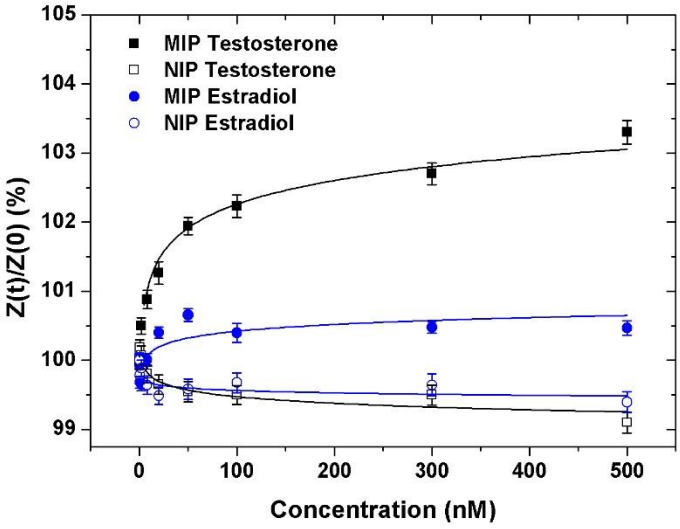

Figure 3.5. EIS dose-response curves of the MIP and NIP sensors exposed to increasing concentrations of testosterone and β-estradiol in EtOH/PBS solution. The curves are based on allometric fits.

The impedance value of the MIP increases more upon increasing concentration of testosterone in comparison to that of the NIP. This means that the MIP sensor is binding more testosterone in comparison with the NIP sensor. A 2 nM testosterone concentration, which is in the physiological range of 0.5 – 60 nM [57-59], was already detectable resulting in an impedance response of 0.42 %. For concentrations higher than 50 nM, which corresponds with an impedance response of 2.4 %, a saturation trend is visible as increasing imprint cavities are getting occupied. The highest testosterone concentration that was added (500 nM) resulted in an impedance response of 4.2 %. To test the selectivity, also a similar

sensor measurement was performed with β-estradiol instead of testosterone. From the graph, it can be concluded that β-estradiol is binding to the MIP to some extent however less in comparison with testosterone. At a concentration of 500 nM β-estradiol, an impedance response of 1.1 % was observed. This effect can be explained with the fact that β-estradiol differs only marginally from testosterone since it contains a hydroxyl functionality instead of a ketone at position C3 and it lacks the methyl group attached to C10. This result is in accordance with our previously reported selectivity studies.[20]

As a final step, the sensor performance was analysed using real biological samples. The same protocol as earlier was used except that the PBS was replaced with filtered fresh urine. The normalized dose-response curves are shown in Figure 3.6. In the supporting information (Figure S3.4), the dose-response curve with a testosterone concentration range plotted in a logarithmic scale is shown.

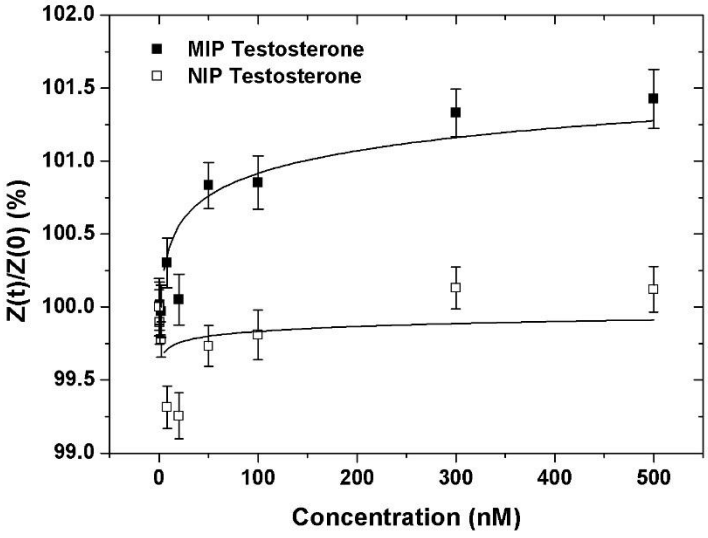

Figure 3.6. EIS dose-response curves of the MIP and NIP sensors exposed to increasing concentrations of testosterone in EtOH/urine solution. The curves are based on allometric fits.

Again, the MIP sensor binds significantly more testosterone in comparison with the NIP, however the absolute response (MIP-NIP) is less pronounced in

comparison with the measurements in PBS buffer. Also, from the error bars, it can be seen that there is more signal noise when the measurements were conducted in urine. The latter two effects can be attributed to the nonspecific absorption of proteins, salts and other small molecules to both the MIP and NIP particles. This absorption causes on the one hand an impedance signal decrease in the MIP sensor because testosterone molecules cannot bind optimally to the imprints anymore and on the other hand a signal increase due to aspecific binding to both MIP and NIP sensors. Regardless, still a reasonable sensor response was obtained: 0.19 % and 1.3 % for the lowest (2 nM) and highest (500 nM) concentration, respectively.

3.5 Conclusions and outlook

In this work, a chemical sensor based on molecularly imprinted polymer sub-micron particles is presented in which a novel immobilization method has been implemented to couple the colloidal particles to the transducer interface. MIP particles with a homogeneous material distribution, shape and a high active sensing surface were obtained by combining the bi-functional crosslinking monomer NOBE with the versatile miniemulsion technique. As a proof of concept, target molecule hormone disruptor testosterone was used because of its biological relevance. After studying the molecular recognition capabilities of the MIP particles using batch rebinding experiments, they were successfully immobilized on a diamond coated silicon substrate functionalized with an amorphous carbon layer. The obtained substrates showed a homogeneous polymer particle distribution. The use of ex-situ prepared MIP particles with an increased surface-to-volume ratio increases the sensor sensitivity. The MIP immobilization method used in this paper is straightforward and simple. It requires minimal effort preparation steps and avoids the use of an interfacial adhesive polymer layer which might block a fraction of the MIP imprint sites resulting in a decreased sensor sensitivity or cause unforeseen material loss during the measurement. The sensor performance of the MIP and NIP particles coupled to the substrates was successfully tested by using impedance spectroscopy as a read-out technique. PBS and urine based solutions spiked with testosterone or structural analogue β-estradiol were used for testing. The sensors were able to selectively bind

testosterone in physiological concentrations both in buffer as in real biological urine samples. It is worth to note that the washing of template molecules can be performed on the substrate after the coupling of the particles thereby allowing for regeneration of the sensor surface in the measuring cell if needed. In concise, colloidal MIP based sensors could be an alternative for the currently used quantification techniques which are expensive and require stringent conditions. In the future, sensor sensitivity will be optimized and the performance of the sensor will be further improved. As the active sensing surface can be increased by decreasing the diameter of the MIP particles and by increasing the amount of MIP particles on the sensor substrate, these steps are currently being undertaken in our laboratories.

3.6 Supporting information

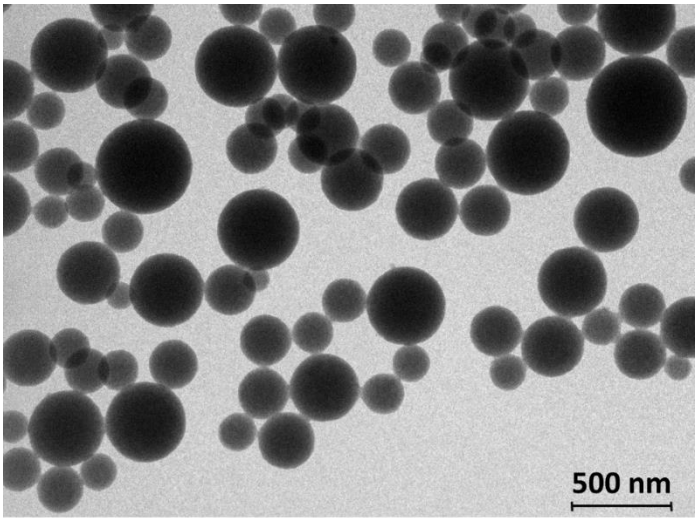

Figure S3.1. TEM image of the miniemulsion NIP particles.

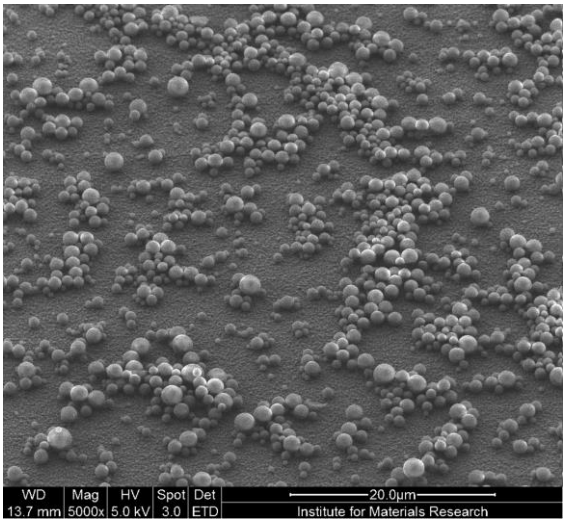

Figure S3.2. SEM image of the miniemulsion NIP particles coupled to a carbon coated diamond substrate.

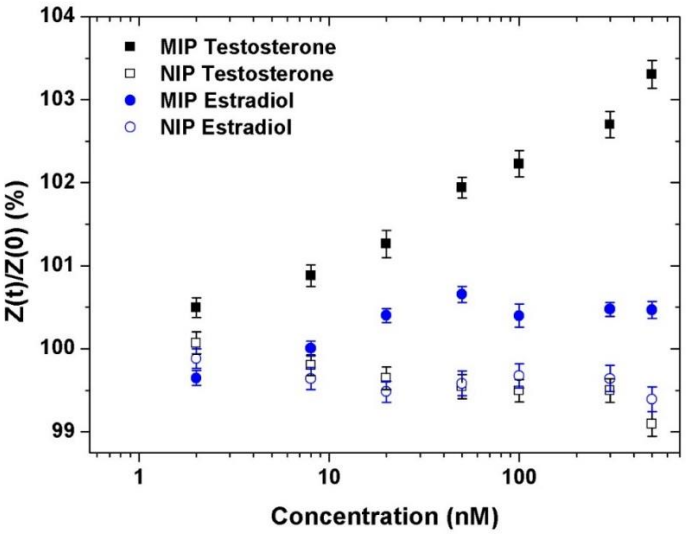

Figure S3.3. EIS dose-response curves of the MIP and NIP sensors in EtOH/PBS solution plotted with a testosterone and β-estradiol concentration range in the logarithmic scale.

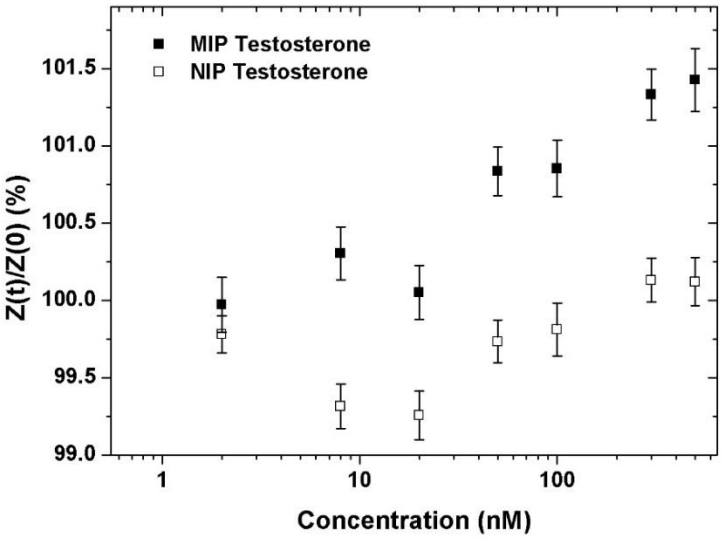

Figure S3.4. EIS dose-response curves of the MIP and NIP sensors in EtOH/urine solution plotted with testosterone concentration range in the logarithmic scale.

3.7 References

[1] W. H. Robinson, C. DiGennaro, W. Hueber, B. B. Haab, M. Kamachi, E. J. Dean, S. Fournel, D. Fong, M. C. Genovese, H. E. Neuman, *Nature Medicine* **2002**, 8, 295.

[2] R. Folly, A. Salgado, B. Valdman, F. Valero, *Brazilian Journal of Chemical Engineering* **1997**, 14.

[3] J. J. Gooding, *Electroanalysis* **2002**, 14, 1149.

[4] M. Liss, B. Petersen, H. Wolf, E. Prohaska, *Analytical chemistry* **2002**, 74, 4488.

[5] A. P. Turner, *Chemical Society reviews* **2013**, 42, 3184.

[6] V. J. Ruigrok, M. Levisson, M. H. Eppink, H. Smidt, J. van der Oost, *The Biochemical journal* **2011**, 436, 1.

[7] K. Haupt, *Chem. Commun.* **2003**, 2, 171.

[8] K. Smolinska-Kempisty, A. Guerreiro, F. Canfarotta, C. Cáceres, M. J. Whitcombe, S. Piletsky, *Scientific Reports* **2016**, 6, 37638.

[9] E. R. Cooper, K. C. Y. McGrath, A. K. Heather, *Sensors (Basel, Switzerland)* **2013**, 13, 2148.

[10] J. A. Cauley, F. L. Lucas, L. H. Kuller, K. Stone, W. Browner, S. R. Cummings, *Annals of internal medicine* **1999**, 130, 270.

[11] Z. Hyde, L. Flicker, K. A. McCaul, O. P. Almeida, G. J. Hankey, S. A. Chubb, B. B. Yeap, *Cancer epidemiology, biomarkers & prevention : a publication of the American Association for Cancer Research, cosponsored by the American Society of Preventive Oncology* **2012**, 21, 1319.

[12] R. Gonzalo-Lumbreras, D. Pimentel-Trapero, R. Izquierdo-Hornillos, *Journal of chromatographic science* **2003**, 41, 261.

[13] F. Gasser, N. Jeandidier, S. Doffoel, F. Klein, R. Sapin, *Immuno. Anal Biol. Spé.* **2003**, 18, 98.

[14] T. G. Shrivastav, A. Basu, K. P. Kariya, *Journal of immunoassay & immunochemistry* **2003**, 24, 205.

[15] F. Vera, R. R. Zenuto, C. D. Antenucci, J. M. Busso, R. H. Marín, *Journal of Experimental Zoology Part A: Ecological Genetics and Physiology* **2011**, 315A, 572.

[16] R. L. Fitzgerald, T. L. Griffin, D. A. Herold, *Methods in molecular biology (Clifton, N.J.)* **2010**, 603, 489.

[17] Y. Wang, G. D. Gay, J. C. Botelho, S. P. Caudill, H. W. Vesper, *Clinica chimica acta; international journal of clinical chemistry* **2014**, 436, 263.

[18] Y. Chen, Y. Liu, X. Shen, Z. Chang, L. Tang, W.-F. Dong, M. Li, J.-J. He, *Sensors* **2015**, 15, 29877.

[19] Y. Fuchs, O. Soppera, A. G. Mayes, K. Haupt, *Advanced Materials* **2013**, 25, 566.

[20] E. Kellens, H. Bové, M. Conradi, L. D'Olieslaeger, P. Wagner, K. Landfester, T. Junkers, A. Ethirajan, *Macromolecules* **2016**, 49, 2559.

[21] A. Poma, A. P. F. Turner, S. A. Piletsky, *Trends in Biotechnology*, 28, 629.

[22] G. Vasapollo, R. D. Sole, L. Mergola, M. R. Lazzoi, A. Scardino, S. Scorrano, G. Mele, *International Journal of Molecular Sciences* **2011**, 12, 5908.

[23] O. Brueggemann, K. Haupt, L. Ye, E. Yilmaz, K. Mosbach, *J. Chromatogr. A* **2000**, 889, 15.

[24] L. Ye, R. Weiss, K. Mosbach, *Macromolecules* **2000**, 33, 8239.

[25] A. G. Mayes, K. Mosbach, *Anal. Chem.* **1996**, 68, 3769.

[26] D. Vaihinger, K. Landfester, I. Kräuter, H. Brunner, G. E. M. Tovar, *Macromol. Chem. Phys.* **2002**, 203, 1965.

[27] B. Pluhar, B. Mizaikoff, *Macromol. Biosci.* **2015**, 15, 1507.

[28] Z. Adali-Kaya, B. Tse Sum Bui, A. Falcimaigne-Cordin, K. Haupt, *Angew. Chem. Int. Ed. (English)* **2015**, 54, 5192.

[29] M. Sibrian-Vazquez, D. A. Spivak, *Macromolecules* **2003**, 36, 5105.

[30] M. Sibrian-Vazquez, D. A. Spivak, *J. Polym. Sci. Part A: Polym. Chem.* **2004**, 42, 3668.

[31] J. LeJeune, D. A. Spivak, *Analytical and bioanalytical chemistry* **2007**, 389, 433.

[32] T. Kamra, S. Chaudhary, C. Xu, N. Johansson, L. Montelius, J. Schnadt, L. Ye, *Journal of Colloid and Interface Science* **2015**, 445, 277.

[33] M. Peeters, F. J. Troost, B. van Grinsven, F. Horemans, J. Alenus, D. Keszthelyi, A. Ethirajan, R. Thoelen, T. J. Cleij, P. Wagner, *Sens. Actuators B Chem.* **2012**, 171-172, 602.

[34] S. Kroger, A. P. Turner, K. Mosbach, K. Haupt, *Analytical chemistry* **1999**, 71, 3698.

[35] K. Reimhult, K. Yoshimatsu, K. Risveden, S. Chen, L. Ye, A. Krozer, *Biosensors and Bioelectronics* **2008**, 23, 1908.

[36] S. Chaudhary, T. Kamra, K. M. A. Uddin, O. Snezhkova, H. S. N. Jayawardena, M. Yan, L. Montelius, J. Schnadt, L. Ye, *Applied Surface Science* **2014**, 300, 22.

[37] K. Yoshiaki, K. Akifumi, U. Tadashi, M. Takashi, *Chemistry Letters* **2014**, 43, 825.

[38] F. Kolarov, K. Niedergall, M. Bach, G. E. Tovar, G. Gauglitz, *Analytical and bioanalytical chemistry* **2012**, 402, 3245.

[39] G. M. Swain, A. B. Anderson, J. C. Angus, *MRS Bulletin* **1998**, 23, 56.

[40] M. Shen, L. Martinson, M. S. Wagner, D. G. Castner, B. D. Ratner, T. A. Horbett, *J Biomater Sci Polym Ed* **2002**, 13, 367.

[41] A. Hartl, E. Schmich, J. A. Garrido, J. Hernando, S. C. Catharino, S. Walter, P. Feulner, A. Kromka, D. Steinmuller, M. Stutzmann, *Nat Mater* **2004**, 3, 736.

[42] J. Rubio-Retama, J. Hernando, B. López-Ruiz, A. Härtl, D. Steinmüller, M. Stutzmann, E. López-Cabarcos, J. Antonio Garrido, *Langmuir* **2006**, 22, 5837.

[43] K. Bakowicz-Mitura, G. Bartosz, S. Mitura, *Surface and Coatings Technology* **2007**, 201, 6131.

[44] S. Wenmackers, V. Vermeeren, M. vandeVen, M. Ameloot, N. Bijnens, K. Haenen, L. Michiels, P. Wagner, *physica status solidi (a)* **2009**, 206, 391.

[45] V. Vermeeren, L. Grieten, N. Vanden Bon, N. Bijnens, S. Wenmackers, S. D. Janssens, K. Haenen, P. Wagner, L. Michiels, *Sensors and Actuators B: Chemical* **2011**, 157, 130.

[46] W. Yang, O. Auciello, J. E. Butler, W. Cai, J. A. Carlisle, J. E. Gerbi, D. M. Gruen, T. Knickerbocker, T. L. Lasseter, J. N. Russell, Jr., L. M. Smith, R. J. Hamers, *Nat Mater* **2002**, 1, 253.

[47] J. Hernando, T. Pourrostami, J. A. Garrido, O. A. Williams, D. M. Gruen, A. Kromka, D. Steinmüller, M. Stutzmann, *Diamond and related materials* **2007**, 16, 138.

[48] B. van Grinsven, N. Vanden Bon, L. Grieten, M. Murib, S. D. Janssens, K. Haenen, E. Schneider, S. Ingebrandt, M. J. Schoning, V. Vermeeren, M. Ameloot, L. Michiels, R. Thoelen, W. De Ceuninck, P. Wagner, *Lab Chip* **2011**, 11, 1656.

[49] N. A. Hutter, M. Steenackers, A. Reitinger, O. A. Williams, J. A. Garrido, R. Jordan, *Soft Matter* **2011**, 7, 4861.

[50] M. Steenackers, R. Jordan, A. Küller, M. Grunze, *Advanced Materials* **2009**, 21, 2921.

[51] H. M. Kuch, K. Ballschmiter, *Environ. Sci. Technol.* **2001**, 35, 3201.

[52] P. Lucci, O. Núñez, M. T. Galceran, *J. Chromatogr. A* **2011**, 1218, 4828.

[53] K. Yoshimatsu, J. LeJeune, D. Spivak, L. Ye, *Analyst* **2009**, 134, 719.

[54] H. Freundlich, *Z. Phys. Chem.* **1906**, 57, 385.

[55] I. R. Umpleby, S. Baxter, A. Rampey, G. Rushton, Y. Chen, K. Shimizu, *J. Chromatogr. B* **2004**, 804, 141.

[56] D. Spivak, *Adv. Drug Deliv. Rev.* **2005**, 57, 1779.

[57] H. Jin, J. Lin, L. Fu, Y. F. Mei, G. Peng, X. Tan, D. M. Wang, W. Wang, Y. G. Li, *Biochemistry and Cell Biology* **2007**, 85, 246.

[58] J. Taieb, B. Mathian, F. Millot, M. C. Patricot, E. Mathieu, N. Queyrel, I. Lacroix, C. Somma-Delpero, P. Boudou, *Clin. Chem.* **2003**, 49, 1381.

[59] J. Dana-Haeri, J. Oxley, A. Richens, *British Medical Journal (Clinical research ed.)* **1982**, 284, 85.

4 A simple and efficient fabrication of reliable and reusable biosensors using patterned molecularly imprinted polymer structures on functionalized diamond substrates for selective detection of target molecules in body fluids.

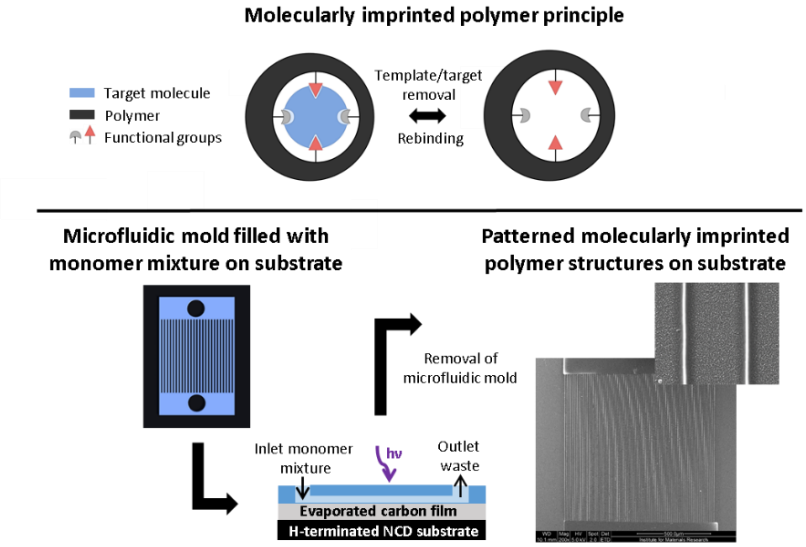

4.1 Abstract

Molecularly imprinted polymers (MIPs) can selectively bind a specific target molecule and can therefore be used as a low-cost and robust alternative to advantageously replace the fragile and expensive natural receptors (such as antibodies and enzymes) in molecular sensing devices. However, one challenging issue in using MIPs for sensor development, is the lack of simple and cost-effective techniques that allow a firm fixation and a controllable and consistent receptor material distribution on the sensor substrate. In this work, a novel method which is simple, efficient, low-cost and less time consuming, is presented, where

microfluidic systems in conjunction with in situ photo-polymerization on functionalized diamond substrates is used. The sensor substrate, nanocrystalline diamond coated silicon, is functionalized with amorphous carbon which is able to react with the vinyl group containing MIP precursor mixture resulting in stable and firm immobilization. Subsequently, a patterned elastic mold is placed on top of the substrate and the MIP precursor mixture is allowed to flow through the pattern. Numerous patterned polydimethylsiloxane (PDMS) molds can be readily obtained by making casts of a single master pattern which was created using e-beam lithography. This technique ensures tunable and consistent MIP material amount and distribution between different sensor substrates and therefore a controllable active sensing surface. After polymerization and removal of the template molecules, the obtained patterned MIP structures are successfully tested as a selective sensor platform to detect physiological concentrations of hormone disruptor testosterone in buffer, urine and saliva samples using electrochemical impedance spectroscopy. Apart from the excellent and selective recognition offered by these patterned MIP structures, they are also extremely stable during and after the dynamic sensor measurements. Therefore, the MIP patterns were easily regenerated by a simple washing procedure for repetitive measurements and reproducible results were possible.

4.2 Introduction

The demand in the fields of molecular screening, clinical diagnostics, and food- and environmental analysis is growing fast. Until recently, target molecule quantification in samples is performed in laboratories using analysis techniques such as immuno assays, gas and liquid chromatography, etc. which are time consuming, laborious, costly and require stringent conditions and specialized personnel.[1-8] Therefore, interest in the development of cheaper, reusable, faster and more user friendly sensors is increasing. Typically in these sensors, recognition elements which are capable of binding target molecules are immobilized on a signal transducer substrate. The binding events can be translated *via* electronic or optical read-out techniques to a concentration-dependent signal.[9-11] Biological macromolecules such as antibodies, enzymes,

and cells are commonly used recognition elements since they possess highly fine-tuned and effective molecular recognition.[12-15] However, typically these natural receptors are on the one hand costly and laborious to obtain and on the other hand they exhibit instability (physically and chemically) and insufficient sensitivity in non-physiological environments.[16] A compelling alternative is the use of so-called synthetic biomimetic receptors, which are highly stable and cost-effective. In this regard, the use of molecularly imprinted polymers (MIPs) has tremendous potential as artificial receptors.[17-20] In general, MIPs are obtained when the target/template molecule is present in the matrix during polymerization. The functional groups of the monomer are arranged around the template molecule through non-covalent or covalent interactions. After polymerization, the subsequent removal of the template leaves nano-cavities. These cavities are complementary to the template in terms of size, shape, and arrangement of the functional groups, allowing these polymer imprints to rebind the target molecule with high affinity and specificity.[21, 22] In contrast with natural receptors, these artificial receptors allow for a long shelf-time storage as well as chemical and physical robustness even in extreme pH-environments.[19, 23, 24]

The geometries of MIPs can be fine-tuned depending on the requirements of the application. For sensor applications, MIPs have been used in the form of ex situ prepared particles which were subsequently immobilized on the sensor substrate [25-27] but also in the form of films or structures which are directly in situ polymerized and grafted on the sensor substrate[28, 29]. Frequently used sensor read-out techniques which quantify the binding between the target molecule and MIP based sensing electrodes include impedance spectroscopy [30], quartz crystal micro balance [31] and surface plasmon resonance [32].

MIPs in the form of ex situ prepared particles are very interesting for sensor applications due to their high and controllable active sensing surface. Bulk polymerization with subsequent grinding is the most conventional, fast and simple method resulting in micron sized particles with irregular shapes and sizes.[33, 34] It is of most importance that the detection of a target molecule in a sample is reliable and consistent. Therefore, all inhomogeneities between different transducer substrates need to be reduced to a minimum. To obtain more control over the shape, particle size and surface area of the MIPs, colloidal MIP synthesis methods such as precipitation [35], suspension [36], and emulsion [37] techniques are

compelling alternatives. Issues which still need to be overcome are: stable MIP attachment to the substrate (even in dynamic conditions) and consistency in amount and distribution of the polymer in and between different sensor substrates. Therefore, there has been a tremendous focus on techniques which allow to create stable and reliable sensing substrates in a reproducible way. MIP particles have been previously deposited using techniques such as stamping, screen printing, drop casting and spin coating, which have all proven their shortcomings.[25, 38-40] Also, particles have been immobilized on the biosensor substrate through linker molecules or by the use of an adhesive polymer layer.[22, 27, 41] Although these immobilization methods have proven their applicability, a stable coupling between the MIP particle and the substrate which is strong enough to endure the dynamic sensor measurement conditions and ensure sensor regeneration for reusability remains challenging. In addition, still many problems are existing with respect to finding a technique which allows control over the MIP particle amount and distribution on the sensor substrate. Alternatively, homogenous MIP films are also deposited on the substrates. However, depending on the thickness of the film, the removal of the template molecules might pose a problem owing to the reduced surface area.

A major advance in the field was the direct in situ coupling and patterning of MIPs on the sensor surface. This way, always the same amount and geometries of imprinted polymer are present to act as molecular recognition layer. For quite some time, photolithographic methods have been extensively employed. Later, advanced fabrication techniques have been developed such as scanning-beam, projection, and interference (holography) photography.[29, 42, 43] Also non-optical based approaches have been used including electrodeposition [44], self-assembly [45], and the use of microfluidic molds [46] or stencils [47]. However, major problems associated with in situ patterning techniques are the multi-step and time-consuming procedures and the use of expensive equipment. Therefore, it is highly desired to have a low-cost and time-efficient method which ensures on the one hand that every time identical amounts of prepolymerization precursor mixture is polymerized in identical geometries with a high active sensing surface and on the other hand an extremely firm attachment of the latter on the sensor substrate. The high surface area allows the total washing time to remove the

template molecules to be reduced to a minimum which leads to a faster regeneration of the substrate. The bond between the MIP material and the sensor substrate should be strong enough so that no polymer detaches during the sensor measurements. This ensures the reliability of the sensor detection results and allows for successful reusability of the sensor substrate.

In this work, we report a simple and elegant fabrication of patterned MIP structures with geometries defined by the microfluidic stamp and the reliable attachment to the diamond electrode surface for the convenient detection of physiological concentrations of testosterone in samples comprising of real biological fluids using an impedimetric set-up under dynamic flow conditions. A doped bio-inert nano-crystalline diamond (NCD) layer deposited on a highly doped silicon wafer was used as a substrate/electrode material. The conductive NCD was used as sensor interface for biological applications because of the materials' unique properties namely the large electrochemical potential window, chemical inertness, physicochemical stability and biocompatibility.[48-54] Due to its poor chemical stability, bare silicon substrates are prone to the formation of a silicon oxide layer which would cause a drift in the impedance signal due to increasing capacitive effects. Various approaches to immobilize (bio-) molecules on diamond thin films have already been investigated [51, 55, 56] and have also been successfully tested further for impedimetric sensing.[57] In this work, for the first time molecularly imprinted polymer structures with controlled morphology using microfluidic molds were immobilized on diamond substrates by means of a simple and efficient carbon coating step. Jordan and co-workers have successfully demonstrated carbon templating on diamond substrates for grafting polymer chains and biofunctionalization.[58, 59] Although a high spatial resolution and a small size range can be achieved, the drawback of the previously used method for carbon templating is that for every sensor substrate, e-beam lithography needs to be performed which is expensive and laborious. Therefore, in here the focus is laid on reducing the multi-step and time consuming synthesis procedures, by using a simple and fast carbon coating step, to deposit a stable thin layer (20 nm) of amorphous carbonaceous material over the whole transducer interface. The reactive bonds of the amorphous carbon allow UV-induced photografting and covalent attachment of polymer structures across the entire sensor surface. To

structure the polymer in to patterned MIP structures with effective transducer surface coverage and defined dimensions, the monomer – target molecule precursor mixture is deposited on the substrate by using a patterned elastic PDMS based microfluidic flow cell. To obtain this PDMS flow cell, first a master structure is created using e-beam lithography. Subsequently, from this master structure, numerous PDMS molds can be obtained by simply using the master as a cast. As a proof of concept, MIP structures for testosterone detection were targeted. A bi-functional crosslinking monomer - N,O-bismethacryloyl ethanolamine (NOBE) [60] - was used as the monomer as we have shown previously that NOBE is a very suitable monomer for imprinting testosterone non-covalently.[61] It is worth to note that by using a bi-functional monomer, the need for additional functional monomers and empirical optimization of the relative ratios in the formulation is eliminated. After the photografting and in situ polymerization of the monomer – target molecule precursor mix, the template molecules were removed from the imprints by washing steps. The emptied cavities are then available for rebinding of the template molecule with high affinity and specificity.

The use of microfluidic systems in combination with MIPs is already described in literature.[46, 62, 63] However, the combination of micropatterned MIP structures and reliable immobilization on an electrochemically inert NCD sensor substrate using a coordinated sequence of surface treatment steps (H-termination followed by thin carbon layer deposition) for selective impedimetric sensing of target molecules is to the best of our knowledge not been reported yet in literature. For every sensor measurement, a non-imprinted polymer (NIP) structure with identical geometries was used. This negative control was synthesized and handled in the same way as the MIP but in the absence of the template molecules during polymerization. To test the selectivity of the MIP structures for the target molecule, the binding characteristics towards molecules that are structurally similar to testosterone, such as estriol and β-estradiol, were tested (Figure 4.1).

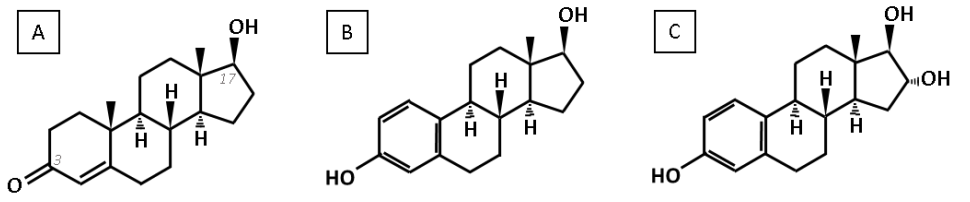

Figure 4.1: Chemical structures of the target molecule testosterone (A) and its structural analogues: β-estradiol (B) and estriol (C).

4.3 Experimental section

4.3.1 Materials

All chemicals and materials, unless otherwise stated, were purchased from VWR or Sigma-Aldrich. Column chromatography was conducted on silicon dioxide (EcoChrom) and 80 g silica cartridges (Grace Davison Discovery Sciences) using a Büchi automatic column chromatography device. For the fabrication of the microfluidic PDMS stamps, the silicone Sylgard elastomer kit 184 was purchased from Dow Corning Corp, and a 1 mm disposable biopsy punch (Miltex) and Teflon tubes with an outer diameter of 1.17 mm (Alpha Wire) were used. Testosterone, estriol and β-estradiol were purchased from Fluka Analytical. Phosphate buffered saline packs were obtained from Thermo Scientific.

4.3.2 Synthesis of N,O-bismethacryloyl ethanolamine (NOBE)

For the synthesis of NOBE, a previously reported procedure was followed.[61] NOBE was synthesized by mixing 0.450 mol ethanolamine and 0.900 mol triethylamine in dry dimethylformamide with 1.125 mol methacryloyl chloride dropwise under nitrogen at 0 °C. The mixture was stirred for 24 h at 40 °C and afterwards diluted with ethyl acetate. The formed ammonia salts were removed by filtration. All water-soluble contents were extracted by washing respectively with saturated sodium bicarbonate, saturated ammonium chloride, water and saturated sodium chloride aqueous solutions. The crude product was dried with magnesium sulphate and passed over a basic alumina column to remove residual acids. For the final

purification, the product was passed over a silica column using ethyl acetate/petroleum spirit (5/95 ratio) as mobile phase. The monomer yield before and after purification are 85 % and 35 % respectively. Since the monomer is prone to self-polymerization, a significant amount of material is lost during purification. For NMR data we refer to previously reported results.[61]

4.3.3 Design and fabrication of microfluidic mold

Prior to spin coating, 1 cm x 1 cm silicon substrates (L14016, Siegert Wafer GmbH) were thoroughly cleaned and dehydrated by heating them for 5 min at 150 °C. The negative photoresist SU-8 2025 (Micro Resist Technology GmbH) was diluted by cyclopentanone from a solid-content of 68.6 % to 44.4 %. These solutions were spin coated according the manufacturer's specifications and cured for 2 min at 95 °C, resulting in an approximately 4.5 µm thick layer. The desired pattern of the MIP structures with different widths and heights were designed with the DesignCad lt 2000 software tool. E-beam lithography was performed with a NPGS system (JC Nabity Lithography Systems) mounted on SEM (FEI Quanta 200F). The e-beam line-exposure was set at 0.12 nC/cm with an acceleration voltage of 30 kV. After exposure, the SU-8 layers were baked again for 3 min at 110 °C. The substrates were developed with SU-8 developer and rinsed with 2-propanol. The master mold was additionally subjected to a hard-baking step for 2 h at 150 °C to release stress from the resulting SU-8 microstructures and to achieve optimal mechanical stability and durability. The mold can then be reused dozens of times without deteriorating performance.

4.3.4 Design and fabrication of microfluidic stamp

A cast from the master mold was made in PDMS. The base polymer and curing agent were mixed thoroughly in a 10:1 weight-ratio in a disposable recipient. The introduced air from mixing was removed at an absolute pressure of 0.55 bar for at least 30 min. Next, the uncured PDMS was poured over the mold and subsequently baked in an oven for 3 h at 60 °C. The resulting PDMS cast of 2.5 mm high was cut out with a scalpel and peeled off from the mold. The inlet and outlet

(hereinafter referred to connection blocks) were cored with a 1 mm biopsy punch and the excess of cured PDMS was removed.

4.3.5 Surface treatment of NCD substrates

Highly doped silicon substrates (resistivity 10 – 20 kΩ, P-type doping, 10 mm x 10 mm x 0.525 mm) grown with a < 200 nm NCD layer (%CH_4 = 4, PPM_{Boron} = 4800) were cleaned by wet etching for 30 min in an oxidizing mixture of boiling potassium nitrate and sulfuric acid (1:10 ratio), followed by washing in an ultrasonic bath with heated ultrapure water. Next, the substrates were thoroughly rinsed with ultrapure water and dried using nitrogen gas. Hydrogenation 141ft he substrates was performed using an ASTeX® reactor equipped with a 2.45 GHz microwave generator: 2 min at 3500 W, 30 Torr, 500 sccm H_2 and 5 min at 2500 W, 15 Torr, 500 sccm H_2. The substrates were cooled in H_2 atmosphere for 40 min. Subsequently, a 20 nm thick carbon layer was deposited at 40 amperes onto the H-terminated substrates (Leica EM ACE600, carbon thread evaporation).

4.3.6 Fabrication of patterned MIP structures

The fabrication of the MIP structures using polymerization ingredients was optimized to achieve high affinity and selectivity for the target molecule testosterone. The optimal mixture used comprised of 0.507 mmol NOBE, 0.012 mmol 2,2-dimethoxy-2-phenylacetophenone, 1.088 mmol chloroform and 0.087 mmol testosterone.

The microfluidic stamp was placed onto the freshly carbon coated NCD substrate and teflon tubes were connected to the inlet and outlet of the stamp. The polymerizable mixture was pumped via the inlet through the microfluidic channels until they were all filled. Next, the tubes were removed and the substrate with the filled microfluidic channels was placed under UV-light (Lawtronics ME5E UV-lamps, 254 nm, 265 mW/cm^2). The UV-transmittance of PDMS at 254 nm ranges between 40 and 60 % (Figure S4.1 in the supporting information). Polymerization was done for 20 h in the presence of oxygen-free nitrogen purge. After polymerization, the stamp was removed from the substrate.

The target molecules were removed from the MIP structures by gently shaking the substrate in a mixture of 1:1 ethanol/ultrapure water (7.5 h, 5x solvent change), a mixture of 1:19 acetic acid/methanol (4 h, 2x solvent change), and a mixture of ethanol/ultrapure water (1 h, 4x solvent change). Non-imprinted polymer structures were synthesized in the absence of the target molecule and washed in the same way as the MIP structures.

4.3.7 Characterization of the patterned polymer structures

The integrity of the structures were characterized using an Axiovert 40 MAT optical microscope (Zeiss) equipped with a digital camera and using the Axiovision AC software. The integrity and geometry of the structures were studied using a SEM microscope (FEI Quanta 200F) operating at an accelerating voltage around 20 kV. The morphology and height of the structures were measured employing the DektakXT profilometer (Bruker).

4.3.8 Electrochemical impedance spectroscopy

The electrochemical testing of the patterned MIP/NIP structures as sensor platform was performed using impedance spectroscopy. The measurements were executed using a custom designed differential impedance sensor-cell set-up (Figure 4.2) which can measure both MIP and NIP substrates simultaneously thereby eliminating the influence of the surroundings (such as temperature fluctuations) and sample variations (such as different biological residue content).

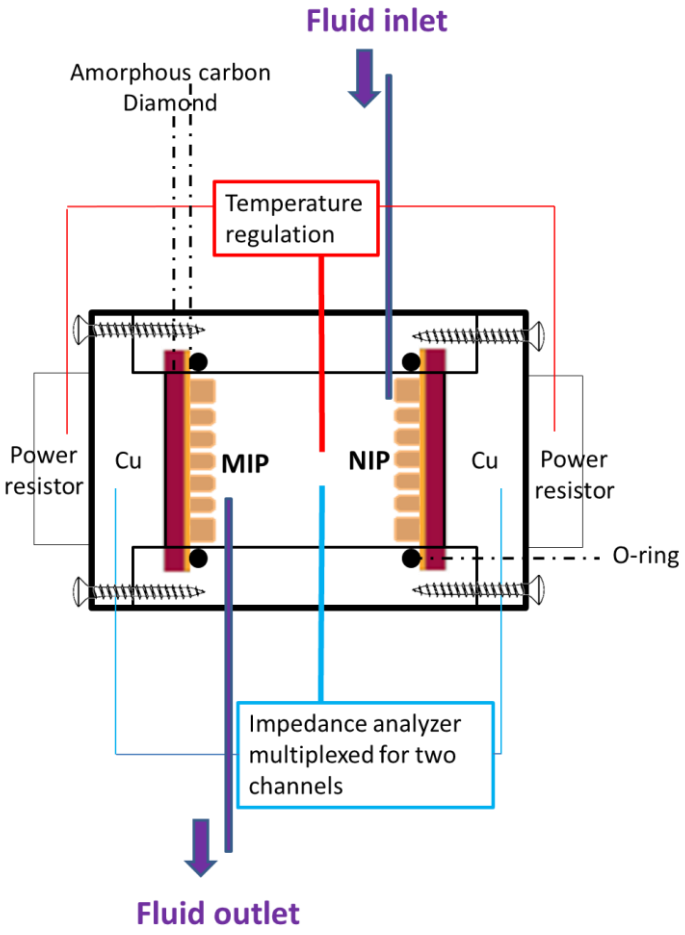

Figure 4.2. Schematic representation of the differential impedimetric flow cell used for the simultaneous measurements of MIP and NIP substrates.

The flow-through cell has an internal volume of 300 µL and is made of polymethyl methacrylate. All measurements were temperature controlled using a proportional integral derivative controller (P = 5, I = 8, D = 0). The MIP- and NIP-coated electrodes were installed symmetrically with respect to a gold wire serving as a common counter electrode. The contact area of each electrode with the liquid was defined by O-rings (28 mm²), and the distance from the sensing substrates to the counter electrode was 1.7 mm. Two other (ground) electrodes were present on the copper block of each substrate. The impedance signals were measured in a

frequency range of 100 Hz to 100 kHz with 10 frequencies per decade and a scanning speed of 5.69 s per sweep. The amplitude of the alternating current voltage was fixed to 10 mV under open circuit conditions. Silver paste was used to improve the contact between the transducer substrate and the copper blocks.

4.3.9 Electrochemical testing of MIP/NIP structures as sensor platform

The binding behavior of the MIP and NIP structures for testosterone was tested using EIS at the physiological pH (7.4) and temperature (37 °C). Testosterone solutions were prepared using ethanol/aqueous media mixtures as the former had limited solubility in water. For these experiments, a mix of ethanol and 1x PBS solution, filtered urine or saliva (in a 20/80 wt. % ratio, passed through Chromafil filters for polar media, pore size 1 and 5 µm) was spiked with testosterone to obtain the following target molecule concentrations: 0.5, 2, 8, 20, 50, 100, 300 and 500 nM. Subsequently, the sensor substrates were integrated in the differential sensor set-up and the impedance signal was allowed to stabilize in the ethanol/buffer or urine or saliva solution containing no target or analogues molecules (blank sample). After stabilization, 1 mL of the spiked samples were added, from low to high concentration with 15 minute intervals. To obtain the dose-response graphs, the mean impedance value of the last 35 data points obtained after administration of a certain concentration (Z(t)) was normalized with the initial impedance stabilization value (blank sample, Z(0)). The obtained value was plotted against that specific testosterone concentration. To test the cross-selectivity, impedance measurements were conducted for the structural analogues β-estradiol and estriol using the following concentrations: 0.5, 2, 8, 20, 50 and 100 nM.

4.4 Results and discussion

In this work, a patterned MIP structure immobilized on a sensor substrate was realized by combining simple and efficient functionalization of diamond substrates using amorphous carbon coating and patterned microfluidic molds. The bi-

functional monomer NOBE, was obtained using a previously reported synthesis method [60, 61] and testosterone was used as template molecule. The resulting MIP structures were characterized by optical light microscopy, dektak profilometry and scanning electron microscopy (SEM). For the proof-of-concept, the sensor performance was tested using EIS in buffer, urine and saliva spiked with testosterone. The highly stable bonds between the polymer structures and the substrate, allowed for successful regeneration of the sensor substrates. The selectivity of the sensor was checked using the testosterone structural analogues, namely, estriol and β-estradiol.

4.4.1 Fabrication of patterned MIP structures

The new design strategy for the immobilization of MIP structures overcomes the aforementioned disadvantages related to ex situ prepared MIP particles and other in situ strategies. It includes the direct synthesis of micron-sized MIP structures onto a hydrogen-terminated and carbon-coated (20 nm thick carbon film) nano-crystalline diamond layer on top of a highly doped silicon transducer substrates by UV-induced photo-polymerization of vinyl groups as well as photografting to the carbon layer (Figure 4.3). This process involves few simple sequential steps: first, carbonaceous material is deposited onto the hydrogen terminated surface of the diamond transducer element to ensure subsequent attachment of the MIP structures to the substrate. The role of carbon functionalization is very crucial as only hydrogen termination of NCD substrates for photografting was not sufficient to yield a stable immobilization of the polymer layer. Further, the MIP precursor mixture, including vinyl-group containing monomers, is pumped through the PDMS stamp microfluidic channels, followed by UV-induced photo-polymerization under inert nitrogen atmosphere. Subsequently, the PDMS stamp is removed resulting in covalently bound cross-linked polymer matrices with a shape and geometry defined by the stamp. The template molecules are removed from the imprints using several washing steps. Non-imprinted polymer (NIP) structures - serving as a negative control - are fabricated in the absence of the template molecules, using identical procedures/treatments as used for the MIP structures.

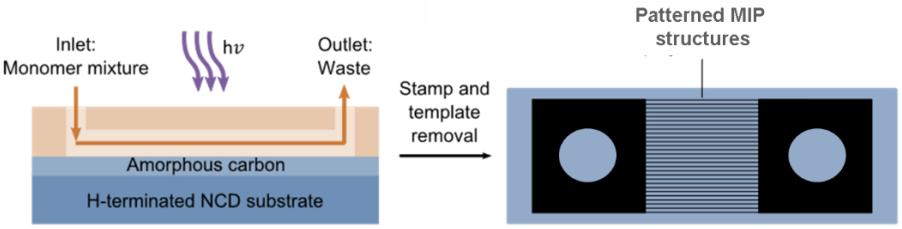

Figure 4.3. Fabrication of the patterned MIP structures. Schematic representation of the cross section of the microfluidic system made of PDMS on an amorphous carbon-coated and H-terminated NCD substrate and top view of the MIP structures obtained via UV-induced photo-polymerization (hυ) of the polymerizable moieties.

4.4.2 Characterization of patterned MIP structures.

For the proof-of-concept, a master structure containing 75 microfluidic channels with well-defined dimensions was fabricated. The height of the structures was fixed to 4.5 µm and was characterized by Dektak profilometry (Figure S4.2 in the supplementary information). The width of the channel is approximately 10 µm at the bottom and 5 µm at the top. Using the master structure, a cast consisting of PDMS was fabricated containing the microfluidic channels. No height profile was made of the stamp since PDMS is too flexible to withstand the force of the stylus. In Figure 4.4 A a microscope image of the PDMS stamp viewed from the top is shown. The black lines are the channel/lane structures and the black dots in the connection blocks are PDMS pillars to prevent these blocks from collapsing. In Figure 4.4 B, a cross-section SEM image of the stamp is shown in order to visualize the geometry of the patterned MIP structures.

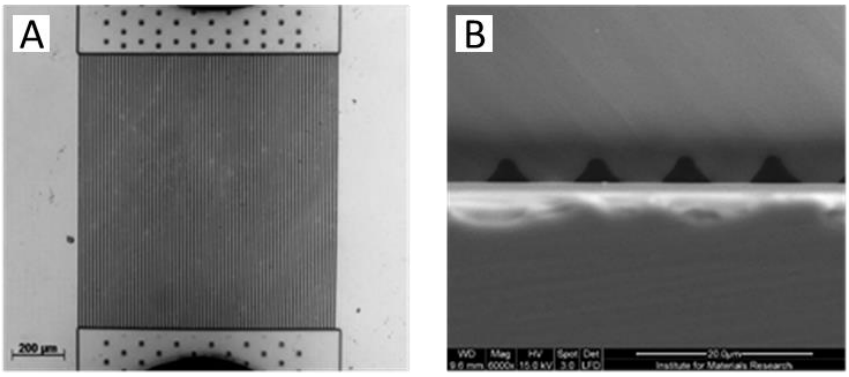

Figure 4.4. PDMS stamp with 75 patterned MIP structures: optical microscope image top view (A) and the cross section SEM microscopy image of the stamp (B).

Subsequently, the stamp was used to synthesize the patterned MIP structures. The latter were characterized using height profilometry using the same conditions as used for the master structure and are shown in Figure S4.3 in the supplementary information. The MIP structures are approximately 1.75 µm high, which is significantly lower than the height of the PDMS stamp channels. This could be attributed to the following reasons: firstly, the chloroform of the precursor mixture partially evaporates prior to polymerization and secondly, there is shrinkage due to the high level of crosslinking. The integrity of these MIP structures on top of the NCD substrates was checked by optical microscopy. From these images, no structural differences can be observed between MIP and NIP structures as shown in Figure S4.4 in the supplementary information. Even after several washing steps the structures were still intact thereby reflecting the stability of the MIP structures on the substrate.

The top view and cross section SEM images were made of these polymer structures (Figure 4.5 A - C). It can be seen from the cross-section image that the polymer structures have a triangular shape with a tip as compared to the PDMS stamp. This observation is in agreement to the reduced dimensions as a result of the shrinkage due to the highly crosslinked polymer network together with chloroform evaporation prior to polymerization.

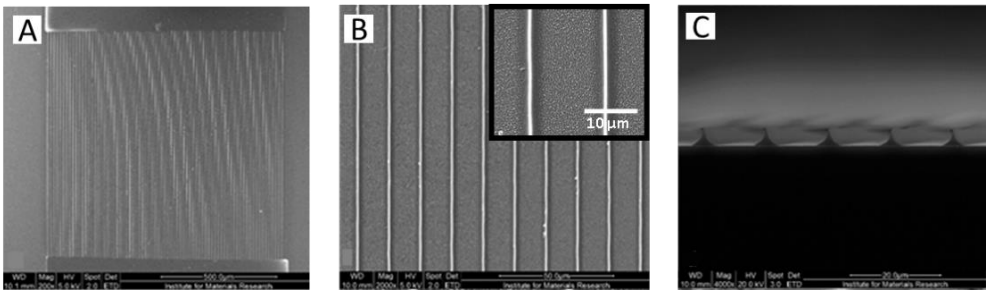

Figure 4.5. SEM images depicting polymer structures on NCD substrates: overview illustrating the patterned structure (A); the top view of structures in higher magnification (B) and the cross-section view of the structures (C).

4.4.3 Impedimetric testing of patterned MIP structures as sensor platform in buffer solution

For the proof-of-concept, the synthesized MIP sensor platform was tested by electronic sensing based on EIS. Both MIP and NIP structures have an identical surface coverage and polymer distribution as they were synthesized using identical PDMS stamps. Therefore, the precondition for differential measurements, having identical surface loadings, was complied.

For the detection using EIS, a custom designed differential set-up was used to measure the binding activity of the MIP and NIP in an identical environment (Figure 4.2, Materials and Methods). The flow-through cell was filled with an ethanol/PBS solution (20/80 wt. %) with a pH of 7.4, to simulate a physiological acidity level. After stabilization at the physiological temperature of 37 °C, 1 mL of increasing known concentrations of testosterone ranging between 0.5 and 500 nM were added stepwise with 15 minute intervals. All dose-response curves for testosterone detection in buffer solutions were determined at a frequency of 1,258 Hz. This frequency was chosen because it resulted in a good signal-to-noise ratio involving a very stable impedance signal with a small standard deviation of approximately 0.18 %.

The resulting dose-response curves are shown in Figure 4.6. The x-axis represents the normalized impedance change and the y-axis the concentration of administered testosterone.

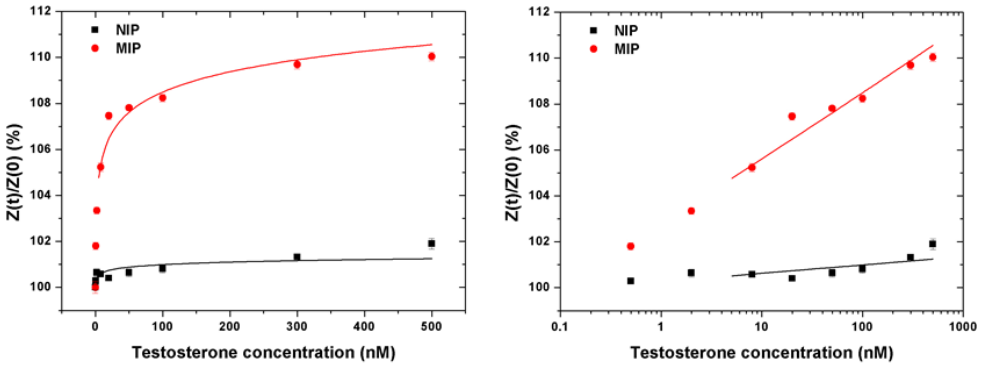

Figure 4.6. EIS dose-response curves (fitted non-linearly) of the MIP and NIP structures exposed to increasing concentrations of testosterone in EtOH/PBS buffer solution (A) and the dose-response curves with the testosterone concentration plotted in logarithmic scale for clearly illustrating the response below 1 nM concentration (B).

The graphs in Figure 4.6 show that there is a significant difference in sensor response between the MIP and NIP upon increasing target molecule concentration. The binding of testosterone to the polymer causes an increase in the complex resistance. The highest added testosterone concentration (500 nM) resulted in an increase of the impedance signal with 10.03 ± 0.19 % for the MIP and 1.89 ± 0.23 % for the NIP. Even the addition of the lowest testosterone concentration (0.5 nM) led to a measurable increase in the MIP signal of 1.8 ± 0.15 %, which is clearly visible from the plot in the logarithmic scale (Figure 4.6 B). This testosterone concentration is well in the physiological range of 0.5 – 60 nM.[64-66] Although the sensor response of the NIP was comparatively low, there is some aspecific binding of testosterone as in accordance with our previously reported studies.[61] The increase in the occupation of the MIP binding sites by testosterone, leads to a trend toward saturation for concentrations higher than 20 nM.

The obtained result clearly proves that by employing this simple fabrication technique, a sensor platform with well-defined MIP structures is achieved resulting in sensitive and high performance measurements. In addition, the sensor substrate can also be regenerated by using the same washing protocol as used to remove the template testosterone molecules as explained in the experimental section. As a proof for regeneration, the substrates that were used to construct Figure 4.6, were washed subsequently for a second time with the same solvent

mixtures to remove bound testosterone from the polymers. The polymer structures remained intact after washing when observed with the optical microscope. Subsequently, another impedance sensor measurement was performed with these substrates and the dose response curve is shown in Figure 4.7.

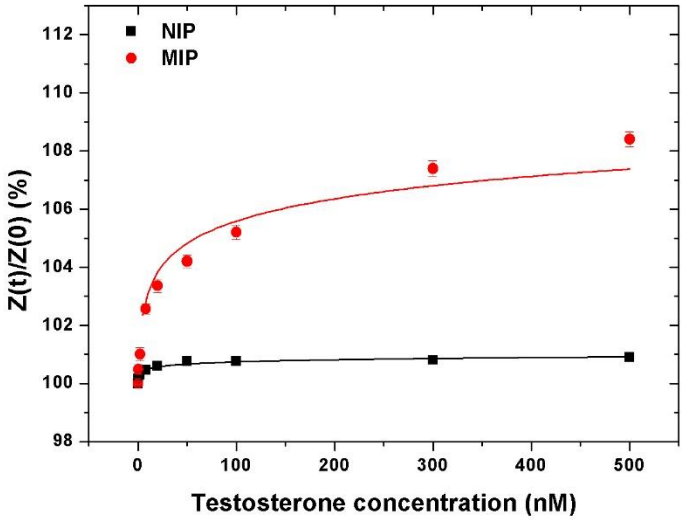

Figure 4.7: EIS dose-response curves of the regenerated MIP and NIP substrates. The curves are based on nonlinear fits.

From Figure 4.7 it can be seen that the MIP structures are still capable of binding a high amount of testosterone in comparison to the NIP structures, even after regeneration. When the highest concentration of testosterone is added (500 nM), the impedance signal increases 8.40 ± 0.26 % for the MIP and 0.90 ± 0.09 % for the NIP. However, these values are not as high as the values obtained from the previous sensor measurement. This effect can be due to incomplete testosterone removal after the second washing procedure, which can be improved by optimizing the washing procedure.

4.4.4 Selectivity testing of the senor in buffer solution

To test the selectivity of these MIP structures, sensor measurements where testosterone was replaced with structurally similar molecules were performed. The obtained dose-response curves recorded at a frequency of 1,258 Hz for the MIP and NIP structures exposed to increasing concentrations of estriol and *β*-estradiol are shown in Figure 4.8.

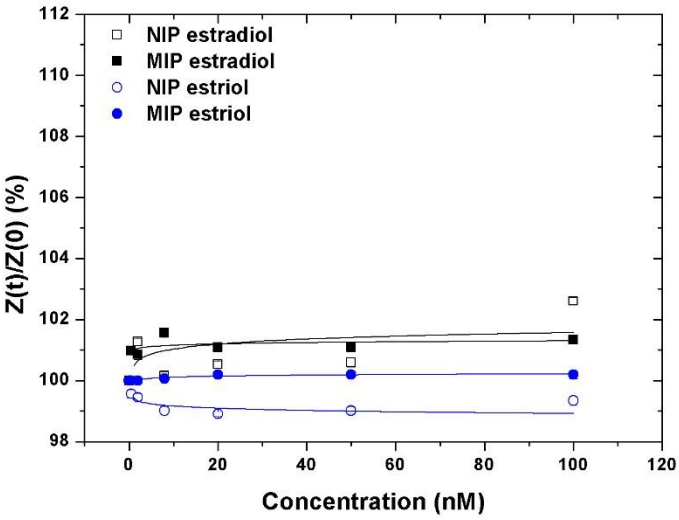

Figure 4.8. EIS dose-response curves of the MIP and NIP structures exposed to increasing concentrations of estriol and *β*-estradiol in EtOH/PBS buffer solution. The curves are based on nonlinear fits.

It can be clearly seen that *β*-estradiol shows some affinity to the MIP structures while estriol shows no binding. A concentration of 100 nM resulted in an increase of the MIP impedance signal with 0.19 ± 0.12 % for estriol and 2.6 ± 0.12 % for *β*-estradiol. Both estriol and *β*-estradiol are different from testosterone since they both lack the methyl group at the C-19 position and have a hydroxyl group at the C-3 position instead of a ketone. Compared to *β*-estradiol, estriol shows the largest structural variation with testosterone because of its excess hydroxyl group at the C-16 position which provides sterical hindrance during the binding to the testosterone imprints. This explains the low or non-existing affinity between the MIP and estriol. *B*-estradiol lacking C-16 hydroxyl group shows a small affinity

however still less pronounced in comparison with the affinity for the template molecule testosterone. These findings are in agreement with our previous report.[61]

4.4.5 Impedimetric testing of the sensor platform in body fluids

After obtaining a selective response from the MIP structures in EtOH/PBS buffer solutions, the same experiments were performed with testosterone-spiked solutions where the PBS buffer was replaced with urine or saliva. These body fluids were obtained from a healthy volunteer and, as a preparation step, they were filtered in order to remove large structures (any residual cells and other large impurities). This way, the binding characteristics of the MIP and NIP structures can be analyzed in the presence of other molecules such as hormones, vitamins, proteins, etc. which are present in real patient samples and can potentially block the imprints. The results obtained with the EtOH/urine solution are shown in Figure 4.9. The optimal frequency where the highest signal to noise ratio is observed for these measurements was 501 Hz due to the presence of proteins, hormones, etc. in urine.

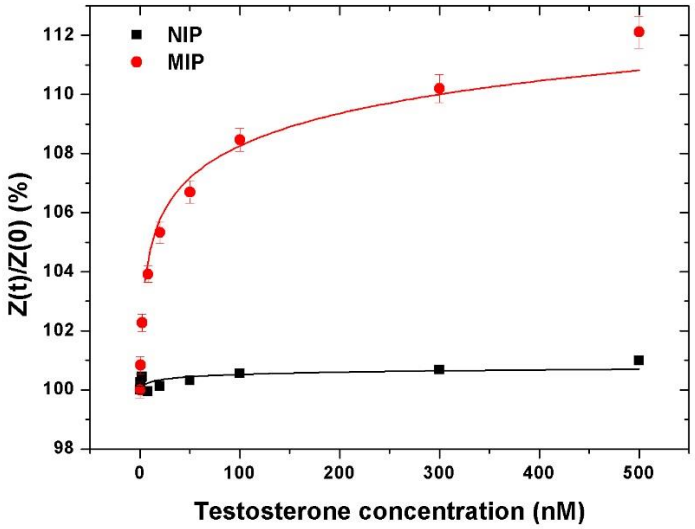

Figure 4.9. EIS dose-response curve of the MIP and NIP structures exposed to increasing concentrations of testosterone in EtOH/urine solution. The curves are based on nonlinear fits.

The maximum impedance increase of the NIP and MIP after adding a concentration of 500 nM testosterone were 0.99 ± 0.09 % and 12.11 ± 0.53 % respectively. At the lower testosterone concentrations of 0.5 and 2 nM, the MIP structures gave a sensor response of 0.84 ± 0.29 % and 2.27 ± 0.29 %, respectively. This limit of detection is in accordance with Batatache *et al.* where they combined MIP film detection with EIS read-out.[30] These results show that even in complex real patient samples, the MIP structure is still able to detect testosterone in a specific way.

Also in saliva based samples, the MIP structures were able to specifically bind testosterone. The results are shown in the supplementary information (Figure S4.5). In saliva, the MIP sensor performance was lower compared to the one obtained in buffer and urine with a maximum impedance increase (at 500 nM testosterone) of 3.63 ± 0.32 %. The impedance increase for the NIP at this testosterone concentration is 1.20 ± 0.24 %. This effect can be explained by the fact that there are more proteins and other molecules present in saliva in

comparison with buffer and urine which substantially block the testosterone imprints. However, this can be circumvented by pretreating the saliva samples. Regardless, the MIP structures show better response than the control NIP structures.

4.5 Conclusions and outlook

Patterned microstructures of molecularly imprinted polymers on functionalized NCD substrates were created with testosterone as target molecule and NOBE as a bifunctional monomer. A master structure, which was obtained using e-beam lithography, was used to fabricate structured PDMS stamps. Using these microfluidic PDMS stamps, polymer structures that are covalently attached to the amorphous carbon coated diamond substrate were obtained. These polymer structures were characterized using optical microscopy, SEM and height profilometry. The structures remained intact on the substrate even after several washing steps. The affinity and selectivity of these sensor substrates for the target molecule testosterone were tested using EIS as a readout technique. The structured polymers were able to detect testosterone in a selective way in buffer and in urine and saliva samples with a detection limit of 0.5 nM and showing saturation at concentrations above 20 nM. In addition, these polymer structures could be conveniently regenerated after a sensor measurement which allows for reusable sensors.

In concise it can be concluded that our approach offers a simple and cost-effective method to produce sensitive, high performance, reproducible and well-defined MIP based sensor platforms for the electronic detection of target molecules. The fabrication method offers design flexibility that can be used for tuning the dimensions and amount of MIP structures by opting for suitable master structures. The latter in combination with a miniaturized measuring cell can eventually lead to achieve an even lower limit of detection. The microfabrication approach employing microfluidic molds can be extended to deposit multiple structures imprinted with different target molecules on the same substrate using independent stamps in order to realize applications requiring multi analyte sensing.

4.6 Supporting information

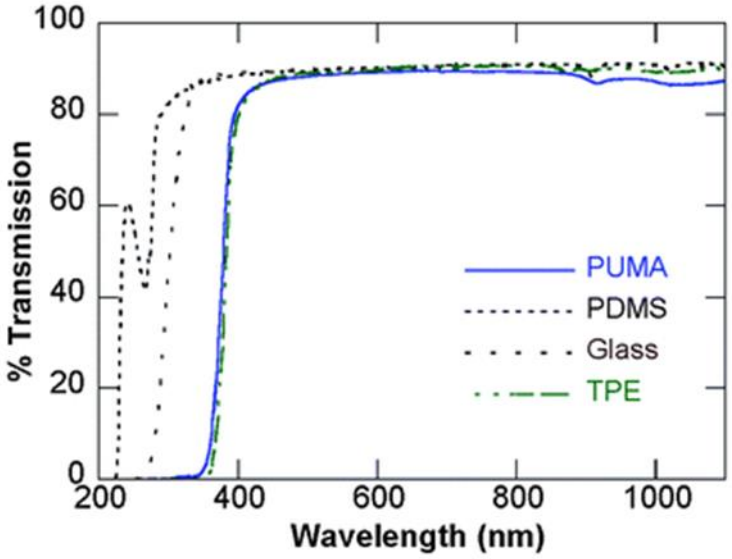

Figure S4.1: The transmission spectrum of polydimethylsiloxane (PDMS) is indicated by the dashed curve. At 254 nm, the transmittance of PDMS is between 60 % and 40 %.[67]

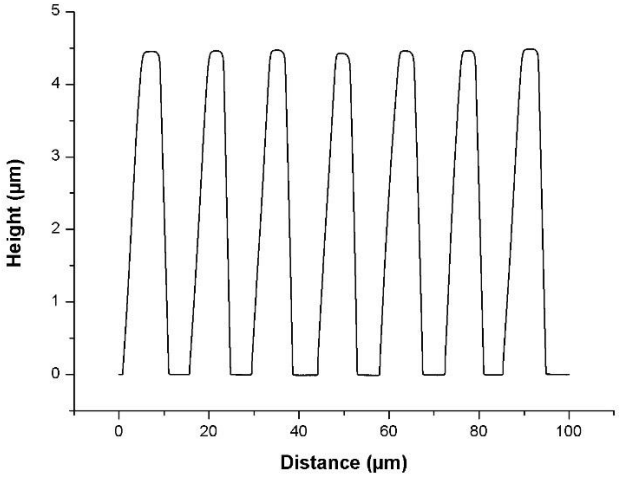

Figure S4.2: Height profile of the master structure (75 patterned structures) using a stylus with a diameter of 2 µm, a stylus force of 1 mg and a scanning speed of 1 µm/s. The height of the patterned MIP structures is 4.5 µm and the width ranges from 5 – 10 µm (from the top to the bottom).

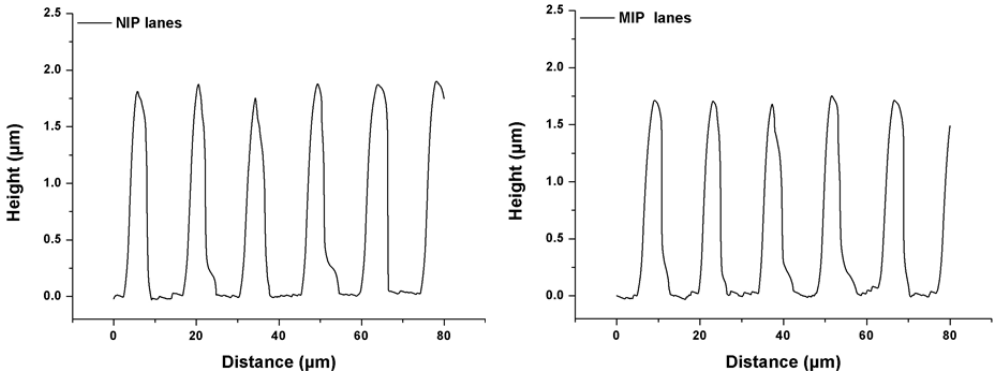

Figure S4.3: Height profiles of both NIP and MIP structures (75 lines) using a stylus with a diameter of 2 µm, a stylus force of 1 mg and a scanning speed of 1 µm/s. The height of the structure is 1.75 µm.

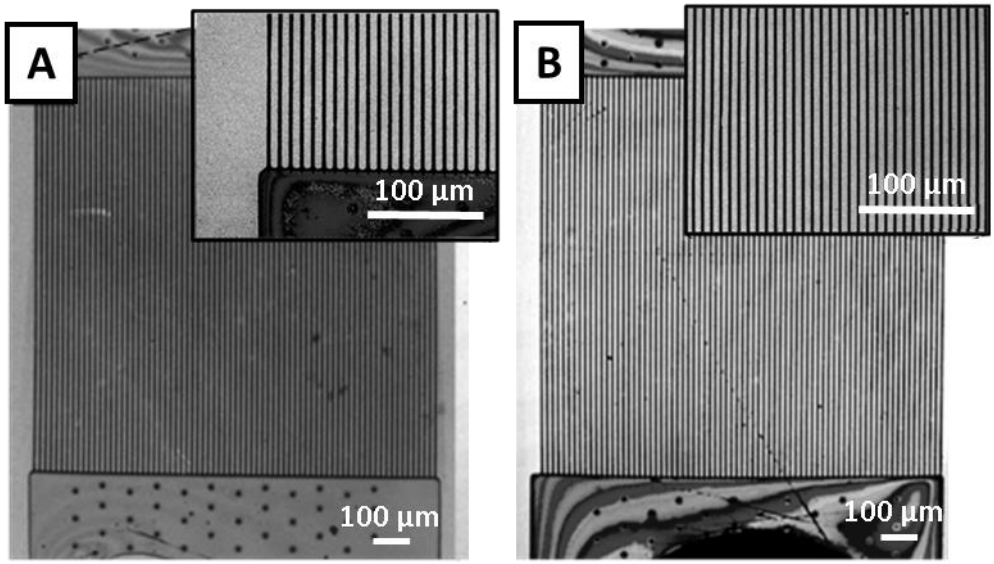

Figure S4.4: Overview and magnified optical microscopy images of the MIP (A) and NIP patterns (B). The enlarged image in (A) also shows the connection block.

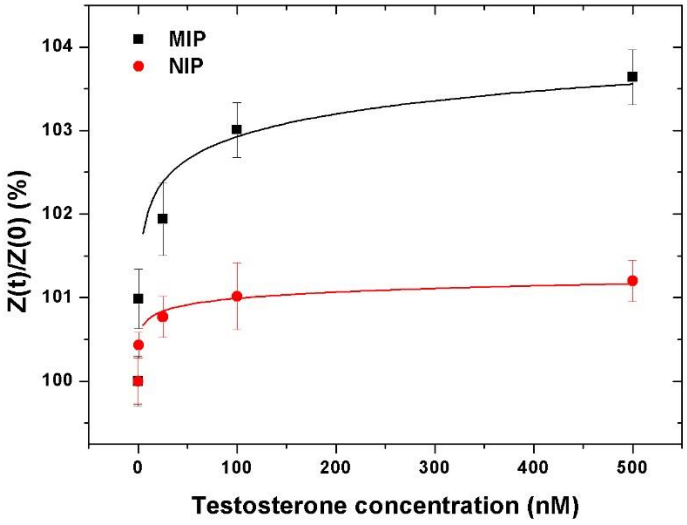

Figure S4.5. EIS dose-response curves of the MIP and NIP structures exposed to increasing concentrations of testosterone in EtOH/saliva solution. The curves are based on nonlinear fits.

4.7 References

[1] D. Wild, *The Immunoassay Handbook (Fourth Edition)*, Elsevier, Oxford **2013**.

[2] W. Jennings, E. Mittlefehldt, P. Stremple, *Analytical Gas Chromatography (Second Edition)*, Academic Press, San Diego **1997**.

[3] R. Gonzalo-Lumbreras, D. Pimentel-Trapero, R. Izquierdo-Hornillos, *Journal of chromatographic science* **2003**, 41, 261.

[4] F. Gasser, N. Jeandidier, S. Doffoel, F. Klein, R. Sapin, *Immuno. Anal Biol. Spé.* **2003**, 18, 98.

[5] T. G. Shrivastav, A. Basu, K. P. Kariya, *Journal of immunoassay & immunochemistry* **2003**, 24, 205.

[6] F. Vera, R. R. Zenuto, C. D. Antenucci, J. M. Busso, R. H. Marín, *Journal of Experimental Zoology Part A: Ecological Genetics and Physiology* **2011**, 315A, 572.

[7] R. L. Fitzgerald, T. L. Griffin, D. A. Herold, *Methods in molecular biology (Clifton, N.J.)* **2010**, 603, 489.

[8] Y. Wang, G. D. Gay, J. C. Botelho, S. P. Caudill, H. W. Vesper, *Clinica chimica acta; international journal of clinical chemistry* **2014**, 436, 263.

[9] B. Barlen, S. D. Mazumdar, M. Keusgen, *Physica Status Solidi (a)* **2009**, 206, 409.

[10] A. Lueking, D. J. Cahill, S. Müllner, *Drug Discovery Today* **2005**, 10, 789.

[11] W. H. Robinson, C. DiGennaro, W. Hueber, B. B. Haab, M. Kamachi, E. J. Dean, S. Fournel, D. Fong, M. C. Genovese, H. E. Neuman, *Nature Medicine* **2002**, 8, 295.

[12] J. Wang, *Electroanalysis* **2001**, 13, 983.

[13] J. J. Gooding, *Electroanalysis* **2002**, 14, 1149.

[14] M. Liss, B. Petersen, H. Wolf, E. Prohaska, *Analytical chemistry* **2002**, 74, 4488.

[15] K. Eersels, B. van Grinsven, A. Ethirajan, S. Timmermans, K. L. Jiménez Monroy, J. F. J. Bogie, S. Punniyakoti, T. Vandenryt, J. J. A. Hendriks, T. J. Cleij, M. J. A. P. Daemen, V. Somers, W. De Ceuninck, P. Wagner, *ACS Appl. Mater. Interfaces* **2013**, 5, 7258.

[16] V. J. Ruigrok, M. Levisson, M. H. Eppink, H. Smidt, J. van der Oost, *Biochemical Journal* **2011**, 436, 1.

[17] K. Mosbach, *Trends Biochem. Sci.* **1994**, 19, 9.

[18] B. Sellergren, *Molecularly Imprinted Polymers. Man-Made Mimics of Antibodies and their Application in Analytical Chemistry*, Elsevier Science, Amsterdam, The Netherlands **2000**.

[19] S. A. Piletsky, S. Alcock, A. P. F. Turner, *Trends Biotechnol.* **2001**, 19, 9.

[20] M. Whitcombe, E. Vulfson, *Advanced Materials* **2001**, 13, 467.

[21] R. Arshady, K. Mosbach, *Die Makromolekulare Chemie* **1981**, 182, 687.

[22] M. Peeters, F. Troost, B. van Grinsven, F. Horemans, J. Alenus, M. S. Murib, D. Keszthelyi, A. Ethirajan, R. Thoelen, T. Cleij, *Sensors and Actuators B: Chemical* **2012**, 171, 602.

[23] B. Sellergren, C. Allender, *Advanced Drug Delivery Reviews* **2005**, 57, 1733.

[24] P. K. Owens, L. Karlsson, E. S. M. Lutz, L. I. Andersson, *TrAC Trends in Analytical Chemistry* **1999**, 18, 146.

[25] G. Wackers, T. Vandenryt, P. Cornelis, E. Kellens, R. Thoelen, W. De Ceuninck, P. Losada-Perez, B. van Grinsven, M. Peeters, P. Wagner, *Sensors (Basel, Switzerland)* **2014**, 14, 11016.

[26] M. Peeters, F. J. Troost, R. H. Mingels, T. Welsch, B. van Grinsven, T. Vranken, S. Ingebrandt, R. Thoelen, T. J. Cleij, P. Wagner, *Analytical chemistry* **2013**, 85, 1475.

[27] T. Kamra, S. Chaudhary, C. Xu, N. Johansson, L. Montelius, J. Schnadt, L. Ye, *Journal of Colloid and Interface Science* **2015**, 445, 277.

[28] Y. Chen, Y. Liu, X. Shen, Z. Chang, L. Tang, W.-F. Dong, M. Li, J.-J. He, *Sensors* **2015**, 15, 29877.

[29] Y. Fuchs, O. Soppera, A. G. Mayes, K. Haupt, *Advanced Materials* **2013**, 25, 566.

[30] A. Betatache, F. Lagarde, C. Sanglar, A. Bonhommé, D. Léonard, N. Jaffrezic-Renault, *Sensors & Transducers Journal* **2014**, 27, 92.

[31] K. Reimhult, K. Yoshimatsu, K. Risveden, S. Chen, L. Ye, A. Krozer, *Biosensors and Bioelectronics* **2008**, 23, 1908.

[32] Y. Tan, L. Jing, Y. Ding, T. Wei, *Appl. Surf. Sci.* **2015**, 342, 84.

[33] C. Alexander, H. S. Andersson, L. I. Andersson, R. J. Ansell, N. Kirsch, I. A. Nicholls, J. O'Mahony, M. J. Whitcombe, *J. Mol. Recognit.* **2006**, 19, 106.

[34] J. Svenson, I. A. Nicholls, *Analytica Chimica Acta* **2001**, 435, 19.

[35] M. Yang, W. Gu, L. Sun, F. Zhang, Y. Ling, X. Chu, D. Wang, *Talanta* **2010**, 81, 156.

[36] N. Pérez-Moral, A. G. Mayes, *Analytica Chimica Acta* **2004**, 504, 15.

[37] D. Vaihinger, K. Landfester, I. Kräuter, H. Brunner, G. E. M. Tovar, *Macromol. Chem. Phys.* **2002**, 203, 1965.

[38] B. K. Lavine, D. J. Westover, N. Kaval, N. Mirjankar, L. Oxenford, G. K. Mwangi, *Talanta* **2007**, 72, 1042.

[39] I. Chianella, S. A. Piletsky, I. E. Tothill, B. Chen, A. P. F. Turner, *Biosensors and Bioelectronics* **2003**, 18, 119.

[40] Y. Tan, H. Peng, C. Liang, S. Yao, *Sensors and Actuators B: Chemical* **2001**, 73, 179.

[41] J. Alenus, P. Galar, A. Ethirajan, F. Horemans, A. Weustenraed, T. J. Cleij, P. Wagner, *Phys. Status Solidi A* **2012**, 209, 905.

[42] B. D. Gates, Q. Xu, J. C. Love, D. B. Wolfe, G. M. Whitesides, *Annual Review of Materials Research* **2004**, 34, 339.

[43] A. V. Linares, A. Falcimaigne-Cordin, L. A. Gheber, K. Haupt, *Small* **2011**, 7, 2318.

[44] R. B. Pernites, S. K. Venkata, B. D. B. Tiu, A. C. C. Yago, R. C. Advincula, *Small* **2012**, 8, 1669.

[45] D. C. Apodaca, R. B. Pernites, F. R. Del Mundo, R. C. Advincula, *Langmuir : the ACS journal of surfaces and colloids* **2011**, 27, 6768.

[46] K. M. Choi, *Bio-chemical sensors based on molecularly imprinted polymers; soft lithography, microfabrication and microfluidic synthesis*, One Central Press **2014**.

[47] C. Ayela, G. Dubourg, C. Pellet, K. Haupt, *Advanced materials (Deerfield Beach, Fla.)* **2014**, 26, 5876.

[48] G. M. Swain, A. B. Anderson, J. C. Angus, *MRS Bulletin* **1998**, 23, 56.

[49] K. Bakowicz-Mitura, G. Bartosz, S. Mitura, *Surface and Coatings Technology* **2007**, 201, 6131.

[50] M. Shen, L. Martinson, M. S. Wagner, D. G. Castner, B. D. Ratner, T. A. Horbett, *Journal of biomaterials science. Polymer edition* **2002**, 13, 367.

[51] A. Hartl, E. Schmich, J. A. Garrido, J. Hernando, S. C. Catharino, S. Walter, P. Feulner, A. Kromka, D. Steinmuller, M. Stutzmann, *Nature materials* **2004**, 3, 736.

[52] J. Rubio-Retama, J. Hernando, B. López-Ruiz, A. Härtl, D. Steinmüller, M. Stutzmann, E. López-Cabarcos, J. Antonio Garrido, *Langmuir : the ACS journal of surfaces and colloids* **2006**, 22, 5837.

[53] S. Wenmackers, V. Vermeeren, M. vandeVen, M. Ameloot, N. Bijnens, K. Haenen, L. Michiels, P. Wagner, *physica status solidi (a)* **2009**, 206, 391.

[54] V. Vermeeren, L. Grieten, N. Vanden Bon, N. Bijnens, S. Wenmackers, S. D. Janssens, K. Haenen, P. Wagner, L. Michiels, *Sensors and Actuators B: Chemical* **2011**, 157, 130.

[55] J. Hernando, T. Pourrostami, J. A. Garrido, O. A. Williams, D. M. Gruen, A. Kromka, D. Steinmüller, M. Stutzmann, *Diamond and related materials* **2007**, 16, 138.

[56] W. Yang, O. Auciello, J. E. Butler, W. Cai, J. A. Carlisle, J. E. Gerbi, D. M. Gruen, T. Knickerbocker, T. L. Lasseter, J. N. Russell, Jr., L. M. Smith, R. J. Hamers, *Nature materials* **2002**, 1, 253.

[57] B. van Grinsven, N. Vanden Bon, L. Grieten, M. Murib, S. D. Janssens, K. Haenen, E. Schneider, S. Ingebrandt, M. J. Schoning, V. Vermeeren, M. Ameloot, L. Michiels, R. Thoelen, W. De Ceuninck, P. Wagner, *Lab Chip* **2011**, 11, 1656.

[58] M. Steenackers, R. Jordan, A. Küller, M. Grunze, *Advanced Materials* **2009**, 21, 2921.

[59] N. A. Hutter, M. Steenackers, A. Reitinger, O. A. Williams, J. A. Garrido, R. Jordan, *Soft Matter* **2011**, 7, 4861.

[60] J. LeJeune, D. A. Spivak, *Analytical and bioanalytical chemistry* **2007**, 389, 433.

[61] E. Kellens, H. Bové, M. Conradi, L. D'Olieslaeger, P. Wagner, K. Landfester, T. Junkers, A. Ethirajan, *Macromolecules* **2016**, 49, 2559.

[62] G. M. Birnbaumer, P. A. Lieberzeit, L. Richter, R. Schirhagl, M. Milnera, F. L. Dickert, A. Bailey, P. Ertl, *Lab on a Chip* **2009**, 9, 3549.

[63] C.-H. Weng, W.-M. Yeh, K.-C. Ho, G.-B. Lee, *Sensors and Actuators B: Chemical* **2007**, 121, 576.

[64] J. Taieb, B. Mathian, F. Millot, M. C. Patricot, E. Mathieu, N. Queyrel, I. Lacroix, C. Somma-Delpero, P. Boudou, *Clin. Chem.* **2003**, 49, 1381.

[65] J. Dana-Haeri, J. Oxley, A. Richens, *British Medical Journal (Clinical research ed.)* **1982**, 284, 85.

[66] H. Jin, J. Lin, L. Fu, Y. F. Mei, G. Peng, X. Tan, D. M. Wang, W. Wang, Y. G. Li, *Biochemistry and Cell Biology* **2007**, 85, 246.

[67] J. S. Kuo, L. Ng, G. S. Yen, R. M. Lorenz, P. G. Schiro, J. S. Edgar, Y. Zhao, D. S. W. Lim, P. B. Allen, G. D. M. Jeffries, D. T. Chiu, *Lab Chip* **2009**, 9, 870.

5 Fabrication of low cost sensors based on molecularly imprinted polymer particles

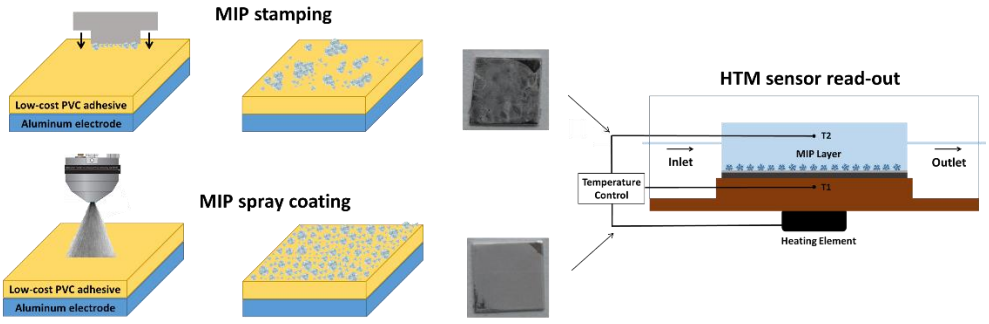

5.1 Abstract

We report the fabrication of low-cost sensors based on molecularly imprinted polymer (MIP) particles as synthetic receptors that allow for easy and convenient upscaling. The MIP particles can be readily obtained using bulk polymerization and can be used as recognition elements on sensor electrodes. As the synthesis of these MIPs is low-cost, the choice of detection technique is crucial for commercialization. In this regard, the heat transfer resistance method (HTM) is very cost-effective due to its simple set-up. However, the MIP particles need to be integrated onto the sensor surface using an adhesive layer. The choice of the adhesive layer and a controllable deposition method is highly important. Previously, a conjugated polymer, namely poly[2-methoxy-5-(3',7'-dimethoxyoctyloxy)-1,4-phenylenevinylene] (MDMO-PPV) was used as adhesive layer. The MIP particles were transferred onto the substrate by stamping followed by annealing to embed the particles partially into the adhesive layer. As PPV is an expensive material and the stamping deposition method is very much dependent on the operator skills, in here for the first time we tested polyvinylchloride, an economically viable readily available common polymer for the adhesive layer in

combination with HTM and a deposition method based on spray coating that allows for high reproducibility and automation for the large scale fabrication of sensor layers. MIP particles capable of detecting serotonin, a clinically relevant biomarker, were used and the sensor layer obtained by spray coating was compared with the previously established stamping method for sensor coverage and their respective sensor performances.

5.2 Introduction

The need for low cost, fast performing and accurate sensors for the detection of relevant molecules in effect relevant concentrations becomes increasingly important, especially in the field of point-of-care medical diagnostics and food- and environmental safety. In a sensor, recognition elements that are able to bind the target molecule are immobilized on a signal transducer. Binding between these receptors and the target can be quantified using electronic or optical read-out techniques.[1, 2] In a biosensor, typically, biological receptors such as DNA, antibodies, enzymes, cells, etc… are used.[3-6] However, these natural receptors are expensive, very time consuming to obtain in sufficient quantities and they show unsatisfactory specificity and physical or chemical stability.[7] Therefore, worthy alternatives for the detection element are 'synthetic' or 'biomimetic' receptors such as molecularly imprinted polymers (MIPs).[8] MIPs are polymers, which contain nanoimprints/nanocavities that have selective affinity for the target molecule.[9-13] These nanocavities are created by the addition of the target/template molecule prior to polymerization so that the functional groups of the monomers can arrange around them through covalent or non-covalent bonds. After polymerization, the subsequent removal of the template molecules leaves nanocavities which have the ability to rebind the target molecule. This property makes the MIPs suitable to be used as detection elements. MIPs can therefore be employed as a low cost receptor in membranes, sensors, affinity chromatography, stationary phase extractions, drug delivery systems and pseudo-immunoassays.[14-19] Because of the broad variety of available functional monomers, MIPs for wide range of molecules can be generated. These versatile MIPs are ideal to be imprinted with small organic molecules such as neurotransmitters [17], but also with ions [20] and larger elements including

proteins [21] and cells [6]. As a negative control, also a non-imprinted polymer (NIP) is synthesized in an identical way, but without the presence of the target molecule during polymerization.

An important aspect in sensors for diagnostic applications is to obtain correct and consistent target molecule quantifications. This property depends, amongst other factors, on the level of homogeneity between various sensing transducer substrates in terms of receptor material amount and distribution. Therefore the reproducibility and scalability of the deposition technique used to apply the MIP particles on the transducer substrate is a critical factor. Possible techniques to deposit MIP particles include stamping, screen printing, spin coating and spray coating.

Wackers et. al. combined bulk MIP particles for the detection of serotonin with the heat transfer method (HTM) read-out technique using a stamping based deposition technique.[22] The polymer particles were manually stamped on a substrate coated with a poly[2-methoxy-5-(3',7'-dimethoxyoctyloxy)-1,4-phenylenevinylene] (MDMO-PPV) layer which serves as an adhesive, by using an elastic polydimethylsiloxaan (PDMS) stamp. To fixate the MIPs, this substrate was heated above the glass transition temperature. This way, the MIP particles partially sunk into the soft adhesive layer. However, this stamping procedure is very much dependent on the handling and skill of the operator and prone to high intra- and inter sample receptor material variations.

Another MIP deposition technique is screen printing which is simple and easily upscalable.[23] The drawback is that this method requires a high concentration slurry, special solvents, fillers and binders. The latter might encapsulate the MIP particles and block the nanoimprint cavities leaving them unable to rebind any target molecule.

Also spin coating can be used as a MIP deposition technique, however, a stable dispersion is required to obtain a homogeneous particle layer. This was done by Lavine et. al. where they spin coated suspension polymerized MIPs (300 nm) dispersed in methanol on top of a gold substrate. Multiple spin coating cycles were required to obtain a uniform and well-covered surface.[24] Another approach is to spin coat a MIP containing polyvinylchloride (PVC)/tetrahydrofuran (THF) mixture. This was done by Chianella et al. and Tan et al. using bulk polymerized MIP particles.[25, 26] Using the latter technique, the PVC might partially block the

imprints of the MIP particles leaving them unable to bind target molecule during the sensor measurement.

In this work, coating of MIP particles using spray coating was tested for the first time. The latter is one of the few techniques to give a higher surface coverage, reduce the intra- and inter sample variation and gives a unique opportunity to have a standardized way to create reproducible and scalable solutions for sensor array production. In addition to the possibility for mass production (spraying of large surfaces) of MIP coated substrates, spray coating also allows to deposit the polymer particles in specific structures with a spatial resolution of 100 µm. This is interesting for multi-analyte sensing like full urine or blood analysis where a number of target molecules in a sample fluid are quantified in the same measurement.

Another important aspect in sensors for diagnostic applications is the cost-effectiveness. Wackers et. al. used the expensive MDMO PPV as an adhesive layer to fixate the MIP particles on the transducer. In this work, the low cost and readily available polyvinylchloride is tested instead. In addition, the simple, affordable and miniaturizable heat transfer resistance method was used as a sensor read-out technique. It circumvents the need of sophisticated equipment since it requires only two thermocouples, a proportional-integral-derivative (PID) controller and an adjustable heat source.[22]

In the context of using the spray coating technique for MIP based sensors, Haupt et al. created a free-standing MIP microcantilever for resonance frequency based mass sensor applications.[27] The MIP prepolymerization mix was sprayed onto a silicon substrate covered with a SU8 based patterned stencil. After photopolymerization, MIP structures of 100 µm in thickness and 500 µm in length were obtained. When compared to bulk MIP particles, these structures show a reduced surface-to-volume ratio which might lead to a lower active MIP sensing surface and sensor sensitivity. In addition, the SU8 photoresist is relatively expensive material which limits its use for cost-effective sensors.

Serotonin (Figure 5.1) has a role in smooth muscle contraction, emotions, sleep and appetite.[28, 29] An imbalance in serotonin body concentrations can be found in patients with hypertension, migraine, fibrotic syndrome, carcinoid tumors and mental disorders.[29-33] The concentration range of serotonin in the portal blood plasma of healthy individuals is 5 – 20 nM.[32, 34] Typically, for the detection of

serotonin in the range of 1 ng/ml, high performance liquid chromatography is used.[35, 36] However, this technique is not cost efficient enough as it needs expensive equipment, making it unsuitable for scalability, fast screening and point-of-care applicability. Other less established options to detect serotonin, found in literature and all in the status of 'proof of concept', are electrochemical techniques like amperometric and voltametric sensing, however, they also do not offer enough selectivity for serotonin to allow for detection in the relevant physiological concentration range.[37-39]

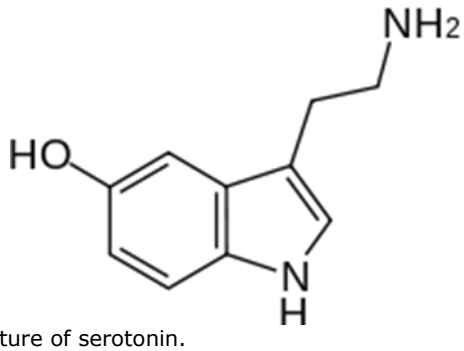

Figure 5.1. Chemical structure of serotonin.

The MIPs used in this work have been synthesized using the widely employed bulk polymerization technique due to its simplicity. After crushing the bulk polymer monolith, a MIP powder consisting of particles with a size ranging from 0.1 to 10 µm was obtained. To test the target molecule rebinding characteristics of these MIPs, equilibrium binding analysis experiments were performed. Subsequently, the MIP particles were deposited on the sensor surface, where the spray coating technique was benchmarked versus the already well known stamping methodology.[17, 22] The deposition of MIP particles using the respective methodology was carried out on a PVC adhesive layer spin coated on top of an aluminum sheet electrode. The read-out technique was based on HTM to detect thermal resistance (R_{th}) changes induced by molecular binding events. The combination of the low cost materials, scalable and reproducible deposition method and cost-effective and miniaturizable read-out, could provide the next step towards a 1 $ sensor for the detection of low molecular weight molecules.

5.3 Experimental section

5.3.1 Materials

Ethylene glycol dimethacrylate (EGDM), methacrylic acid (MAA), acrylamide (AM), dimethylsulfoxide (DMSO), dopamine, acetic acid, PVC and THF were purchased from Sigma Aldrich. The stabilizers in the monomers MAA and EGDM were removed by filtration over basic alumina (Sigma). Azobusisobutyronitrile (AIBN) and the target molecule serotonin were obtained from Fluka and Alfa Aesar respectively. All solvents (analytical grade) were obtained from VWR and used as such. Phosphate buffered saline packs were purchased from Thermo Scientific.

5.3.2 MIP synthesis

The MIP synthesis procedure used in this work is an adapted version of Peeters et. al.[17] MAA (2.84 mmol), AM (8.50 mmol), EGDM (22.72 mmol), AIBN (0.61 mmol) and the target molecule serotonin (5.67 mmol) were dissolved in 7.7 g DMSO. After degassing this solution with nitrogen, it was polymerized in a UV chamber for 20 h. As a negative control, a NIP was synthesized in an identical way, but without the presence of the target molecule. Subsequently, the bulk polymer was ground (using the pulverisette 7, Fritsch at 500 rpm for 300 s) and the obtained particles were in the size range of 0.1 to 10 µm. The size and the shape of the polymer particles were characterized by optical microscopy (Axiovert 40 Carl Zeiss). As a final step the MIP and NIP particles were washed by Soxhlet extraction with ethanol (48 h), a mixture of acetic acid/acetonitrile (1/1) (48 h) and methanol (24 h) in order to remove the target molecule serotonin from the imprint sites. After these washing steps, no template molecules were observable in the solvent waste by using UV-Vis spectroscopy (λ_{max} serotonin = 276 nm, Nanodrop 2000c, Thermo Scientific, 10 mm quartz cuvette). Subsequently, the polymer particles were dried on a vacuum pump.

5.3.3 Optical batch rebinding experiments

To test the binding capacity of the bulk serotonin MIPs, batch rebinding experiments were performed. For this, 30 mg of MIP and NIP powder was

suspended in 2 ml of 1 x phosphate buffered saline (PBS) solution (pH 7.4) containing different amounts of serotonin concentrations (0.10, 0.15, 0.20, 0.25, 0.30 and 0.35 mM). The resulting suspensions were shaken overnight (16 h) at room temperature to reach an equilibrium between bound and free target molecules. Subsequently the dispersions were centrifuged for 20 minutes at 10.000 rpm and filtered (0.2 µm Chromafil PTFE syringe filters) to separate the polymer from the supernatants. The serotonin solutions used for calibration were also filtered to make sure that there is negligible target molecule retention during this step. The free concentration (C_f) of serotonin in the supernatant was measured by UV-Vis spectroscopy.

5.3.4 Preparation of the PVC coated transducer substrate

In order to fixate the bulk MIP and NIP particles to an aluminum sheet transducer element (10 x 10 mm and a thickness of 0.5 mm), the latter was coated with a PVC adhesive layer. To obtain a homogeneous layer with a thickness of around 180 nm, a 2 w% PVC/THF solution was spincoated (Laurell WS-400BX-6NPP/LITE, 5000rpm, 1650 m/s2, 1 minute, at room temperature) on the aluminum substrates. The thickness of the layer was examined using dektak (XT profilometer Bruker) measurements.

5.3.5 Stamping of MIPs and NIPs on the transducer element

The dried MIP and NIP powders were manually stamped on top of the PVC coated aluminum substrate using an elastomer PDMS stamp by hand using a light force. Subsequently the substrates are heated above the glass transition temperature (T_g) of PVC (120°C, 15 min). This way the polymer particles sink into the soft PVC adhesive layer. Subsequently, the substrates are cooled and rinsed with water in order to remove MIPs and NIPs that were not immobilized. The surface of the substrates coated with the particles were further characterized using an optical microscope (Axiovert 40 Carl Zeiss) and a scanning electron microscope (SEM, Quanta 200F SEM, FEI, 20kV). In addition, to study how deep the polymer

particles are embedded in the PVC layer, also the cross section of these substrates was investigated. Using a dual-beam focused ion beam (FIB) FEI Helios Nanolab 600i operating with an acceleration voltage of 30.0 kV and a milling current of 0,28 nA and subsequently 48 pA, the cross sections were prepared. The SEM images were taken using a through-lens detector with a voltage of 5.0 kV and a 0,69 nA current.

5.3.6 Spraycoating of MIPs and NIPs on the transducer element

A 2 w% MIP/ethanol dispersion was sprayed on the PVC coated transducer elements using a Sono-Tek Exacta Coat with a flow rate of 0.5 ml/min. The nozzle had a run power of 3.2 W and moved with a speed of 15 mm/s. The nozzle moved 10, 20, 30 and 40 times back and forth over different sets of substrates, adding particles to the substrates on each passing. Ultrasonic vibrations were applied to avoid particle aggregation which ensures a homogeneous material deposition on the substrates. Subsequently, the sensor electrodes were heated above the T_g (120 °C, 15 min) of the adhesive PVC layer to immobilize the polymer particles. After rinsing, these substrates were characterized in the same way as the substrates prepared using the stamping technique (optical microscope and SEM).

5.3.7 Design of the sensor setup

The substrates with the immobilized MIPs or NIPs on top (either by stamping or by spraycoating) were placed on a copper plate which was connected to a power resistor heating element (22 Ω, MPH20S, Farnell, Grace-Hollogne, Belgium). To monitor the temperature of this copper block, a thermocouple (type K, diameter 500 µm, TC Direct, Nederweert, The Netherlands) was inserted. The temperature of the copper block (T1) was kept at 37.00 ± 0.02 °C with a PID (P = 1, I = 8, D = 0.1) controller. A second thermocouple is inserted into the PBS to measure the temperature in the liquid (T2) at a fixed height (2 mm) above the aluminum sheet electrode. In Figure 5.2, a schematic representation of the sensor set-up is shown. The temperature of the copper (T1) is regulated and the heat flows through the MIP or NIP covered substrate to the liquid where the temperature (T2) is

measured. As the target molecule binds to the cavities in the MIP, the heat flow is blocked resulting in an increase in thermal resistance.

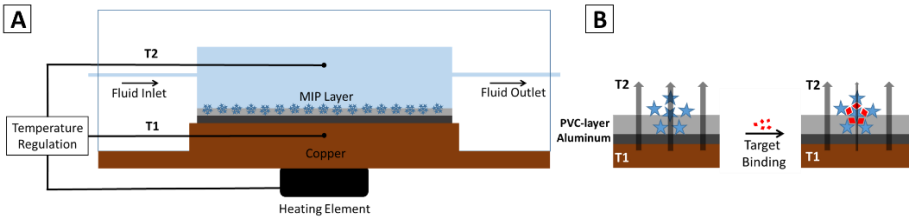

Figure 5.2. Schematic illustration of the Rth set-up (A). Visualization of the 'pore blocking model' [40] (B).

For the sensor measurements, the aluminum substrates on which MIPs or NIPs were deposited using 40 spray coat passes, were installed in the sensor set-up and the R_{th} signal was allowed to stabilize for 2 hours in static conditions (no flow) with degassed 1 x PBS buffer (pH 7.4 and 37.00 ±0.02 °C). The obtained stabilized R_{th} value is set to zero. After the stabilization time, 1 mL of degassed PBS solutions containing 100, 200, 500 and 1000 nM of serotonin, were added with one hour intervals resulting in changes in temperature of the fluid in the measuring chamber (T2). The power needed to keep the set-up at 37 °C was determined and was subsequently used to calculate the R_{th} using the formula in equation 5.1 in which P is the power in Watt (W), T1 is the temperature in degrees Celsius (°C) of the heat sink (copper block), and T2 is the temperature of the fluid (°C). After the measurement, a graph can be constructed in which the x-axis represents the duration of the measurement and the y-axis the change in R_{th}.

$$R_{th} = \frac{(T1 - T2)}{P} \qquad \text{Eq. 5.1}$$

5.4 Results and discussion

MIP particles were synthesized using the bulk polymerization technique to detect the target molecule serotonin. These particles were deposited by either stamping or spray coating on a sensor transducer substrate comprising of a low cost PVC adhesive layer spin coated on top of an aluminum substrate. Both MIP deposition techniques are compared in terms of sensor coverage and their respective sensor performances using the simple and miniaturizable HTM technique.

5.4.1 Characterization of bulk MIP and NIP particles

After obtaining the bulk MIP and NIP monoliths by bulk polymerization, they were crushed to obtain particles with a size ranging from 0.1 – 10 µm. In Figure 5.3 an optical microscopy image of the MIP particles is shown. As no visible difference can be observed between the MIP and NIP particles, an optical microscopy image of the NIP particles is shown in Figure S5.1.

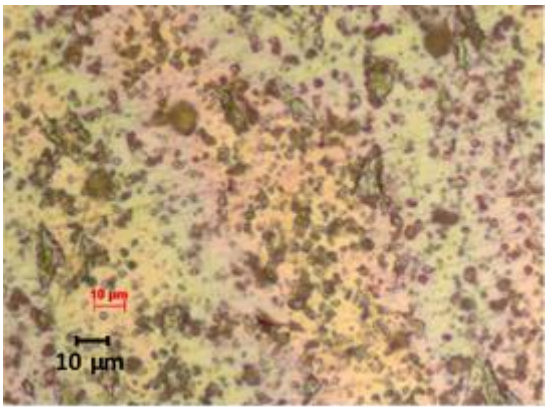

Figure 5.3. Optical microscopy image of crushed bulk MIP particles.

The binding capacity of the bulk MIPs for serotonin was analyzed by batch rebinding experiments. For these experiments, 30 mg of MIP or NIP powder was added to 2 ml of 1x PBS solution (pH 7.4) with serotonin concentrations of 0.10, 0.15, 0.20, 0.25, 0.30 and 0.35 mM. The resulting suspensions were shaken overnight at room temperature and subsequently centrifuged for 20 minutes at 10,000 rpm and filtered. The free concentration (C_f) of serotonin in the supernatant was measured by UV-VIS spectrometry and the amount of bound target molecule per gram MIP or NIP (S_b) was calculated. Based on these values, the binding isotherms were constructed (Figure S5.2). MIPs that bind the target molecule based on the non-covalent interaction principle contain a heterogeneous distribution of binding sites and affinity constants, therefore, the Freundlich model is used to describe the binding isotherms.[41, 42] An allometric fitting ($S_b = AC_f^v$, where S_b is the amount of target molecule bound to the polymer particles, A is the Freundlich constant, C_f is the free concentration of target molecule and v is

the Freundlich heterogeneity parameter) was used to fit the data.[12] The imprint factor, which is the ratio of the amount of target molecules bound per gram of the MIP to that of the NIP (S_b MIP/S_b NIP), was calculated to evaluate the amount of specific versus nonspecific binding. There is a clear difference between the MIP and the NIP isotherm: for every target molecule concentration, the MIP particles show more serotonin binding as compared to their NIP counterparts. At the concentration C_f = 0.5 mM, the imprint factor (IF) is 1.66 which means that at this free concentration the binding of the MIP to the target molecule is 1.66 times better in comparison with the NIP.

5.4.2 MIP deposition

As a next step, these polymer MIP and NIP particles are immobilized on a substrate to serve as the active sensing element in a sensor. In this work, aluminum was used as transducer material as it is cheap and has good heat conduction properties. A 180 nm thick PVC layer serving as adhesive was spin coated on top of these aluminum substrates. In Figure S5.3, optical microscopy images of a bare and a PVC coated aluminum sensor electrode are shown. The thickness of the PVC layer was characterized using profilometry (Figure S5.4). As a next step the polymer particles were deposited via stamping or spray coating (10, 20, 30 and 40 passes) and subsequently the substrates were heated to 120 °C (for 15 minutes) which is above the glass transition temperature of PVC. This allows the MIP and NIP particles to partially sink into the softened adhesive layer. After cooling and rinsing the substrates, the polymer particles are trapped in the adhesive layer. The results are shown in Figure 5.4 and 5.5. In order to ensure that during this heating step, the PVC does not flow off of the substrate, profilometry measurements (Figure S5.5) were also performed on a PVC coated substrate (in absence of MIP/NIP particles) that went through the heating treatment (120 °C, 15 min). Since only a small difference of about 10 nm in PVC layer thickness can be observed (between non-baked and baked substrates), it can be safely assumed that all the PVC material remains on the substrate during the heating step.

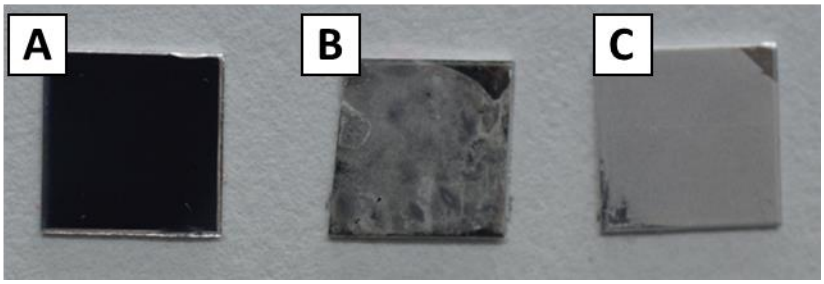

Figure 5.4. Photograph of a PVC coated aluminum electrode containing: no MIP particles (A), MIP particles deposited using the stamping technique (B) and MIP particles deposited using the spray coating technique (40 passes, C).

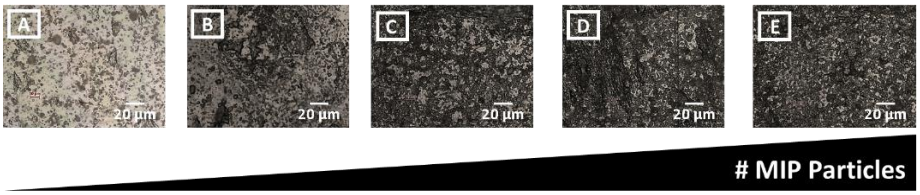

Figure 5.5. Optical microscopy images of a PVC coated aluminum electrode containing MIP particles deposited using stamping (A) or spray coating using 10 (B), 20 (C), 30 (D) or 40 (E) passes.

In Figure 5.4, bare PVC coated aluminium electrode and particles deposited using stamping and spray coating are shown. The photographs visually depict the distribution of particles and the surface coverage on the substrate. The polymer particles which were manually stamped on the substrate using a PDMS elastomer stamp as described by Peeters et. al. are visibly not homogeneously distributed over the substrate.[17] When using MIP and NIP coated substrates for sensing applications, the receptor material distribution variation in and between different substrates should be kept to a minimum by excluding all manual errors during the deposition of the particles. As can be seen in Figure 5.4 C, spray coating offers a more homogeneous material distribution of the MIP particles compared to the stamping alternative. From Figure 5.5, it can be seen that the stamped substrate contains the least amount of polymer particles while the 10 pass spray coated substrate already contains a higher amount of material. With increasing number of passes -10 to 40 passes of spray coating- the amount of particles deposited gradually increases as expected. In Figure 5.6 optical and scanning electron

microscopy images of substrates with stamped and sprayed polymer particles are shown.

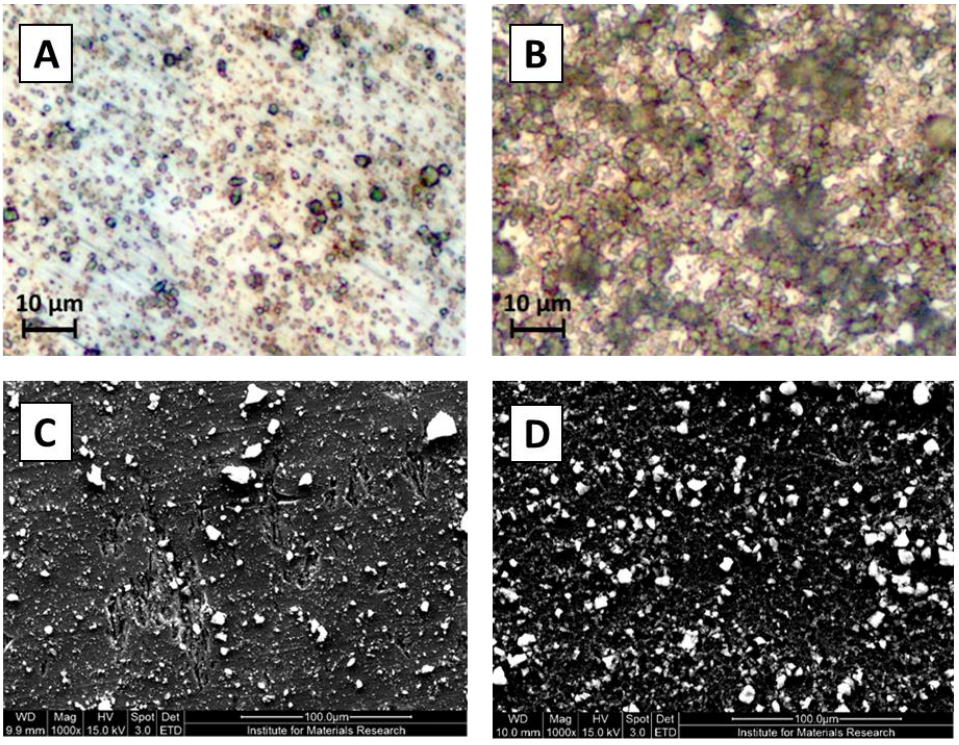

Figure 5.6. Optical (A and B) and scanning electron (C and D) microscopy images of MIPs deposited with different techniques on a PVC coated aluminum substrate: Stamped MIPs (A and C) and sprayed MIPs (40 passes, B and D).

It can be estimated from the SEM images using Image J software, that the spray coated substrates contain approximately 23 % more polymer particles on the surface in comparison with the stamped ones.

5.4.3 Sensor measurements

In this section, the HTM based sensor performance of substrates with MIPs deposited using stamping and spray coating are discussed.

5.4.3.1 Stamping as particle deposition technique

The R_{th} sensor measurements for substrates on which MIP or NIP particles were deposited using the stamping technique, are shown in Figure 5.7. Graph A shows the raw data of the R_{th} signal as a function of time and graph B shows the average change of R_{th} which is plotted with the respective concentration of serotonin. In table 5.1 the absolute values are given together with the absolute difference (delta) in R_{th} signal between MIP and NIP. This way, aspecific binding of serotonin to the NIP and external factors such as fluctuations of the environmental temperature and influence of heat conduction capacity of serotonin are eliminated. Therefore, these delta values represent only the specific binding between the MIP and serotonin. The R_{th} of the MIP increases more in comparison with the R_{th} of the NIP with increasing concentration of serotonin. This effect is due to a higher amount of serotonin binding to the MIP imprints since the thermal resistance of serotonin is higher with respect to the thermal resistance of PBS which was filling the imprints before. The binding of serotonin therefore leads to a more effective heat blocking and a higher heat resistance in accordance to the pore blocking model.[40] Also an R_{th} measurement was successfully performed using dopamine (Figure S5.6) which is structurally similar to serotonin to prove the selectivity of the MIP layer. These results are shown in Figure S5.7.

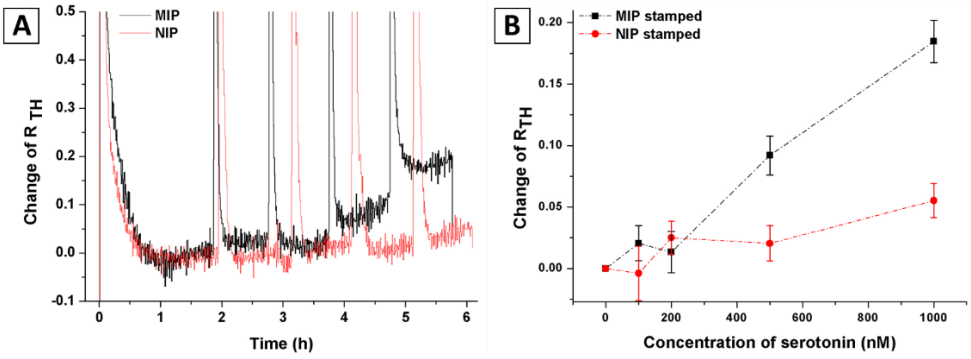

Figure 5.7. R_{th} measurement results for MIP and NIP based sensors obtained using the stamping deposition technique upon addition of increasing serotonin concentrations (100, 200, 500 and 1000 nM) plotted as a function of time (A) and the average change in R_{th} plotted against the concentration of target molecule (B).

Table 5.1. Average change of R_{th} for a given concentration of serotonin together with the absolute difference (delta) between MIP and NIP for sensor substrates prepared using the stamping technique.

Serotonin concentration (nM)	Average change of R_{th} stamped MIP	Average change of R_{th} stamped NIP	Delta average change of R_{th} (stamped MIP-NIP)
100	0.02052	-0.00393	0.02445
200	0.01329	0.02504	-0.01174
500	0.09199	0.02038	0.07161
1000	0.18467	0.05522	0.12945

5.4.3.2 Spray coating as particle deposition technique

In figure 5.8, the R_{th} measurement results with increasing concentrations of target molecule serotonin (100, 200, 500 and 1000 nM) are shown for the substrate with 40 spray coat passes of MIP and NIP ethanol dispersion. Also here the MIP covered substrate is binding significantly more serotonin in comparison with the negative control since the R_{th} increases relatively more for the MIP upon increasing concentration of serotonin. Also for these graphs, the absolute and delta values are given in Table 5.2.

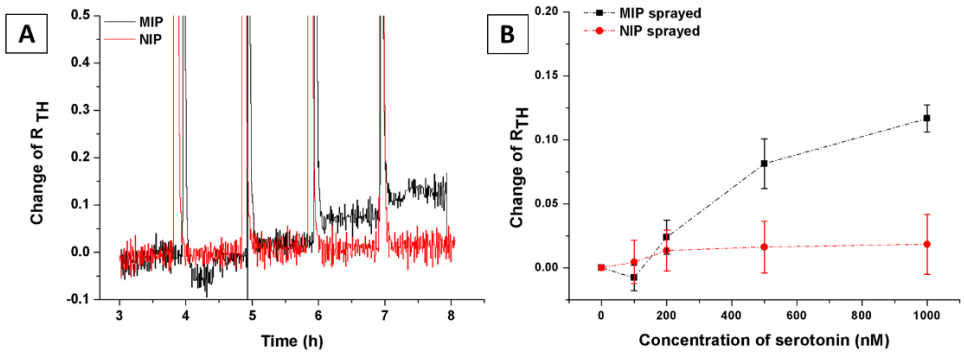

Figure 5.8. R_{th} measurement results for MIP and NIP based sensors obtained using the spray coating deposition technique upon addition of increasing serotonin concentrations (100, 200, 500 and 1000 nM) plotted as a function of time (A) and the average change in R_{th} plotted against the concentration of target molecule (B).

Table 5.2. Average change of R_{th} for a given concentration of serotonin together with the absolute difference (delta) between MIP and NIP for sensor substrates prepared using the spray coating technique.

Serotonin concentration (nM)	Average change of R_{th} sprayed MIP	Average change of R_{th} sprayed NIP	Delta average change of R_{th} (sprayed MIP-NIP)
100	-0.00778	0.00458	-0.01236
200	0.02396	0.01355	0.01041
500	0.08139	0.01620	0.06519
1000	0.11666	0.01837	0.09829

When the delta average change of R_{th} values of the stamped and spray coated substrates are compared at a serotonin concentration of 500 nM, it can be concluded that the sensor employing the stamping deposition technique gives around 10 % more response. The responses of both sensors are not compared at the highest target molecule concentration (1000nM) since at this concentration, the spray coated sensor is already showing saturation. From this result it can be concluded that the amount of MIP material on the sensor substrate is not the only factor that is decisive for the sensor response as the stamped sensor contained less MIP particles then the spray coated sensor. Therefore, to further investigate the effect of the polymer particle deposition technique, the baseline R_{th} (PBS without the presence of target molecule) of the different sensor substrates was measured. The results are shown in Figure 5.9.

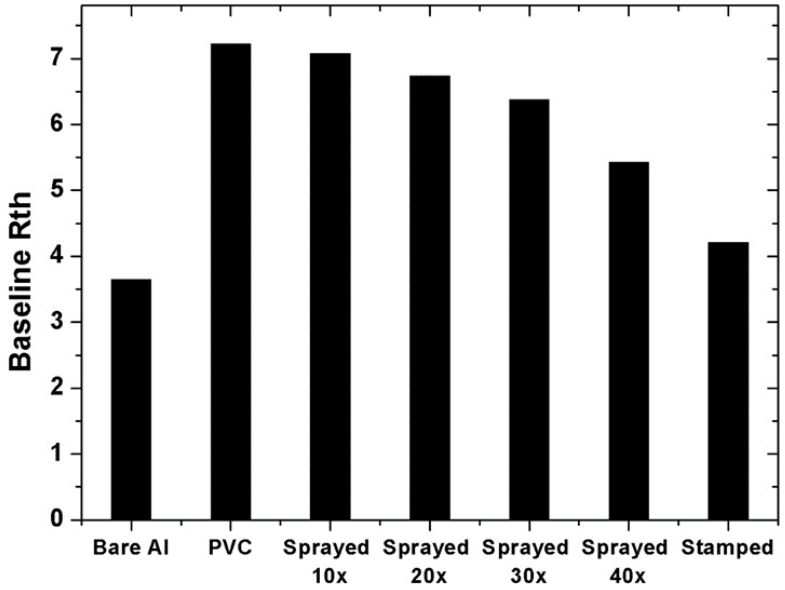

Figure 5.9. Baseline R_{th} values of spray coated MIP samples with increasing MIP particle load (10 – 40 passes). As a reference, the baseline values of a bare and PVC coated aluminum substrate and a stamped MIP substrate are also shown.

From the graph in Figure 5.9, it can be seen that the thermal resistance is at its minimum for bare aluminum and that it reaches a maximum when a uniform layer of PVC is spin coated on top of it. The thermal resistance decreases gradually as more particles (more spray coat passes) are deposited on the substrate. This effect can be due to the fact that the PVC layer gets more inhomogeneous when more particles sink in during the immobilization step. The more rough and inhomogeneous the PVC layer is, the thinner the thermal insulation layer is in specific areas leading to a reduced thermal resistance. This also explains why the substrate with the stamped MIPs shows the lowest baseline R_{th} since here a mechanical force is applied which pushes the particles even deeper into the PVC layer leaving it more inhomogeneous as compared to the spray coated substrates. To further understand these results, FIB cross sections of both stamped and spray coated (40 passes) sensor substrates were made and visualized using SEM (Figure 5.10).

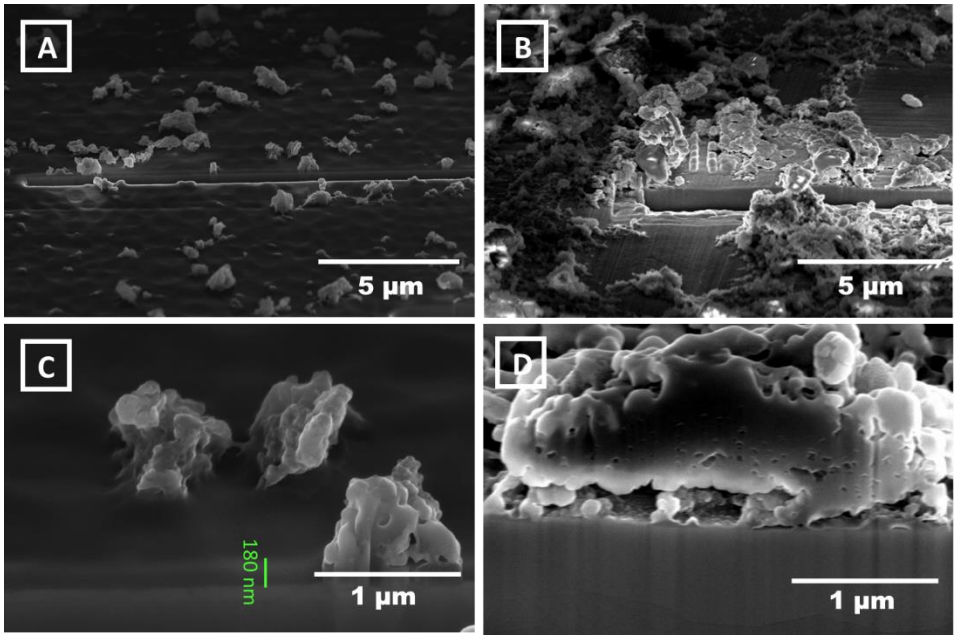

Figure 5.10. FIB cross sections tilted at 52 ° SEM images of the stamped (A and C) and spray coated (B and D) MIP based sensor substrates.

In these images, it can be seen once again that the spray coated substrates contain more MIP particles in comparison with the stamped ones. It is also visible that the mechanical force used during the stamping procedure, caused the particles to be pressed deeper in the PVC layer which allows them to be more in contact with the underlying aluminum substrate. While no pressure was used on the spray coated substrate, the MIP particles are only touching the PVC layer at its surface rather than being embedded in it. These results are also in correlation with the findings in Figure 5.9. When looking at the pore blocking model in Figure 5.2 B, it becomes clear that binding events between the target and MIP that happen further away from the substrate (which is the case for the spray coated substrates) are more difficult to detect using HTM as a read-out technique in comparison with the binding that occurs closer to the surface (which is the case for the stamped substrates). This might be a plausible explanation of why the spray coated sensor shows a lower response and faster saturation in comparison with the stamped one.

5.5 Conclusions and outlook

In this work towards low-cost MIP based sensors, as a proof of concept, spray coating is used as a scalable, and automated technique to deposit polymer particles on transducer substrates to reduce human error that occurs during stamping. In addition, the previously used expensive MDMO-PPV serving as an adhesive layer was successfully replaced with the cheap polymer PVC and the cost-effective miniaturizable HTM set-up was implemented for sensor read-out.
The MIP particles were successfully obtained using the bulk polymerization technique and tested for their capability to rebind the target molecule using batch rebinding experiments. After the deposition on low-cost PVC, the spray coated polymer particles showed a more homogeneous distribution in comparison with the stamped ones. Upon the administration of different concentrations of target molecule, both stamped and spray coated MIP based sensors show a stronger increase in R_{th} in comparison with the negative control which indicates specific binding. When dopamine was used instead of the structurally similar target molecule, the MIP sensor showed no response which proves its selectivity for serotonin. The MIP and NIP particles were deposited using stamping and spray coating techniques and were studied for the amount of material deposited and surface coverage on the substrate using optical and scanning electron microscopy. The results indicate that with spray coating high amounts of MIP covering the substrate can be easily achieved by simply tuning the number of nozzle passes. The sensor measurements on substrates coated using stamping and spray coating techniques shows that the results are comparable and within the same range. However, the sensor measurement on the spray coated sample is not yet optimal as compared to sensors based on the more established stamping technique in terms of signal increase, despite the higher amount of material on the substrate in case of the former. The results clearly indicate that for the sensor response, the amount of MIP material on the sensor substrate is not the only factor that is decisive and that also the proximity of the receptor material to the aluminium electrode is a crucial factor. Though the performance of the spray coated substrates are not optimal, this work clearly shows the feasibility of the deposition technique towards automation and upscaling. To conclude, the combination of the

low cost materials, scalable and reproducible deposition method and cost-effective and miniaturizable read-out, is a significant step towards a cheap sensor for the detection of low molecular weight (bio-) molecules.

In the future, the spray coat conditions (such as the substrate particle load) and the thickness of the PVC adhesive layer, will be optimized to achieve a higher signal response. In addition, to achieve an improved contact between the sprayed MIP particles and the sensor substrate, a mechanical step to press the spray coated particles deeper in the PVC layer will be investigated. Because of the high spatial resolution offered by spray coating in comparison to stamping, different structures each consisting of MIPs that can bind different target molecules can be realized. This is especially interesting for multi-analyte sensing applications towards low-cost sensors for full sample analysis.

5.6 Supporting information

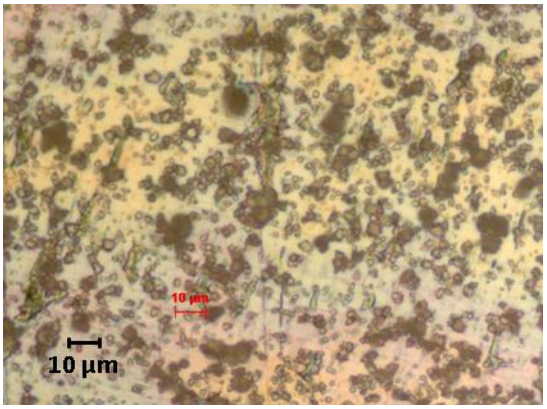

Figure S5.1. Optical microscopy image of crushed bulk NIP particles.

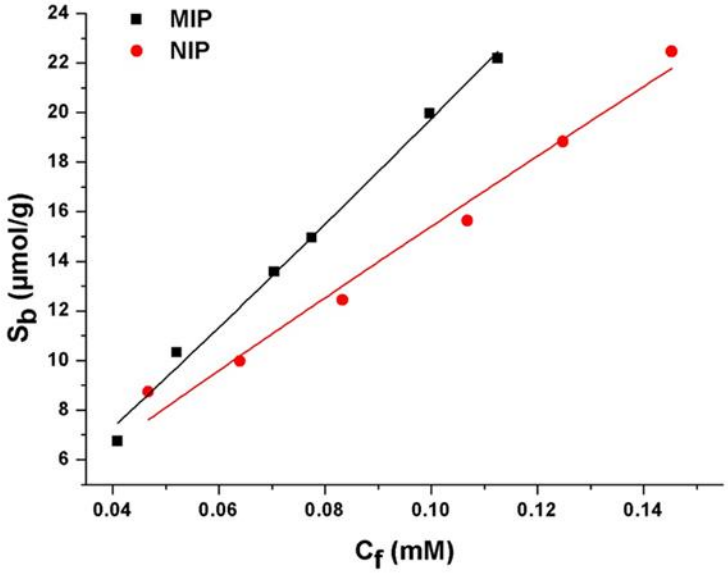

Figure S5.2. Binding isotherms for MIP and NIP particles at pH 7.4 fitted with an allometric fit (non-linear, $R^2 = 0.98$) with added concentrations of serotonin ranging from 0.1 to 0.35 mM.

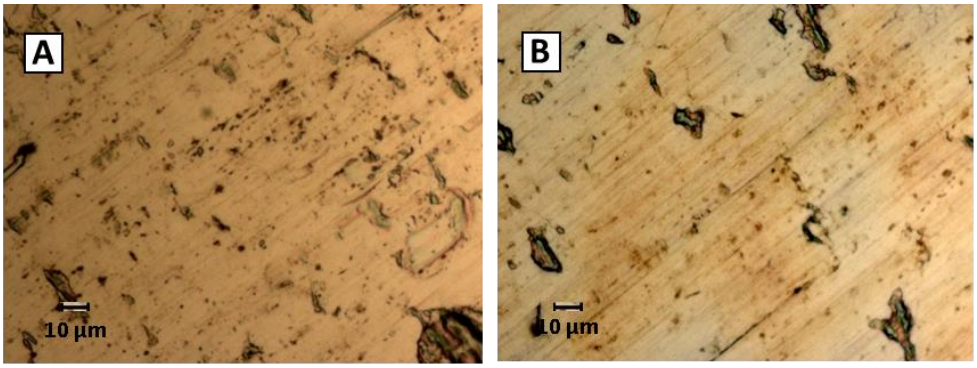

Figure S5.3. Optical microscopy images of aluminum substrates during different stages of sample preparation: Bare aluminum substrate (A), after deposition of 180 nm thick PVC layer on aluminum substrate (B).

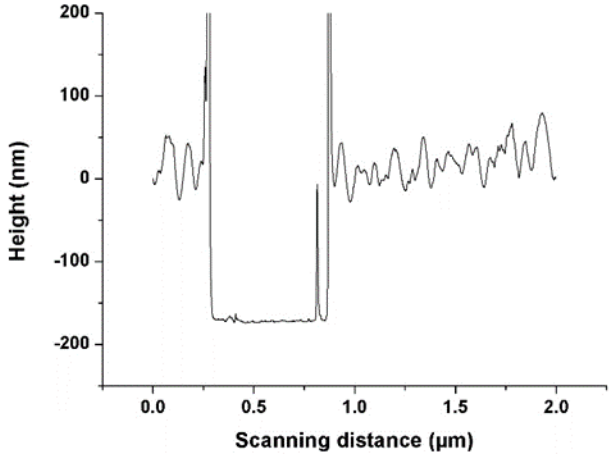

Figure S5.4. Dektak profile of the aluminum with a spin coated layer of PVC (about 190 nm).

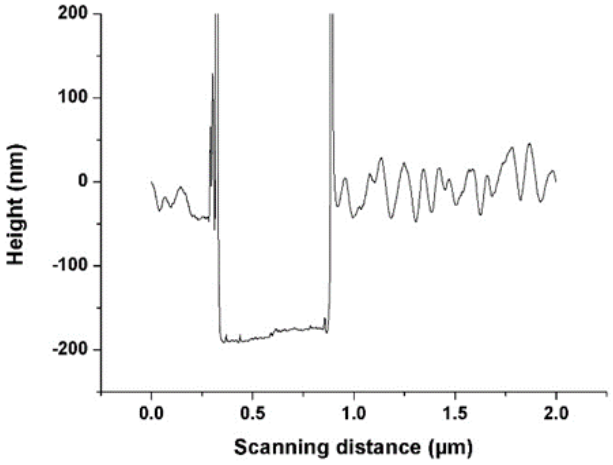

Figure S5.5. Dektak profile of the aluminum with a spin coated layer of PVC baked at 120 °C (about 180 nm).

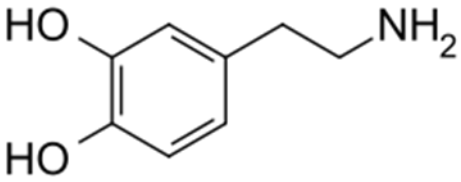

Figure S5.6. Chemical structure of dopamine.

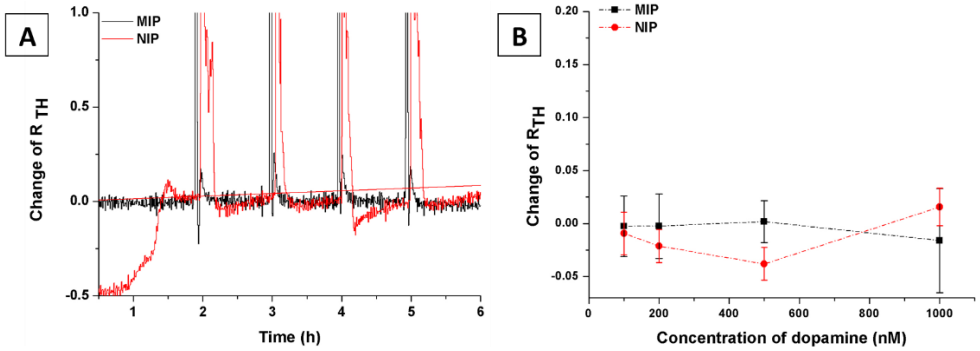

Figure S5.7. R_{th} measurement results for MIP and NIP based sensors obtained using the stamping deposition technique upon addition of increasing dopamine concentrations (100, 200, 500 and 1000 nM) plotted as a function of time (A) and the average change in R_{th} plotted against the concentration of target molecule (B).

5.7 References

[1] B. Barlen, S. D. Mazumdar, M. Keusgen, *Physica Status Solidi (a)* **2009**, 206, 409.

[2] A. Lueking, D. J. Cahill, S. Müllner, *Drug Discovery Today* **2005**, 10, 789.

[3] Q. Zheng, H. Wu, Z. Shen, W. Gao, Y. Yu, Y. Ma, W. Guang, Q. Guo, R. Yan, J. Wang, K. Ding, *Analyst* **2015**, 140, 6660.

[4] T. R. J. Holford, F. Davis, S. P. J. Higson, *Biosensors and Bioelectronics* **2012**, 34, 12.

[5] R. Folly, A. Salgado, B. Valdman, F. Valero, *Brazilian Journal of Chemical Engineering* **1997**, 14.

[6] K. Eersels, B. van Grinsven, A. Ethirajan, S. Timmermans, K. L. Jiménez Monroy, J. F. J. Bogie, S. Punniyakoti, T. Vandenryt, J. J. A. Hendriks, T. J. Cleij,

M. J. A. P. Daemen, V. Somers, W. De Ceuninck, P. Wagner, *ACS Appl. Mater. Interfaces* **2013**, 5, 7258.

[7] R. S. Marks, C. R. Lowe, D. C. Cullen, H. H. Weetall, I. Karube, *Handbook of Biosensors and Biochips*, Vol. 2, **2007**.

[8] K. D. Shimizu, C. J. Stephenson, *Current Opinion in Chemical Biology* **2010**, 14, 743.

[9] K. Mosbach, *Trends Biochem. Sci.* **1994**, 19, 9.

[10] B. Sellergren, *Molecularly Imprinted Polymers. Man-Made Mimics of Antibodies and their Application in Analytical Chemistry*, Elsevier Science, Amsterdam, The Netherlands **2000**.

[11] G. E. M. Tovar, I. Kräuter, C. Gruber, *Top. Curr. Chem.* **2003**, 227, 125.

[12] D. Spivak, *Adv. Drug Deliv. Rev.* **2005**, 57, 1779.

[13] C. Alexander, H. S. Andersson, L. I. Andersson, R. J. Ansell, N. Kirsch, I. A. Nicholls, J. O'Mahony, M. J. Whitcombe, *J. Mol. Recognit.* **2006**, 19, 106.

[14] R. J. Ansell, *J. Chromatogr. B: Anal. Technol. Biomed. Life Sci.* **2004**, 804, 151.

[15] S. Wei, B. Mizaikoff, *J. Sep. Sci* **2007**, 30, 1794.

[16] M. Abdouss, E. Asadi, S. Azodi-Deilami, N. Beik-mohammadi, S. Amir Aslanzadeh, *J. Mater. Sci. Mater. Med.* **2011**, 22, 2273.

[17] M. Peeters, F. Troost, B. van Grinsven, F. Horemans, J. Alenus, M. S. Murib, D. Keszthelyi, A. Ethirajan, R. Thoelen, T. Cleij, *Sensors and Actuators B: Chemical* **2012**, 171, 602.

[18] J. Alenus, A. Ethirajan, F. Horemans, A. Weustenraed, P. Csipai, J. Gruber, M. Peeters, T. J. Cleij, P. Wagner, *Anal. Bioanal. Chem.* **2013**, 405, 6479.

[19] E. Asadi, S. Azodi-Deilami, M. Abdouss, D. Kordestani, A. Rahimi, S. Asadi, *Korean J. Chem. Eng.* **2014**, 31, 1028.

[20] K. Yang, M. M. Berg, C. Zhao, L. Ye, *Macromolecules* **2009**, 42, 8739.

[21] O. Hayden, P. A. Lieberzeit, D. Blaas, F. L. Dickert, *Advanced Functional Materials* **2006**, 16, 1269.

[22] G. Wackers, T. Vandenryt, P. Cornelis, E. Kellens, R. Thoelen, W. De Ceuninck, P. Losada-Perez, B. van Grinsven, M. Peeters, P. Wagner, *Sensors (Basel, Switzerland)* **2014**, 14, 11016.

[23] N. Kirsch, J. P. Hart, D. J. Bird, R. W. Luxton, D. V. McCalley, *Analyst* **2001**, 126, 1936.

[24] B. K. Lavine, D. J. Westover, N. Kaval, N. Mirjankar, L. Oxenford, G. K. Mwangi, *Talanta* **2007**, 72, 1042.

[25] I. Chianella, S. A. Piletsky, I. E. Tothill, B. Chen, A. P. F. Turner, *Biosensors and Bioelectronics* **2003**, 18, 119.

[26] Y. Tan, H. Peng, C. Liang, S. Yao, *Sensors and Actuators B: Chemical* **2001**, 73, 179.

[27] C. Ayela, G. Dubourg, C. Pellet, K. Haupt, *Advanced materials (Deerfield Beach, Fla.)* **2014**, 26, 5876.

[28] V. Erspamer, G. Boretti, *Archives internationales de pharmacodynamie et de therapie* **1951**, 88, 296.

[29] I. P. Kema, E. G. E. de Vries, F. A. J. Muskiet, *Journal of Chromatography B: Biomedical Sciences and Applications* **2000**, 747, 33.

[30] P. M. Vanhoutte, in *Serotonin and the Cardiovascular system*, (Ed: R. Press), New York **1985**.

[31] D. G. Grahame-Smith, *The American Journal of Cardiology* **1968**, 21, 376.

[32] A. N. M. Wymenga, W. T. A. van der Graaf, I. P. Kema, E. G. E. de Vries, N. H. Mulder, *The Lancet* **1999**, 353, 293.

[33] J. E. Blundell, *The American journal of clinical nutrition* **1992**, 55, 155s.

[34] G. M. Anderson, J. M. Stevenson, D. J. Cohen, *Life Sciences* **1987**, 41, 1777.

[35] G. M. Anderson, in *Kynurenine and Serotonin Pathways: Progress in Tryptophan Research*, (Eds: R. Schwarcz, S. N. Young, R. R. Brown), Springer New York, Boston, MA **1991**, 51.

[36] B. A. Patel, M. Arundell, K. H. Parker, M. S. Yeoman, D. O'Hare, *Journal of Chromatography B* **2005**, 818, 269.

[37] B. V. Sarada, T. N. Rao, D. A. Tryk, A. Fujishima, *Analytical chemistry* **2000**, 72, 1632.

[38] K. Wu, J. Fei, S. Hu, *Analytical Biochemistry* **2003**, 318, 100.

[39] B. E. K. Swamy, B. J. Venton, *Analyst* **2007**, 132, 876.

[40] M. Peeters, P. Csipai, B. Geerets, A. Weustenraed, B. van Grinsven, R. Thoelen, J. Gruber, W. De Ceuninck, T. J. Cleij, F. J. Troost, P. Wagner, *Analytical and bioanalytical chemistry* **2013**, 405, 6453.

[41] H. Freundlich, *Z. Phys. Chem.* **1906**, 57, 385.

[42] I. R. Umpleby, S. Baxter, A. Rampey, G. Rushton, Y. Chen, K. Shimizu, *J. Chromatogr. B* **2004**, 804, 141.

6 Summary and outlook

Sensors which are able to accurately detect and quantify a biologically relevant target molecule in physiological concentrations in a consistent way while still being user friendly, cheap and accessible for a broad public, are highly interesting for point-of-care medical diagnostics and food- and environmental safety. Today, the quantification of a target molecule in a sample is mostly performed with expensive and time consuming detection techniques such as immunoassays and liquid and gas chromatography in specialized labs and by specialized personnel. Therefore, as an alternative, researchers are focussing on a user friendly, low cost and reliable diagnostic sensor which can also be used outside of the lab. Biosensors typically use biological receptors as sensing elements which are very specific and selective when it comes to target molecule detection. However, these biological receptors also show major drawbacks regarding cost and stability. In addition, there are many target molecules for which sufficiently stable biological receptors do not exist. In this regard, a compelling alternative is the synthetic molecularly imprinted polymer (MIP) receptor which has multiple advantages over the biological receptors in terms of stability and cost while still offering sufficient affinity and selectivity for the target molecule. MIPs are made by polymerizing functional and crosslinking monomers in the presence of the target/template molecule. After polymerization and removal of the template molecule, an imprint is left which is complementary to the template regarding size, shape and functional groups. Therefore, these imprints are able to rebind the target molecule with high affinity and specificity. As a negative control, non-imprinted polymers (NIPs) are used. MIP based sensors for different target molecules have already been established at the host institute and have been continuously developed and optimized for improving their performance, reliability and reusability.

At the start of my PhD, bulk MIP sensor based detection of nicotine, histamine, caffeine and serotonin in biological samples was already established using stamping and matrix entrapment as deposition and immobilization techniques respectively. Impedance spectroscopy, heat transfer method (HTM) and quartz crystal microbalance were used as read-out techniques. However, bulk polymerization as a MIP synthesis method resulted in irregularly shaped particles

with a broad size distribution (0.1 – 50 µm) and a relatively low sensing surface which limits their applicability for commercial diagnostic sensors. Also the manual MIP deposition method that was used, is time consuming and very much dependent on the operator skills which leads to high variations in and between different sensor substrates regarding MIP material amount and distribution. In addition, the embedding of particles by physical entrapment physically blocks many imprint sites and might loosen up during the sensor measurement. This might lead to a reduced sensor sensitivity and unforeseen erroneous detection, and limits the possibility for reusable sensors. In this thesis, each chapter deals with different efficient and simple strategies to tackle the aforementioned problems. As it is highly desired and necessary to achieve low-cost, high performing, reproducible and reusable sensors for the detection of (bio-) molecules in biological samples in physiological concentration ranges, each chapter is devoted to realize one or more of these requisites.

The important results from this work are summarized below chapter wise along with future perspectives.

In the first part of my doctoral studies (**chapter 2**), the focus was laid on creating MIP particles with enhanced recognition which are on the one hand homogeneous regarding size, shape and material distribution and on the other hand provide an increased sensing surface owing to their small sub-micron size. To achieve this goal, two strategies were combined. The first strategy was the implementation of the versatile miniemulsion technique which resulted in colloidal MIPs in the form of water-based dispersions. The obtained colloidal MIP particles had a small diameter (± 500 nm), spherical shape, and a relatively narrow size distribution. Next, to go one step further and also gain control over the homogeneity of the material distribution within MIP entities, a second strategy, was implemented. Usually, MIPs are obtained by combining a functional monomer (± 10 – 20 %) containing a functional group that can interact with the template molecules, with a crosslinking monomer (± 80 – 90 %). To ensure a homogeneous distribution of crosslinker and functional monomer in the polymer matrix, the latter two need to be structurally similar. Therefore, one has to choose the appropriate functional monomer with respect to the template/target molecule together with an appropriate crosslinker and the quality of the final MIP depends also on the

concentration ratios of the individual components. Alternatively, a previously established single bifunctional crosslinking monomer: N,O-bismethacryloyl ethanolamine (NOBE) was used. With that concept, a simplified route to design colloidal MIPs was developed where the need for additional functional monomers and empirical optimization of the relative ratios of functional monomers, crosslinkers, and template was eliminated.

NOBE based bulk and miniemulsion MIPs templated with testosterone were successfully prepared. To prove that colloidal MIPs were indeed superior to the conventional bulk MIPs, a comparative study was performed. This was possible because both bulk and miniemulsion polymerized NOBE MIPs were formulated employing the same relative ratios of target molecule, monomer, initiator and porogen. The molecular recognition capacity of the different MIPs was studied using equilibrium binding analysis in aqueous solutions. The binding properties of the bulk MIPs and NIPs were tested first at various pH values. After selecting the optimal pH, batch rebinding studies were performed with the miniemulsion colloidal MIP-NIP duo. From these experiments, it could be seen that the colloidal NIP showed significantly less aspecificity as compared to the bulk NIP. The colloidal MIPs show significant advantages owing to their small size, homogeneity and increased surface area resulting in largely increased imprint factors (6.8 vs 2.2) and improved selectivity in comparison with bulk MIPs. Finally, both the bulk and miniemulsion polymerized particles were tested for their selectivity against different structural analogues of testosterone namely methyl testosterone, β-estradiol and estriol. It was found that the recognition of the structural analogues is strongly dependent on the extent of their structural resemblances to the imprinted molecule. To conclude, for the first time colloidal MIPs for the recognition of testosterone and its structural analogues were developed using the simplified synthesis protocol based on a single monomer in aqueous solution. In the future, the miniemulsion MIP synthesis recipe can be fine-tuned to obtain particles with a lower polydispersity index. To achieve this, a co-stabilizer may be added to the system. However, the fact that the latter might alter the bonding between the monomer and the target molecule should be taken into consideration. Also other bi-functional monomers such as 2-methyl-*N*-(3-methyl-2-oxobut-3-enyl)acrylamide (NAG) can be tested to obtain even higher performing MIPs. NAG

might show an improved resolution in cavity formation as a consequence of its shorter cross-linker size in comparison to NOBE. Also monomers containing different functionalities can be used to imprint target molecules with complementary functional groups. Using the non-covalent imprinting approach, not only hydrogen bonding can be established between the functional monomer and the target molecule, but also electrostatic, hydrophobic, etc. interactions are interesting options.

After obtaining these superior miniemulsion MIPs, our focus was on their integration in a real sensor application (**chapter 3**). There are two widely employed routes to fixate MIPs on a sensor substrate. One way is by using a polymer adhesion layer (like a glue) and the second way is by chemical coupling. As MIP immobilization in an adhesion layer blocks a certain amount of the imprint sites (resulting in reduced sensor sensitivity) and might loosen up during the sensor measurement resulting in unforeseen material loss, direct chemical coupling to the transducer surface was preferred. A doped silicon substrate covered with a doped nanocrystalline diamond layer was functionalized with amorphous carbon by using carbon evaporation. Subsequently, the miniemulsion particles which display vinyl surface groups are covalently coupled to the carbon layer by using UV light. This direct coupling method avoids the impairment of the MIP functionality and reduces sample preparation steps while still offering a strong and reliable bond. In addition, in comparison with approaches where linker molecules such as silanes are employed, the direct coupling to the transducer substrate via a carbon layer allows the receptor to be in much closer proximity to the sensor substrate that is crucial for surface sensitive detection techniques. After the removal of unbound MIP particles, the scanning electron microscopy (SEM) images show a uniform MIP particle distribution on the surface. To test the ability of these MIP sensor substrates to effectively and selectively detect the target molecule in biological samples, both buffer and urine samples spiked with several testosterone or structural analogue β-estradiol concentrations were used. As a read-out technique, electrochemical impedance spectroscopy was employed. From these sensor measurements, it was indeed confirmed that testosterone can be selectively detected in urine samples in the physiological nM concentration range. To conclude, the MIP immobilization method used in this chapter is

straightforward and simple. It requires minimal effort preparation steps and avoids the use of an interfacial adhesive polymer layer. In the future, to improve the active sensing surface, optimizations can be made by decreasing the diameter of the MIP particles or by improving the sensor coverage by increasing the areal density of MIP particles. Also the sensor flow cell set-up can be optimized and miniaturized to obtain lower limits of detection and faster response times.

Another interesting strategy that was developed in order to achieve reliable high performing sensors, is the *in situ* polymerization and grafting of patterned MIP structures with confined geometries directly on the sensor substrate using microfluidic systems (**chapter 4**). A master structure which contains a specific lane pattern to maximize the eventual sensing surface area, was obtained using electron beam lithography. From this master structure, an elastic cast/mold was obtained using polydimethylsiloxane. This mold was placed on top of an amorphous carbon functionalized diamond coated silicon substrate. The structures were subsequently filled with the testosterone containing NOBE prepolymerization (monomer) mixture. Next, the *in situ* polymerization and the coupling to the substrate, were initiated upon exposure to UV-light. This simple and cost effective technique allows a more firm fixation and a controllable, homogeneous and reproducible receptor material distribution on the sensor surface. In addition, this method is low-labour as numerous cast molds can be readily obtained from a single master structure. This means that the expensive and time consuming e-beam lithography only needs to be performed once. After the removal of the elastic mold and the template molecules, the selective sensor performance of these substrates was tested in buffer, urine and saliva samples spiked with testosterone or its structural analogues β-estradiol and estriol. As a read-out technique, EIS was used. A differential flow-cell sensor setup was designed in which both MIP and NIP particles immobilized substrates are measured simultaneously in the same environment. The latter aspect eliminates the influence of surrounding and sample variations (complex mixtures). The sensor measurements showed that the MIP structures were able to selectively bind testosterone both in buffer and in the biological samples. Even the addition of the lowest testosterone concentration of 0.5 nM (physiological range), led to a measurable increase of the sensor signal. Although the response in urine samples

is comparable with the ones obtained in buffer, when saliva was used, a reduced but still significant sensor response was obtained. This might be attributed to the reason that saliva contains much more proteins and other molecules as compared to urine. This excess of proteins might block a significant amount of MIP binding sites resulting in a lower sensor sensitivity. However, this can be circumvented in the future by using treated saliva samples. After the sensor measurements in which the MIP structures are subjected to a dynamic liquid flow, optical microscopy showed that the structures were still intact. Due to the large MIP surface area and the highly stable bond between the polymer and the substrate, regeneration of the sensor was successfully performed with a simple washing step. A second sensor measurement was performed and resulted again in a clear concentration dependent sensor response upon administration of testosterone. To conclude, a technique that offers a cost-effective and straightforward method to produce sensitive, high performance, reproducible and well-defined MIP based sensor platforms for the electronic detection of (bio-) molecules was developed. The latter also offers design flexibility that allows for tuning the dimensions and amount of MIP structures by opting for suitable master structures. As a next step to achieve an even lower limit of detection (pM range), adaptations in the system can be made such as an increased active sensing surface and optimization and miniaturization of the sensor flow cell set-up and read-out. An increased active sensing surface will also allow shorter sensor regeneration times. Additionally, MIP structures imprinted with different target molecules can be immobilized on the same sensor substrate. This concept will allow the detection of multiple analytes in a sample simultaneously in one sensor measurement.

In **chapter 5**, a new MIP deposition technique in combination with a low-cost MIP immobilisation adhesive and sensor read-out technique, was explored for the fabrication of cheap and scalable sensors. After obtaining bulk MIP particles (0.1 – 10 µm) imprinted with serotonin, they were successfully tested for their ability to rebind the target molecule using batch rebinding experiments. As a next step, they were immobilized on a cheap planar aluminium electrode by using an adhesive layer. For this, the previously used expensive conjugated polymer namely poly[2-methoxy-5-(3’,7’-dimethoxyoctyloxy)-1,4-phenylenevinylene] (MDMO-PPV), was replaced with the economically viable and readily available

common polymer polyvinylchloride (PVC). A PVC solution was spin coated on top of the aluminium electrodes to obtain a 180 nm thick layer. Also the previously used stamping deposition method which is very much dependent on the operator skills, was replaced with the spray coating technique as it allows for high reproducibility and automation for the large scale fabrication of sensor layers. After the deposition of the MIP and NIP particles, the substrates were heated slightly above the glass transition temperature of PVC. This way, the adhesive becomes soft and the particles can partially sink in thereby fixating the particles on the substrate. In order to compare the two different MIP deposition techniques in terms of surface coverage, both stamped and spray coated sensor substrates were compared using both optical microscopy and scanning electron microscopy. With spray coating, high amounts of MIP particles can be easily deposited on the substrate by tuning the number of spray coat passes. On the one hand, the spray coated substrates contain significantly higher amounts and a more homogeneous distribution of MIP and NIP material on the surface in comparison with the stamped ones. On the other hand, as the polymer particles are mechanically pressed on the sensor substrate using the stamping technique, with the cross-section SEM analysis, it could be seen that the MIPs are embedded deeper in the PVC layer. While, with the spray coating deposition technique, the MIPs are not sufficiently embedded but mostly touching the PVC layer at its surface. To test their sensor performances, the cost-effective and simple heat transfer method is used as a read-out technique. The latter circumvents the need of sophisticated equipment since it requires only two thermocouples, a proportional-integral-derivative (PID) controller and an adjustable heat source. From these measurements, it was concluded the results are comparable and within the same range for both the deposition techniques. However, the stamped sensor showed 10 % more response and less saturation at a target molecule concentration of 500 nM serotonin in comparison with the spray coated sensor. This result indicates that the sensor performance is influenced more by the way the MIP particles are embedded in the adhesive layer and their proximity to the aluminium electrode rather than the MIP quantity present on the substrate. Although the sensor performance of the spray coated substrates are not optimal yet, this deposition technique clearly shows its feasibility towards automation and upscaling. The combination between the cost-effective PVC, the scalable and reproducible (as it

can be automated) deposition technique and the miniaturizable read-out, offers the development of a low-cost sensor to detect low molecular weight (bio-) molecules. As a next step, the spray coat conditions (such as the substrate particle load) and the thickness of the PVC adhesive layer, has to be optimized to achieve a higher signal response. In addition, to achieve an improved contact between the sprayed MIP particles and the sensor substrate, a mechanical step to press the spray coated particles deeper in the PVC layer has to be investigated. Lower detection limits and faster response times can be obtained by optimizing and miniaturizing the HTM sensor set-up. Because of the high spatial resolution offered by spray coating in comparison to stamping, different structures each consisting of MIPs that can bind different target molecules can be realized. This is especially interesting for multi-analyte sensing applications towards low-cost sensors for full sample analysis.

Within this PhD work, different MIP based sensor fabrication concepts were tested in order to develop reliable and cost-effective high performance sensors. The results clearly show that with a little optimization, these sensors have the potential for commercial use in the near future.